2021

PHARMACOPHORIC EVALUATION OF 5-HT2A AND 5-HT2B SEROTONIN RECPEPTORS

Prithvi Hemanth
Virginia Commonwealth University

PHARMACOPHORIC EVALUATION OF 5-HT_{2A} AND 5-HT_{2B} SEROTONIN RECEPTORS

A dissertation submitted in partial fulfillment of the requirements for the degree of Doctor of Philosophy at Virginia Commonwealth University

By

PRITHVI HEMANTH
Bachelor of Science, Virginia Commonwealth University, United States, 2017

Director: Dr. MAŁGORZATA DUKAT, PHD
ASSOCIATE PROFESSOR
DEPARTMENT OF MEDICINAL CHEMISTRY

Virginia Commonwealth University
Richmond, Virginia
August, 2021

Acknowledgements

I would like to begin by giving a huge thank you to my advisor and mentor Dr. Małgorzata Dukat. You were kind and patient from the moment you accepted me into your lab even though you weren't sure if you could accept a PhD student that year, until my dissertation/defense preparation during which you provided me the necessary guidance to create this wonderful dissertation. I am in awe of the disparity of the naïve child I was when you first took me under your wing compared to the much more mature and scientifically-trained child I am now, and you and Dr. Richard Glennon had huge roles in making that happen. Thank you both for being tough with me and always pushing me to apply myself completely in every setting; I feel now that I am so hardened, I could go to war. Dr. Richard Glennon, you are an inspiration both in a sense of accomplishment and in the shear breadth of your experiences. I have very much enjoyed your stories and I would love the opportunity to listen to more of them, after I successfully receive my doctorate degree, and ideally each of us enjoying a glass of fine cognac.

Thank you Dr. Jose M. Eltit for essentially serving as my third mentor along with Drs. Dukat and Glennon. Without you, I would not have been able to analyze the compounds I synthesized in this project and this amazing dissertation would have been a fraction of the size it is now and would have made for a much less interesting story. I owe you a huge debt of gratitude for all your training and guidance in conducting my assays and creating my cell line. Thank you Dr. Javier Gonzalez-Maeso for allowing me to learn the fundamentals of the fluorescence assay in your lab. Your wonderful post-doctoral student, Dr. Urjita H. Shah was instrumental in teaching me the techniques of the assay while establishing in me a scrupulous attention to proper laboratory technique. I would like to also thank the rest of my extremely supportive graduate committee members, Drs. Glen E. Kellogg and Laura J. Sim-Selley. You have all given me wonderful advice and direction throughout this project. I would be remiss and would never hear the end of it if I did not acknowledge Claudio Catalano. Without you nobody in the department would have done any

modeling during the last four years. Thank you to all past and present lab members, Dr. Abdelrahman E. S. Shalabi, Dr. Ahmed S. Abdel Khalek, Dr. Malaika D. Argade, Dr. Barkha Yadav, Dr. Rachel A. Davies, Pallavi Nistala, C.J. Jones, and Jeremy Rolquin for making the lab an awesome place to be.

One of my proudest accomplishments of my experience as a graduate student is making the dopest friends a guy could make. Because of them, Friday nights would at times seem like a beacon of hope during an otherwise stressful week. To list them: Claudio Catalano, Connor O'Hara, C.J. Jones, Sara Trujillo, Serena Bonasera, Barkha Yadav, Pallavi Nistala, and Shravan Morla. I have thoroughly enjoyed our times together and I look forward to our continued friendship.

A special shoutout to the NOVA crew, specifically the Westfield crew and the Village Center Dr. crew. You guys were/are the brothers and sisters I never had and my personality and sense of humor is almost entirely shaped by you. I would like to thank my incredible mother who has always been supportive of me since day one. Thank you for all the sacrifices you have made to allow me to have lived a life full of comfort and love. Thank you to my aunt Rheka Chikki, uncle Sathi Mama, and little cousin Shrihan for making the visits home such a wonderful escape – I am very lucky to have such cool family in my hometown. Last but not least, I would like to thank my late father, Dr. Hemanth K. Thippeswamy to whom this dissertation is dedicated for being a great inspiration. I would not be where I am today if it weren't for you.

Table of Contents

List of Tables

List of Figures

List of Schemes

List of Abbreviations

[^{11}C]-MBL	N^1-([^{11}C]-methyl)-2-Br-LSD
5-HIAA	5-Hydroxyindoleacetic acid
5-HT	Serotonin
5-HTP	5-Hydroxy-L-tryptophan
AADC	L-Aromatic amino acid decarboxylase
AC	Adenylyl cyclase
Ac_2O	Acetic anhydride
AD	Aldehyde dehydrogenase
$AlCl_3$	Aluminum chloride
Ar-C-C-N	Aryl-carbon-carbon-nitrogen
BBB	Blood-brain barrier
$CaCl_2$	Calcium chloride
cAMP	Cyclic AMP
CNS	Central nervous system
DAG	Diacylglycerol
DRE	Deconstruction, reconstruction, elaboration
EPS	Extrapyramidal stimulation
Fen	Fenfluramine

FST	Forced swim test
GABA	Gamma-aminobutyric acid
GAD	Glutamic acid decarboxylase
GAT	Glutamate transporter
GI	Gastrointestinal
GPCR	G-protein-coupled receptor
$H_2NOH \cdot HCl$	Hydroxylamine hydrochloride
HCOOH	Formic acid
HINT	Hydropathic INTeraction
His	Polyhistidine
HTR	Head-twitch response
IP_3	1,4,5-Triphosphate
LGICR	Ligand-gated ion channel receptor
LTP	Long-term potentiation
MAO	Monoamine oxidase
mCPP	1-(3-Chlorophenyl)piperazine
MDMA	3,4-Methylenedioxymethamphetamine
NAD^+	Nicotinamide adenine dinucleotide
nFen	Norfenfluramine
PAG	Pulmonary artery banding

PCP	Phencyclidine
PET	Positron emission tomography
PLC	Phospholipase C
SAR	Structure-activity relationship
SERT	Serotonin transporter
$SOCl_2$	Thionyl chloride
SSRI	Selective serotonin reuptake inhibitors
TFMPP	1-(3-Trifluoromethylphenyl)piperazine
TH	Tryptophan hydroxylase
THB	Tetrahydrobiopterin
TM	Transmembrane
VGAT	Vesicular GABA transporter

Abstract

PHARMACOPHORIC EVALUATION OF 5-HT_{2A} AND 5-HT_{2B} SEROTONIN RECPEPTORS

By Prithvi Hemanth

A dissertation submitted in partial fulfillment of the requirements for the degree of Doctor of Philosophy at Virginia Commonwealth University

Virginia Commonwealth University

Director: Dr. MAŁGORZATA DUKAT, PHD
ASSOCIATE PROFESSOR
DEPARTMENT OF MEDICINAL CHEMISTRY

Serotonin (5-HT) receptors represent a class of receptors involved in a variety of physiological processes including regulation of mood, perception, cognition, appetite, and heart function, and thus serve as drug targets of several drugs such as antipsychotic agents, hallucinogenic drugs, and appetite suppressant drugs. Due to the structural similarity of certain

5-HT receptor subtypes, particularly 5-HT_2 receptors (5-HT_{2A}, 5-HT_{2B} receptors) determination and refinement of pharmacophore models of these receptor subtypes can greatly improve the therapeutic efficacy of drugs that target them.

The goals of this study were to define and/or refine existing pharmacophore models for 5-HT_{2A} and 5-HT_{2B} receptors. Investigation of 5-HT_{2A} receptors involved analysis of a previously published pharmacophore for 5-HT_{2A} receptors based on the structure of the atypical antipsychotic risperidone. Investigation of a 5-HT_{2A} receptor agonist quipazine and its positional isomers/analogues also aided in the elaboration of 5-HT_{2A} receptor binding. Finally, to determine structural requirements for 5-HT_{2B} agonist action, a series of phenyl-substituted amphetamine analogues and a series of 4-substituted-2,5-dimethoxyamphetamines (DOX-type phenylisopropylamine compounds) were analyzed for their 5-HT_{2B} receptor functional activity.

In the present study, a previously known pharmacophoric 5-HT_{2A} antagonist compound was synthesized along with its N-propyl analogue. The pharmacophoric compound, along with several others in a series in which the piperidine substituent varies in both length and bulk, were screened across serotonin, dopamine, and adrenergic receptors to determine if high affinity and selectivity can be achieved for 5-HT_{2A} receptors. The affinity screen revealed that, as the size and bulk of the piperidine substituent increases, affinity and selectivity for 5-HT_{2A} receptors increased albeit with an accompanying increase in D_2 receptor affinity – antagonism at D_2 receptors is responsible for extrapyramidal stimulation (EPS) symptoms associated with several antipsychotics. Because D_2 receptor affinity could not be abolished, it was determined that extending the chain size of the piperidine substituent is not an effective method for achieving more selective 5-HT_{2A} antagonists.

Computational analysis of quipazine and its analogues was conducted to determine their binding modes at 5-HT_{2A} receptor crystal structures. Higher affinity ligands 1-NP and 2-NP were found to bind in a distinct pocket relative to the lower affinity ligands quipazine and isoquipazine.

It was predicted that the binding pocket occupied by 1-NP and 2-NP contains numerous hydrophobic amino acids and that hydrophobic interactions with these residues confer the high affinity for this class of compounds.

Finally, evaluation of 5-HT_{2B} receptors involved analyzing several 5-HT_{2B} ligands in a Ca^{2+}-release assay to determine their functional activity. In particular, analogues of norfenfluramine (nFen) and DOB were analyzed and it was determined that the agonist activity of nFen is driven by hydrophobic interactions of its 3-CF_3 substituent. To determine the SAR of related phenylisopropylamines at 5-HT_{2B} receptors, a series of DOX analogues was analyzed for their functional activity. It was discovered that larger, more lipophilic 4-position halogens such as bromine (DOB) and iodine (DOI) are more accommodated than smaller less lipophilic halogens such as fluorine (DOF). Supporting the importance of a hydrophobic interaction with the 4-position substituent, DOPR and DOTB containing propyl and *t*-butyl 4-position substituents, respectively, produced potencies on par with that of DOI. These studies resulted in formulation of the first ever pharmacophore for agonist activity at 5-HT_{2B} receptors.

I. Introduction

Serotonin (5-HT) is a monoamine neurotransmitter that binds to and elicits many of its effects through serotonin receptors (5-HT_{1-7} family of serotonin receptors). Serotonin, along with all other monoamine neurotransmitters, contains a common scaffold: a basic nitrogen atom separated by a two-carbon alkyl chain from an aromatic moiety. The similarity of the structures of monoamine neurotransmitters (e.g., serotonin, dopamine, norepinephrine, epinephrine) is representative of the similarities in the binding site residues of all monoamine receptors. Thus, many drugs designed to target one of these receptors are likely to also display activity at the others, making the designing of selective compounds a challenging task. However, techniques such as the application of the Deconstruction, Reconstruction, and Elaboration (DRE) approach and the development of pharmacophore models can greatly ease difficulties in this area by determining minimal structural features necessary to produce biological activity. Once a simple scaffold is established, it can be elaborated by the addition of substituents that might result in selective compounds. This project is concerned with the development/refinement of pharmacophore models for 5-HT_{2A} and 5-HT_{2B} receptors.

One area in which the development of more selective compounds can have an enormous impact is antipsychotic therapy. The issue with current antipsychotic drugs is that although they antagonize the desired 5-HT_{2A} receptor, they also display desired antagonism at D_2 receptors. This D_2 antagonism also underlies the undesired extrapyramidal stimulation (EPS) side effects observed in patients prescribed certain antipsychotic medication. Unfortunately, although current antipsychotic drugs are very effective in treating schizophrenia, EPS symptoms cause patients to experience Parkinsonism-like symptoms such as tremors and dyskinesia. Thus, the development of more selective 5-HT_{2A} antagonizing antipsychotic agents would alleviate the suffering experienced by millions of schizophrenic patients around the world. Here, we attempt to exploit a

new 5-HT_{2A} receptor antagonist pharmacophore to identify compounds with an improved 5-HT_{2A} receptor versus D_2 receptor profile.

Quipazine, a known but relatively non-selective 5-HT_{2A} receptor agonist, represents an enigmatic ligand in that it does not conform to the structures of other known 5-HT_{2A} agonists. In as much as it might provide new insight to how quipazine interacts with the receptor, quipazine, a related agonist, 2-NP, and two structurally-related antagonists will be examined at models of the active and inactive states, respectively, of 5-HT_{2A} receptor models.

Unlike 5-HT_{2A} receptors which are mostly expressed in the central nervous system (CNS), 5-HT_{2B} receptors are mostly expressed peripherally in regions such as the liver, lung, heart, and kidney. One region of particular interest is the heart where 5-HT_{2B} receptors regulate proper heart morphology and function. In fact, certain drugs such as the very effective anorectic drug fenfluramine have been removed from the market due to incidences of cardiac valvulopathy in patients – a condition characterized by thickening of the heart valves – resulting from the activation of cardiac 5-HT_{2B} receptors. Thus, in the interest of preserving the therapeutic effects of these drugs (e.g., anorectic effect of fenfluramine) while dispelling negative side-effects (e.g., cardiac valvulopathy) produced by the activation of 5-HT_{2B} receptors, pharmacophoric features for activation can be elucidated and these features can be omitted in the structures of drugs developed in the future, thus reducing the chances of activating 5-HT_{2B} receptors and producing negative cardiac side-effects. These studies will involve molecular modeling, and the synthesis and pharmacological evaluation of known and novel agents.

II. Background

A. Overview of Serotonin Receptors

Serotonin (**1**) (5-HT, Figure 1), one of the most abundant signaling molecules,[1] plays numerous physiological roles including the modulation of aggression, appetite, cognition, emesis, endocrine function, gastrointestinal function, motor function, neurotrophism, perception, sensory function, sex, sleep, and vascular function.[1,2] It was initially found in the gastrointestinal mucosa (where it is in most abundance and produced by enterochromaffin cells) during the discovery that it produced contraction of the smooth muscle of rat uterus in 1937,[3] it was later found in the brains of numerous animals in 1953[4] where it is produced by a cluster of cells within the raphe nuclei.[5] Since this discovery, numerous insights have been made in regard to serotonin's function, including the crucial discovery that it is involved in the modulation of psychiatric disorders.[5]

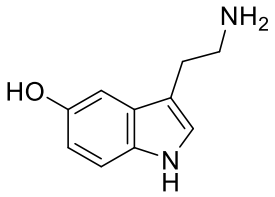

Serotonin (5-HT; **1**)

Figure 1. Structure of serotonin (**1**).

In the human body, serotonin is peripherally biosynthesized primarily in enterochromaffin cells and centrally in presynaptic serotonergic neurons, particularly in cell bodies known as the raphe nuclei.[6] Its synthesis is consistent irrespective of location and involves two steps. First, the amino acid tryptophan is hydroxylated at the 5-position of the indole ring by tryptophan hydroxylase (TH) using the cofactor tetrahydrobiopterin (THB), forming 5-hydroxy-L-tryptophan (5-HTP, Figure 2). Second, 5-HTP is decarboxylated by L-aromatic amino acid decarboxylase (AADC) forming serotonin which is then stored in intracellular vesicles in enterochromaffin cells,

platelets, and serotonergic neurons, ready to be released extracellularly upon external stimuli. The binding of serotonin to presynaptic autoreceptors (i.e., 5-HT_{1A} and 5-HT_{1B} receptors) creates a negative feedback loop, resulting in the termination of serotonin's effect via uptake through serotonin transporters (SERT) and storage into vesicles or cytoplasmic degradation by monoamine oxidase (MAO).[6] MAO converts serotonin into 5-hydroxyindoleacetaldehyde which is then oxidized by aldehyde dehydrogenase (AD) using the cofactor nicotinamide adenine dinucleotide (NAD^+) forming the primary metabolite 5-hydroxyindoleacetic acid.

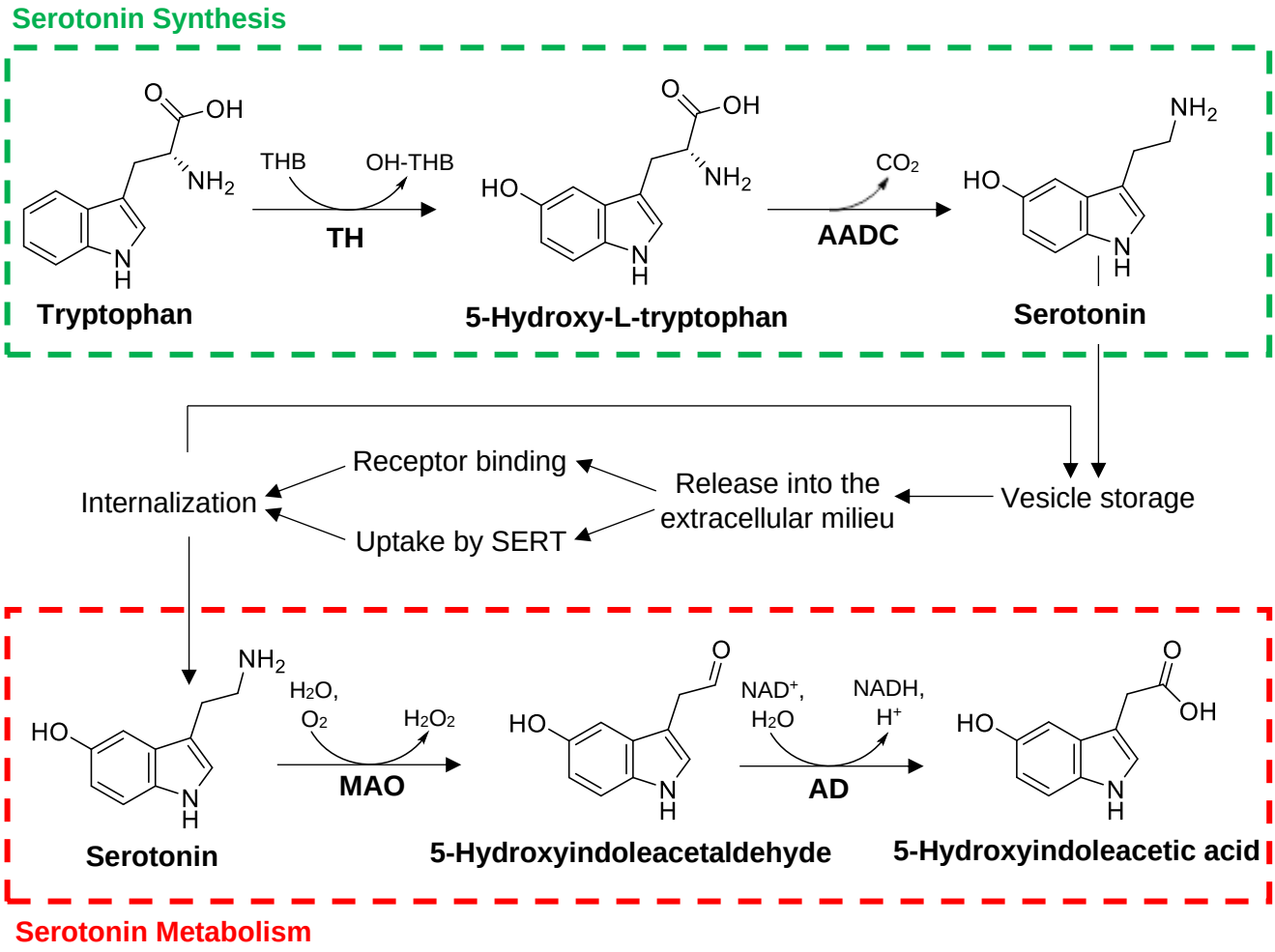

Figure 2. Synthesis and metabolism of serotonin.[7]

Serotonin produces its effects through the modulation of proteins known as the serotonin receptor family. This family currently consists of seven transmembrane protein subfamilies (5-HT_{1-7}), of which the 5-HT_3 channel is the only ligand-gated ion channel receptor (LGICR) while the others are type A rhodopsin-like G-protein-coupled receptors (GPCRs). Serotonin receptors were originally classified into two groups, “D” type and “M” type receptors. “D” type receptors were found to be involved in the contraction of smooth muscle, the effect of which was blocked by the antagonist dibenzyline,[8] whereas “M” type receptors, produced a depolarization effect of cholinergic neurons that was blocked by morphine.[8] In 1979 Peroutka and Snyder reclassified serotonin receptors as 5-HT_1 and 5-HT_2 (previously “D” type receptors) receptors, based on the binding of agonists/antagonists at two distinct serotonin binding sites.[9] in 1986, Bradley and colleagues reclassified type “M” type receptors as 5-HT_3 receptors.[10] Today, the seven sub-types of serotonin receptors are typically grouped according to which G-protein the receptor is coupled to during downstream signaling. 5-HT_4, 5-HT_6, and 5-HT_7 receptors are coupled to the G-protein $G\alpha_s$ which results in the activation of the effector protein adenylyl cyclase (AC) and an increase in the levels of the second messenger cyclic AMP (cAMP) , 5-HT_1 and 5-HT_5 receptors couple to $G\alpha_{i/o}$ and deactivate AC and decrease levels of cAMP and 5-HT_2 receptors couple to $G\alpha_q$ resulting in activation of the effector protein phospholipase C (PLC) and increase in the levels of the second messenger inositol 1,4,5-triphosphate (IP_3) (Figure 3) and diacylglycerol (DAG). Upon IP_3 binding to IP_3 receptors located on the endoplasmic reticulum (ER), Ca^{2+} is transported from the interior of the ER to the cytoplasm (this mechanism serves as a basis for Ca^{2+} binding assays employed to measure functional activity of ligands).[11]

The 5-HT_2 receptor subfamily consists of three receptor subtypes: 5-HT_{2A}, 5-HT_{2B}, and 5-HT_{2C} receptors. The 5-HT_{2A} receptor contains a binding site which was originally labeled the “D” receptor site. After Leysen et al. discovered a serotonergic component to neurons labeled with [^{3}H]spiperone in 1978,[12] these receptors were later classified as 5-HT_2 receptors by Peroutka and

Snyder in 1979. Eventually these receptors were designated 5-HT_{2A} receptors. Examination of the distribution of 5-HT_{2A} receptor mRNA in post-mortem humans revealed the presence of mRNA in pyramidal neurons (especially in layer V of the neocortex) and in very small levels in the hippocampus.[13] Positron emission tomography (PET) imaging studies of living human brains using the imaging agent *N*[1]-([[11]C]-methyl)-2-Br-LSD ([[11]C]-MBL) revealed that 5-HT_{2A} receptors label highest in regions of the brain associated with cognition and sensory input (e.g., frontal, temporal, and parietal lobes) and lowest in regions associated with motor functions such as the caudate nucleus and putamen,[14] providing evidence for its involvement in the modulation of behavior. In the periphery, 5-HT_{2A} receptors have been demonstrated to be expressed in cardiac cells and the modulation of cardiac hypertrophy;[15] they have also been found on the membranes of blood platelets, serving a role in platelet aggregation.[16]

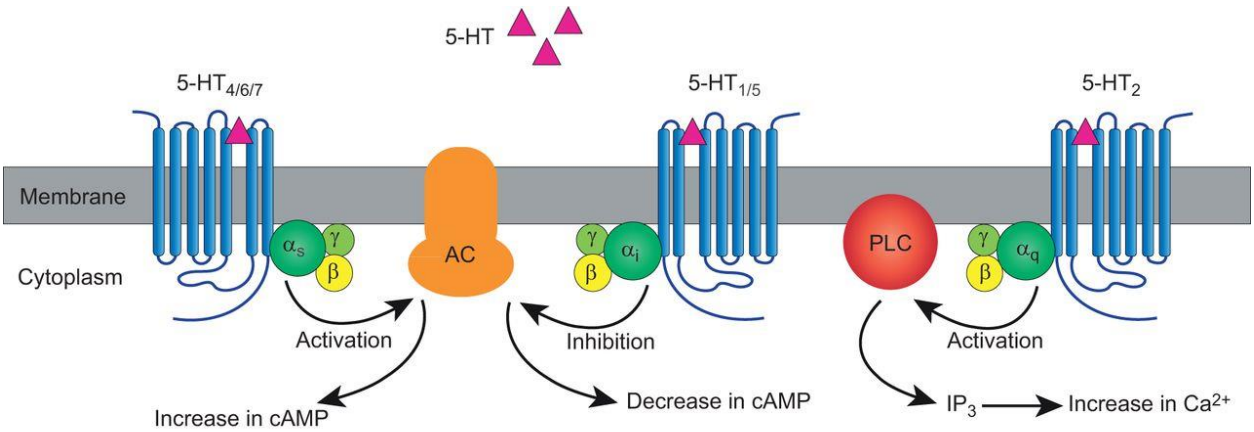

Figure 3. Schematic diagram of classification of serotonin receptors based on their functional selectivity.[17]

The 5-HT_{2B} receptor, although not called as such at the time, was one of the first serotonin receptors to be characterized pharmacologically when in 1957, it was found to facilitate contraction of the rat stomach fundus in response to serotonin.[18] Unlike 5-HT_{2A} receptors, 5-HT_{2B} receptors, originally designated 5-HT_{2F} receptors,[19] express very minimally in the central nervous

system (CNS) and more so in the human liver, lung, heart, and kidney (as elucidated by northern blot containing human RNA samples).[20] Immunohistochemical analysis of rat brain sections showed that relative to the other 5-HT_2 receptors, the few 5-HT_{2B} receptors expressed in the CNS display a distribution pattern indicating involvement in locomotion, food behavior, perception, and aversion.[21] In the lungs, activation of 5-HT_{2B} receptors with dexfenfluramine is shown to lead to pulmonary hypertension symptoms independent of a vasoconstriction method,[22] indicating its up-stream involvement in the regulation of proper lung arterial pressure. The most infamous involvement of 5-HT_{2B} receptors is in the heart, where they are involved in controlling proper morphology and function, an effect which will be discussed in greater detail below.

5-HT_{2C} receptors, initially labelled 5-HT_{1C}, are shown in rat brains to be expressed in highest abundance in the amygdala, choroid plexus, cortex, hippocampus, thalamus, subthalamus and in several neurons associated with motor functions.[23,24] This receptor is implicated in the regulation of anxiety[25] and inhibition of drug abuse potential,[26] both involving their activation. The latter effect is considered to be a result of the inhibition of dopamine release upon activation of 5-HT_{2C} receptors.[27] These receptors have also been implicated in regulating depression as shown by the initial anxiogenic effects of selective serotonin reuptake inhibitors (SSRIs) caused by 5-HT_{2C} activation during the first few weeks of administration, followed by the intended antidepressant effects coupled with a downregulation of 5-HT_{2C} receptors.[28] Lastly 5-HT_{2C} receptors are thought to be involved in the regulation of obesity. Antagonism of 5-HT_{2C} receptors increases food intake and weight gain,[29] while 5-HT_{2C} receptor agonists decrease food intake,[30] as seen with the previously-marketed weight-loss drug, fenfluramine.

B. Schizophrenia Hypotheses

1. Serotonin hypothesis of schizophrenia: The serotonin hypothesis of schizophrenia has its origins in the pharmacological research of hallucinogens, in particular LSD (**2**) (Figure 4). Due to the structural similarity between LSD and serotonin, in that they both contain an indolamine structural scaffold, and the similarity between the hallucinogenic effects of LSD and the psychotic symptoms of schizophrenia, research commenced into the possible relationship between serotonin and schizophrenia.[31] Studies showing that indoles antagonize the effects of serotonin, in particular LSD antagonizing the contraction of uterine smooth muscle in rats,[32] led researchers to initially believe that schizophrenia resulted from a reduction of serotonergic activity in the brain. This version of the serotonin hypothesis was amended, when numerous pharmacological studies were conducted revealing the similarities between the action of serotonin and LSD,[33,34] Specifically it was revealed that LSD produced contraction of oligodendroglia similar to that produced by serotonin, an effect that was not blocked by serotonin.[34] Moreover, LSD stimulates the hearts of clams and raises the blood pressure of anesthetized dogs, similar to serotonin.[33] The dissimilarities in the mouse behavioral effects between administration of LSD versus other antiserotonin agents were also noted.[34] The new hypothesis stated that the psychotic symptoms of schizophrenia were caused by an excess, as opposed to a deficit, of serotonergic activity in the brain. Soon after, researchers turned their interest to other hallucinogens, in particular mescaline which has a phenethylamine structural scaffold. It was revealed that mescaline produces a cross tolerance with LSD when administered to humans,[35] indicating that the two compounds with distinct structural scaffolds, could be behaving in a similar manner physiologically. Several years later in 1984, Glennon et al. revealed significant correlations between the 5-HT_{2A} binding affinities of a series of hallucinogens that included tryptamines and phenethylamines and their ED_{50} values in drug discrimination assays, as well as with their hallucinogenic potencies in humans.[36] It was later revealed that the schizophrenia-like effects

produced by psilocybin, an indoleamine hallucinogen, are blocked by the 5-HT_{2A} antagonist ketanserin and the atypical antipsychotic drug risperidone in humans,[37] further indicating a 5-HT_{2A} involvement in the hallucination symptoms of schizophrenia.

A more accurate model of serotonin's involvement in the pathogenesis and pathology of schizophrenia is excessive serotonergic activity in certain areas of the brain and diminished activity in others, as revealed by examination of postmortem human schizophrenic brains. In these studies, serotonin concentration was significantly lower in the hypothalamus, medulla oblongata, and hippocampus of schizophrenic brains compared with controls.[38] Another group reported increased levels of serotonin and its primary metabolite 5-hydroxyindoleacetic acid (5-HIAA) in the nucleus accumbens and globus pallidus in postmortem schizophrenic brains.[39] Therefore, it has been postulated that schizophrenia might be characterized as an "increase in 5-HT transmission in subcortical areas…and a decrease in cortical regions."[39] In support of this theory, several studies have reported a dysregulation in the density of 5-HT transporters and 5-HT_{2A} receptors in the prefrontal cortex of schizophrenic patients.[39]

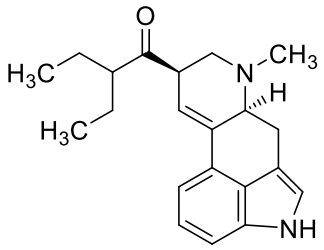

LSD (**2**)

Figure 4. Structure of LSD (**2**).

2. Dopamine hypothesis of schizophrenia: Interest into the relationship between dopamine and schizophrenia began when it was revealed that administration of typical antipsychotic drugs haloperidol and chlorpromazine resulted in accumulation of dopamine in mouse brain through inhibition of monoamine oxidase (MAO).[40] These results in combination with results of a previous study indicating that the tranquilizing effects of reserpine, a drug previously used to treat

psychosis,[41] can be reversed by administration of the dopamine precursor 3,4-dihydroxyphenylalanine,[42] provided the framework for the dopamine hypothesis of schizophrenia. Specifically, it was stated that excessive neurotransmission of dopamine might be one of the reasons for psychosis.[43] Further studies into the mechanistic relationship between dopamine and schizophrenia revealed a reduction of dopaminergic activity in the prefrontal cortex (where D_1 receptors are located) in schizophrenia patients[44] and an inverse relationship between prefrontal cortex and subcortex (where D_2 receptors are located) dopamine levels,[44–46] providing evidence for a link between schizophrenia and prefrontal hypodopaminergia and subcortical hyperdopaminergia. The original hypothesis was further revised to include a theory that negative symptoms of schizophrenia are correlated with the former and positive symptoms are correlated with the latter.[44] The pathophysiology of schizophrenia does not stop with the neurotransmission of dopamine as there is also evidence for dopamine neurons innervating and affecting the modulation of glutamatergic and GABAergic neurons.[47]

3. Glutamate hypothesis of schizophrenia: Studies utilizing the general anesthetic phencyclidine (PCP) that revealed similarities in the behavioral effects of PCP and the psychotic symptoms of schizophrenia[48] initiated the research into the possible link between glutamate neurotransmission and schizophrenia. PCP was thought to mimic psychotic symptoms more closely than LSD – the former producing more of the perceptual and cognitive deficits associated with schizophrenia while the latter producing more of the "secondary" effects such as visual and auditory hallucinatory events.[49] Moreover, PCP was shown to exacerbate and reinforce preexisting psychotic symptoms in schizophrenia patients and produced symptoms in acute schizophrenic patients.[49] PCP was first found to antagonize the excitatory effects of the NMDA channel (for which L-glutamate is the endogenous neurotransmitter) in the vertebrae of rats and cats.[50] Furthermore, it was found that PCP binds at a distinct site relative to L-glutamate, thus producing its antagonism through a noncompetitive manner.[51,52] Glutamate is known to be important for learning and memory,

processes that are dependent on glutamate's ability to induce hippocampal long-term potentiation (LTP) which is related to synaptic plasticity. Lastly, a specific subunit (NR2A) of NMDA receptors is downregulated in GABAergic neurons of schizophrenia brains and disruptions in the modulation of GABA have also been linked to schizophrenia.[53] Together, with the results of research with PCP and the physiological role of glutamate, it can be postulated that glutamate and its excitatory effects are crucial to maintaining healthy cognition and disruptions in its effects (antagonism) can produce behavioral effects similar to the psychotic symptoms of schizophrenia.

4. GABA hypothesis of schizophrenia: As opposed to glutamate, which is an excitatory neurotransmitter, gamma-aminobutyric acid (GABA) is the primary inhibitory neurotransmitter in the mature central nervous system, effecting its inhibition on pyramidal neurons located in the hippocampus, cerebellum, thalamus, and neocortex (based on GABA-A receptor channel isoform and $GABA_{B1}$/$GABA_{B2}$ receptor distribution),[54,55] all areas of the brain affected by schizophrenia. In contrast, GABA has been shown to act as an excitatory neurotransmitter in the developing brain.[56] Disruptions in both the excitatory and inhibitory neural transmission of glutamate have been implicated in the pathogenesis of schizophrenia.[57,58] GABA is synthesized in GABAergic presynaptic neurons where glutamate is decarboxylated by glutamic acid decarboxylase (GAD) to form GABA. It is then packaged into vesicles by the vesicular GABA transporter (VGAT) and is released into the synapse to bind at GABA receptors A and B upon depolarization of the membrane, after which its signal is terminated in part due to reuptake by the glutamate transporter (GAT).[58] It has been reported that mRNA of GAD67, the enzyme responsible for maintaining basal levels of GABA, is significantly reduced in layers 3, 4 and 5 of the prefrontal cortex but is largely unaffected in most GABAergic neurons in postmortem brains of schizophrenia patients.[59] This reduction of GAD67 levels is directly correlated with the reduction of the mRNA of parvalbumin,[60] an enzyme found in subsets of GABAergic neurons characterized by their high rate of firing action potentials, which might imply that the reduction in the levels of GAD67 mRNA is specific to a

subset of GABAergic neurons containing the enzyme parvalbumin.[61] There is also evidence for the reduction of GAT-1 mRNA levels,[62,63] a subset of GABA transporters that are responsible for the majority of GABA modulation, and also for the reduction of the α2 subunit of $GABA_A$ type receptor, a subunit found on a vast majority of pyramidal neurons synapsed by GABAergic neurons, in postmortem schizophrenia brains. This would suggest that the schizophrenia is associated with a reduction of GAT-1 and a subset of $GABA_A$ receptors and as a result of an increase in the level of GABA and inhibition of postsynaptic neurons. This is in contrast to the increased excitation that would result from a reduction GAD67 and therefore a reduction of GABA synthesis, suggesting that schizophrenia is characterized by hypofunction of both the excitatory and inhibitory pathways of GABA. Others have reported downregulation of several other $GABA_A$ receptor subunits including α1, α4, α5, γ2, and δ. These results illuminate the complex and multi-faceted relationship between GABAergic neurotransmission and schizophrenia.

C. Antipsychotic Drugs

Prior to the 1950s, treatment of schizophrenia was limited to crude methods such as electroconvulsive therapy, treatment with nonspecific sedatives such as morphine, opium, and codeine, physical restraint, and administration of insulin.[64,65] It wasn't until the discovery of chlorpromazine (**3**), a phenothiazine derivative originally used as part of a sedative concoction in surgery,[66] and reserpine (**4**) (Figure 5), originally used as a antihypertensive,[67] that research into the treatment of psychosis started to look promising. These discoveries spawned what is known as the "psychopharmacological revolution"[64] after both drugs were found to be efficacious in the alleviation of psychotic symptoms in schizophrenic patients through their tranquilizing effects and became widely used clinically.[67,68] Their use clinically encouraged researchers to investigate the pharmacological action of these drugs and they found a dopaminergic component to chlorpromazine[40] and a serotonergic component to reserpine.[69] Discovery of other antipsychotic drugs soon followed including haloperidol (**5**), thiothixene (**6**), thioridazine (**7**), and trifluoperazine

(**8**) (Figure 5), among others, which formed a class of drugs known as typical antipsychotic drugs along with chlorpromazine and reserpine.[66]

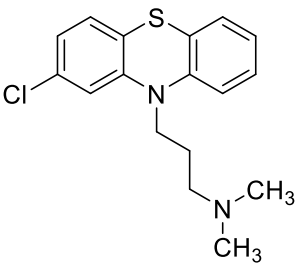

Chlorpromazine (**3**)

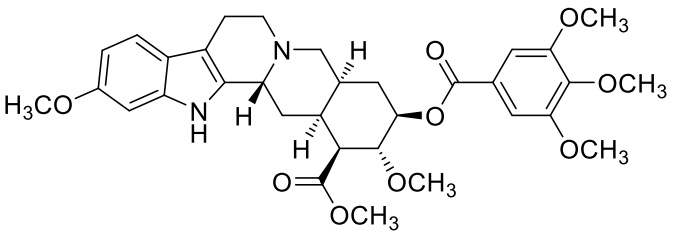

Reserpine (**4**)

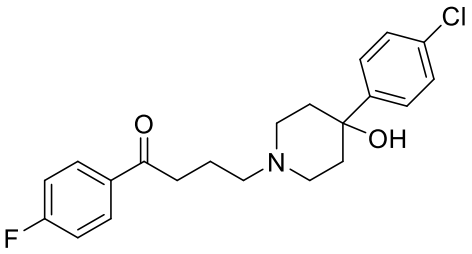

Haloperidol (**5**)

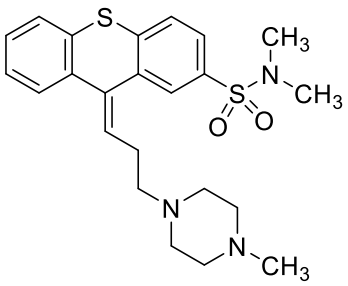

Thiothixene (**6**)

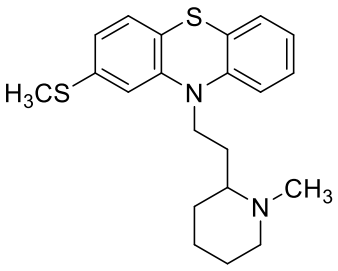

Thioridazine (**7**)

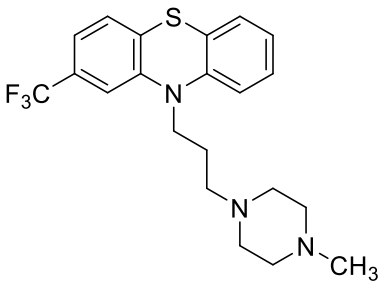

Trifluoperazine (**8**)

Figure 5. Structure of typical antipsychotic drugs chlorpromazine (**3**), reserpine (**4**), haloperidol (**5**), thiothixene (**6**), thioridazine (**7**), and trifluoperazine (**8**).

The problems with typical antipsychotic drugs are that they result in high incidences of extrapyramidal stimulation (EPS) symptoms related to primary antagonism of D_2 receptors,[70] such as Parkinsonism,[68] and that they fail to alleviate the negative symptoms of schizophrenia such as

apathy and lack of motivation.[65] In the 1970s, the dibenzodiazepine antipsychotic clozapine (**9**) (Figure 6) was discovered and was shown to be very effective clinically in treating schizophrenia, including the negative symptoms, and did not produce EPS symptoms. Drugs exhibiting these characteristics became known as atypical antipsychotic drugs, display 5-HT_{2A}/D_2 receptor antagonism,[70] and later included drugs discovered in the 1990s risperidone (**10**), olanzapine (**11**), sertindole (**12**), and quetiapine (**13**) (Figure 6).[66] The latter group of drugs were essential because they failed to produce the agranulocytosis side effects seen with clozapine administration[66]

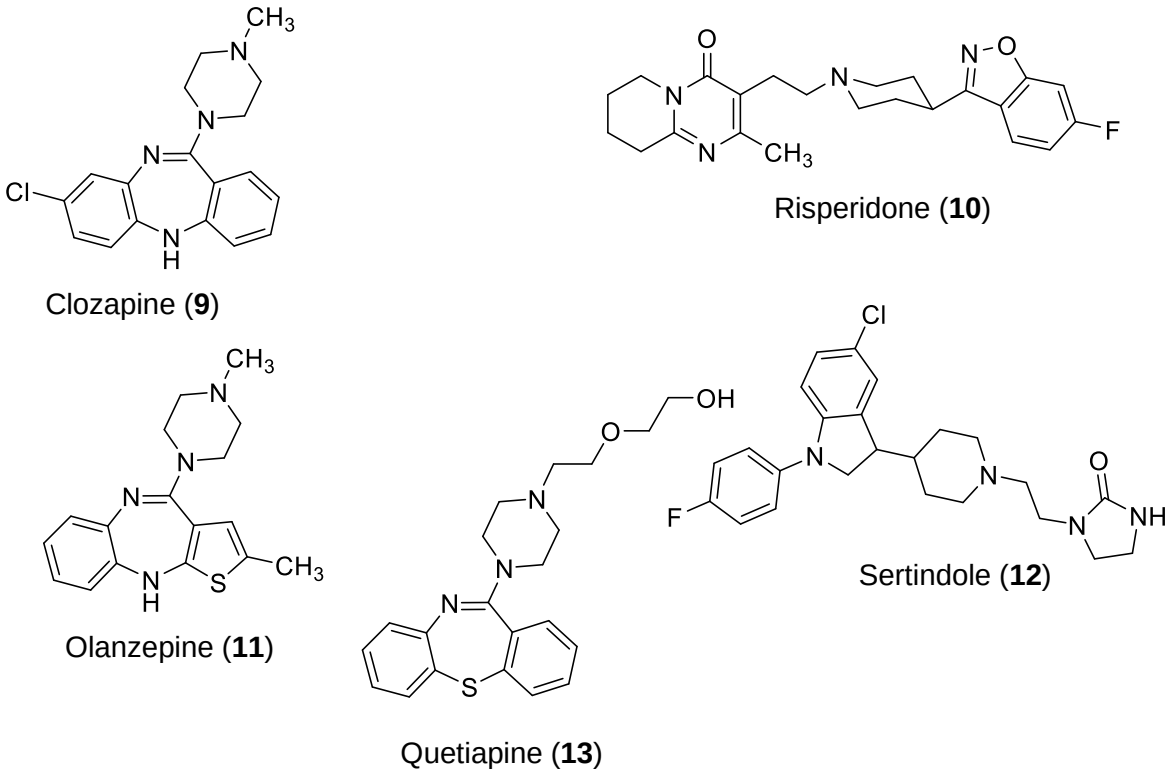

Figure 6. Structure of atypical antipsychotic drugs clozapine (**9**), risperidone (**10**), olanzepine (**11**), sertindole (**12**), quetiapine (**13**).

D. 5-HT_{2A} Receptor Antagonist Pharmacophore

Since the discovery of atypical antipsychotic drugs, numerous studies have been conducted in an attempt to understand the structure-activity-relationship (SAR) of these drugs[71–73] to further increase their efficacy and decrease their incidence of EPS. One particular area of interest is in the pharmacophoric evaluation of risperidone (**10**) (Figure 6) at 5-HT_{2A} receptors.[74–77] Risperidone was chosen for examination because it is used clinically and maintains a high affinity and potency at 5-HT_{2A} receptors (K_i = 5.29 nM and IC_{50} = 5.59 μM, respectively).[76] Our group has previously published results of a deconstruction study of risperidone in order to determine its minimal structural features necessary (pharmacophore) for antagonism of 5-HT_{2A} receptors.[76,77]

Developing a pharmacophore for a receptor is a highly illuminating method for rational drug design. This method usually involves the deconstruction step of the Deconstruction, Reconstruction, Elaboration (DRE) approach, first established by Glennon.[78] In this step, a molecule is stripped down to determine essential substituents for activity. In the reconstruction step, the molecular scaffold is synthesized containing only these essential substituents and omitting nonessential ones. In the elaboration approach, substituents are added to the molecule in a rational way (usually incorporating the Craig Plot or Topliss Tree methods) to optimize activity.[78]

5-HT_{2A} receptors were the focus in this study because a reduction of EPS symptoms of atypical antipsychotic drugs is correlated with greater 5-HT_{2A} activity and lower D_2 activity and so a greater understanding of the structural requirements for antagonism of 5-HT_{2A} receptors might aid researchers in developing more selective 5-HT_{2A} receptor antagonists, and thus safer antipsychotic drugs.

A typical pharmacophoric model for 5-HT_{2A} antagonism based on the structural requirements and distance investigations of 5-HT_{2A} ligands by various groups[79–82] is shown in Figure 7 (as summarized by Younkin et al.[76]) which consists of two aromatic centers separated by given distances from a basic nitrogen atom. The initial deconstruction of risperidone conducted by our laboratories revealed that the entire structure of risperidone is not required for antagonism at 5-HT_{2A} receptors, a result corroborated by the comparable antagonist actions of compounds **14** (K_i = 71.41 nM; IC_{50} ± 2.24 μM) and **15** (K_i = 12.27 nM; IC_{50} = 7.40 ± 1.45 μM) to that of risperidone. In particular, only one aromatic center might be required for antagonist activity.

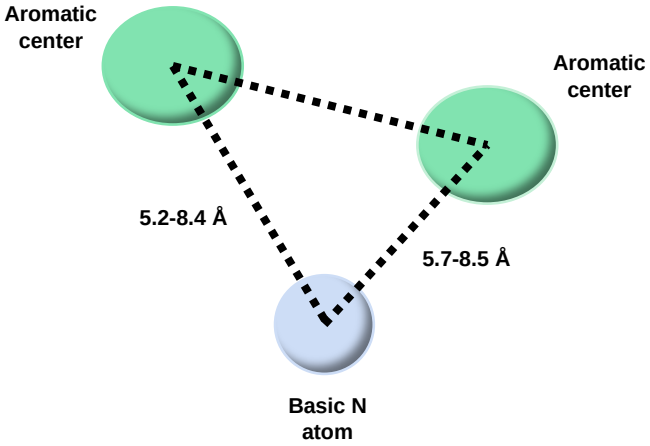

Figure 7. Composite of pharmacophoric model developed by various groups.[76]

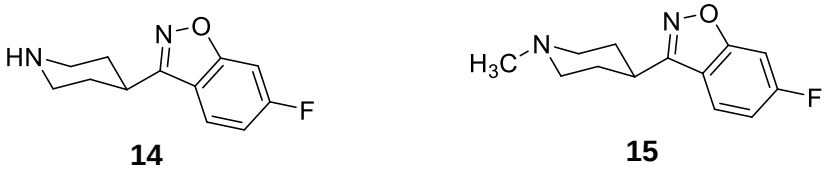

Figure 8. Structure of abbreviated compounds **14** and **15**.

In a more comprehensive deconstruction analysis of risperidone (**10**) and ketanserin (**16**) (Figure 9) by our group, Shah et al. examined several deconstructed analogues of risperidone (5.29 nM and 5.59 μM at 5-HT_{2A} receptors) and ketanserin (K_i = 15.5 nM, IC_{50} = 32.4 μM at 5-HT_{2A} receptors) as well as hybrid molecules of the two.[77] In this study, compound **14** was further

deconstructed by removing the 6-fluoro substituent on the benzisoxazole ring. The des-fluoro analog of **14** retained nanomolar affinity and micromolar potency (K_i = 271 nM and IC_{50} = 3.49 μM), showing that, although beneficial for activity, the 6-fluoro substituent is not essential. The results of this study were utilized to revise the existing pharmacophoric model for 5-HT_{2A} antagonism producing the model shown in Figure 10.

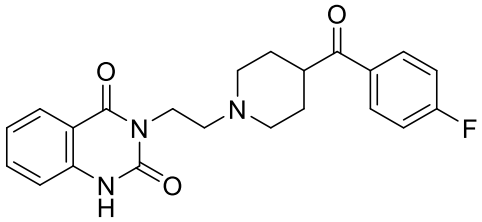

Ketanserin (**16**)

Figure 9. Structure of ketanserin.

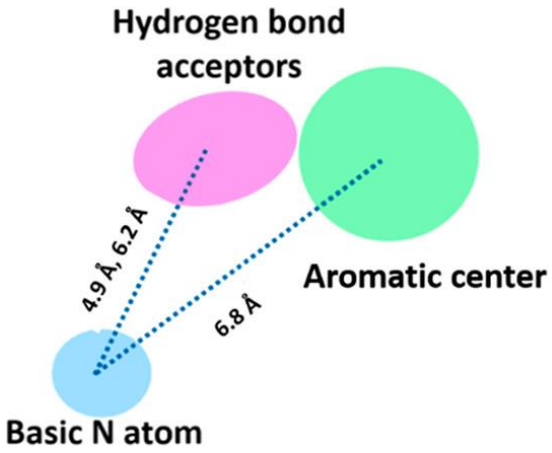

Figure 10. Revised pharmacophoric model for 5-HT_{2A} antagonism.[77]

In the initial deconstruction study, results indicated that only the “right half” portion (benzisoxazole/piperidine-containing portion) of risperidone (**10**) is necessary for antagonist action at 5-HT_{2A} receptors. This might suggest that the binding of this portion might be magnified by the presence of the “left half” portion (pyrimidinone-containing moiety). To test this hypothesis, two agents were developed in the new study containing either the right or left portions of

risperidone and the right or left portions of ketanserin. Agents containing only the left half portion of risperidone did not have appreciable affinity for 5-HT_{2A} receptors ($K_i \geq 5{,}000$). However building onto these agents by adding the right half portion of ketanserin (**16**) as seen in Figure 11 produces a compound (**17**) with greater affinity and potency than ketanserin (K_i = 3.02 nM and IC_{50} = 25.7 μM). The other hybrid compound containing the left half portion of ketanserin (**16**) and the right half portion of risperidone (**10**) (Figure 6) **18** displayed greater affinity and potency (K_i = 0.37 nM and IC_{50} = 0.7 μM) than either risperidone or ketanserin. It was also revealed that a tertiary amine is optimal for binding i.e. the piperidine nitrogen atom of risperidone. These results reveal multiple insights with regard to the structure-activity relationships of risperidone antagonism at 5-HT_{2A} receptors.

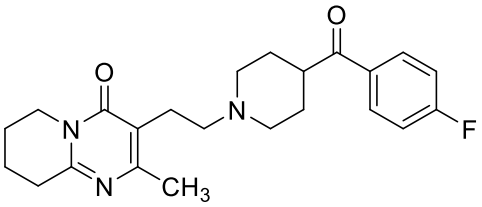

17

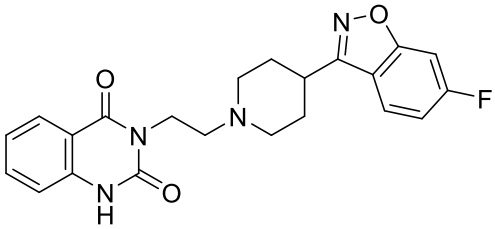

18

Figure 11. Structure of hybrid molecules with the “left half” portion of risperidone and the “right half” portion of ketanserin (**17**) and the “right half” portion of ketanserin and the “left half” portion of risperidone (**18**).

E. Significance of 5-HT_{2B} Receptors

Although 5-HT_{2B} receptors are generally considered to be anti-targets due to the prevalence of cardiac valvulopathic effects precipitated by their activation, the study of these receptors is still very crucial for drug development. Early studies reported that high levels of serotonin excreted into the blood stream by carcinoid tumors result in fibrosis of particular heart valves, supporting the role of serotonin in the modulation of cardiac function.[83,84] Additionally,

SSRIs are associated with abnormal heart function including arrhythmias, bradycardia, atrial fibrillation, and tachycardia.[85] Despite this, there is evidence for 5-HT_{2B} receptors being implicated in the therapeutic action of SSRIs with one group showing that the response of mice (i.e., mobility) in the forced swim test (FST) is absent in 5-$HT_{2B}^{-/-}$ mice[86] and later showing that these mice fail to respond to long-term administration of SSRIs in a novelty-suppressed feeding test.[87] However, focus has remained on the heart abnormalities that result upon activation of this receptor and 5-HT_{2B} receptors in particular have been linked to the shape and morphology of the heart, with one group reporting a reduction of ventricular mass in 5-HT_{2B} receptor mutant mice.[88] Furthermore, a later study reported that overexpression of 5-HT_{2B} receptors in the heart leads to cardiac hypertrophy in mice.[89] The research into the link between 5-HT_{2B} receptor activation and cardiac dysfunction has led those in the field to investigate the possible therapeutic uses of 5-HT_{2B} antagonists. One group demonstrated that administration of 5-HT_{2B} antagonists SB204741 and terguride diminishes induced right ventricle fibrosis following pulmonary artery banding (PAB) treatment in mice.[90]

Studies with fenfluramine (**19**) (Fen, Figure 12), a 5-HT_{2B} agonist, prompted extensive research into the relationship between 5-HT_{2B} receptors and cardiac abnormalities. Fen was initially prescribed as an anti-obesity drug in 1973, but was removed from the market in 1997 due to occurrences of cardiac disorders, specifically cardiac valvulopathy and pulmonary hypertension, in patients.[91,92] The cardiac valvulopathy associated with Fen has been characterized by thickening of the aortic, mitral, and tricuspid valves with plaque-like deposits along the leaflets and chordae tendineae, as well as regurgitation of blood through the valves.[92] These symptoms are similar to those seen in patients with carcinoid valve disease.[92] Fen and its metabolites act as both 5-HT_{2B} agonists and serotonin releasers at serotonin transporters (SERT).[93] However, the mitogenesis associated with the cardiac valvulopathic effect is thought to be precipitated by the downstream action of Gq-mediated activation and beta arrestin recruitment

rather than serotonin release;[94] in fact, Fen was actually found to decrease platelet and plasma levels in both humans and animals.[95–97] The popular street drug MDMA (or 3,4-methylenedioxymethamphetamine, also a 5-HT_{2B} receptor agonist), produces significant mitogenic changes in human heart valve interstitial cells and valvular regurgitation and morphological changes in patients.[98,99] Administration of other 5-HT_{2B} receptor agonists such as anti-Parkinsonism drugs, pergolide and cabergoline, induces cardiac valve regurgitation in patients.[100] These results provide further evidence for the association between the activation of 5-HT_{2B} receptors and the incidence of cardiac valvulopathy.

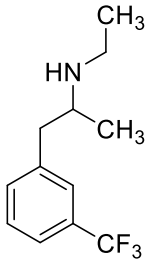

Fen (**19**)

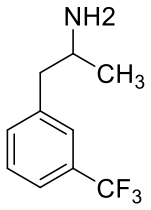

nFen (**20**)

Figure 12. Structure of fenfluramine (Fen; **19**) and its active metabolite norfenfluramine (nFen; **20**).

Despite its adverse cardiological effects, Fen is a very effective anorectic[101,102] shown to result from 5-HT_{2C} receptor activation,[103,104] and was very popular when available on the market (5 million US patients used prescription Fen between 1996-1998).[98] Fen has recently been reevaluated for the treatment of Dravet's syndrome and is currently in clinical trials. A low dose of Fen significantly diminished epilepsy-associated seizures, with patients experiencing freedom from seizures in as little as 3 days and a median reduction in seizure frequency of 80%.[105] The antiepileptic effect of Fen is thought to be precipitated through action at 5-HT_{1D}, 5-HT_{2A}, 5-HT_{2C}, and sigma-1 receptors.[105–108] Fen clearly has therapeutic potential and structural modification to abolish its affinity for 5-HT_{2B} receptors (and thus its adverse cardiac effects) can open the door to more effective treatment options without dangerous side effects.

Fenfluramine's most active N-deethylated metabolite is norfenfluramine (nFen, **20**) (Figure 12), which has much higher affinity and functional activity at 5-HT_{2B} receptors (Table 1). (±)nFen has an affinity of over 79-fold greater than that of (±)Fen, which also corresponds with almost two-fold greater V_{max} values of the isomers of nFen relative to those of Fen. This effect is also seen with regard to 5-HT_{2A} receptors at which fenfluramine/norfenfluramine and their metabolites posess greater affinity and functional activity. Considering the greater activity of nFen compared with Fen at 5-HT_{2B} receptors, it is believed that the majority of 5-HT_{2B} activation and thus induction of cardiac valvulopathy that occurs upon Fen administration is due to the action of nFen and not Fen.[93] Both nFen and Fen belong to a class of compounds known as phenylisopropylamines.

Table 1. Affinity K_i values and V_{max} values of the isomers of fenfluramine and its most active metabolite norfenfluramine.[109]

	5-HT_{2A} K_i [nM] (rat: [^{3}H]Ketanserin)	**5-HT_{2B} K_i [nM]** (human: [^{3}H]5-HT)	**5-HT_{2A} V_{max}** (% of 5-HT response; PI hydrolysis)	**5-HT_{2B} V_{max}** (% of 5-HT response; PI hydrolysis)
(±)Fen	5216	4134	15	ND
(+)Fen	11107	5099	ND	38
(-)Fen	5463	5713	43	47
(±)nFen	2316	52.1	ND	ND
(+)nFen	1516	11.2	88	73
(-)nFen	3841	47.8	93	71

F. Phenylisopropylamines

Phenylisopropylamines can have a broad range of activities from stimulant effects as seen with amphetamine[110] to hallucinogenic effects as seen with classical hallucinogens in the DOX series (Table 2),[111,112] to anorectic effects as seen with fenfluramine (**19**).[102] The Ar-C-C-N (aryl-carbon-carbon-nitrogen) moiety contained in the phenylisopropylamine scaffold is so common in a wide variety of drugs because they resemble neurotransmitters containing the same moiety (e.g. serotonin, dopamine, norepinephrine) with which they might share the same target proteins.[113] The simplest version of a related class of compounds is phenethylamine (Figure 13) (**43**) which has no substituents on its phenyl ring or its alkyl chain. Phenethylamine is not known to produce significant central stimulating effects upon administration; however, adding an α-methyl substituent, forming amphetamine (**42**) (Table 2) (a phenylisopropylamine), adds a central stimulant component to the drug.[113] With regard to phenylisopropylamine hallucinogens, mescaline is the prototypical phenethylamine compound.[114] Modification of its structure by addition of an α-methyl substituent results in the phenylisopropylamine trimethoxyamphetamine (TMA; **38**) (Table 2). Shulgin, later, after investigating a series of substitution patterns of TMA, concluded that the 2,4,5-methoxy substitution pattern was optimal in terms of hallucinogenic activity as seen with TMA-2 (**27**) (Table 2).[112] It should be noted that although the α-methyl substituent distinguishes phenethylamines from phenylisopropylamines, the α-methyl does not seem to improve the affinity[101] or efficacy[115] at 5-HT_{2A} receptors in vitro. However, an improvement is seen in the ED_{50} values of phenylisopropylamines vs. phenethylamines in drug discrimination assays as represented by the lower ED_{50} value of DOM (**25**) (ED_{50} = 1.8 μmol/kg) than of its des-α-methyl counterpart 2C-D (**44**) (Figure 13) (ED_{50} = 5.6 μmol/kg). One reason for this effect is that the α-methyl substituent may be adding lipophilic character to the compound and thus is able to cross the blood-brain barrier (BBB) more effectively to exert its central effects.

Table 2. Selected examples of the DOX series of phenylisopropylamines.

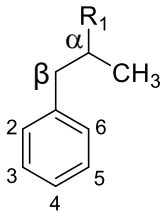

Compound	Name	R_1	R_2	R_3	R_4	R_5	R_6
21	DOF	NH_2	OCH_3	H	F	OCH_3	H
22	DOB	NH_2	OCH_3	H	B	OCH_3	H
23	DOI	NH_2	OCH_3	H	I	OCH_3	H
24	DOC	NH_2	OCH_3	H	Cl	OCH_3	H
25	DOM	NH_2	OCH_3	H	CH_3	OCH_3	H
26	2,5-DMA	NH_2	OCH_3	H	H	OCH_3	H
27	TMA-2	NH_2	OCH_3	H	OCH_3	OCH_3	H
28	MEM	NH_2	OCH_3	H	OCH_2CH_3	OCH_3	H
29	DOAc	NH_2	OCH_3	H	$COCH_3$	OCH_3	H
30	DON	NH_2	OCH_3	H	NO_2	OCH_3	H
31	DOCN	NH_2	OCH_3	H	CN	OCH_3	H
32	DOPR	NH_2	OCH_3	H	Propyl	OCH_3	H
33	DOHx	NH_2	OCH_3	H	Hexyl	OCH_3	H
34	DOTB	NH_2	OCH_3	H	*t*-Butyl	OCH_3	H
35	DOBz	NH_2	OCH_3	H	Benzyl	OCH_3	H
36	DOCT	NH_2	OCH_3	H	Octyl	OCH_3	H
37	DOPP	NH_2	OCH_3	H	3-(Phenyl)propyl	OCH_3	H
38	TMA	NH_2	H	OCH_3	OCH_3	OCH_3	H
39	M-154	$N(CH_3)_2$	OCH_3	H	Br	OCH_3	H
40	D-367	NH-C_3H_7	OCH_3	H	Br	OCH_3	H
41	QDOB	$N^+(CH_3)_3$	OCH_3	H	Br	OCH_3	H
42	Amphetamine	NH_2	H	H	H	H	H

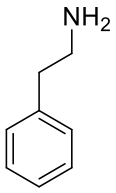

Phenethylamine (**43**)

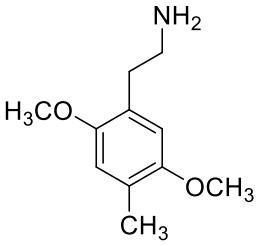

2-CD (**44**)

Figure 13. Structures of phenethylamine (**43**) and 2C-D (**44**).

Phenylisopropylamines have chiral centers at the α-carbon and the *R*(-) enantiomers are generally the most potent agonists at 5-HT_{2A} receptors (fenfluramine/norfenfluramine and metabolites being exceptions). Glennon et al. investigated the additions of hydroxy and methoxy substituents to the β position of 1-(4-bromo-2,5-dimethoxyphenyl)-2-aminopropane DOB (Table 2) (**22**), the brominated analogue in the DOX series of hallucinogens.[116] β-Hyroxylation and β-methoxylation, forming new chiral centers with the designation 1*R*,2*R* is well tolerated and produces compounds with similar affinities and efficacies as DOB at 5-HT_{2A} receptors. However, the 1*R*,2*R*, β-methoxylated compound is the only one that has a significantly higher potency as compared with DOB (almost 2-fold).

Greater interest in phenylisopropylamine hallucinogens prompted researchers to determine the ideal substitution of methoxy substituents with regard to affinity and efficacy. It was revealed that the 2,5-dimethoxy pattern is best tolerated.[117] Glennon et al. further reported that substitution of the 2-methoxy substituent with a 2-hydroxy substituent in DOM (Table 2) (**25**) produced similar behavioral responses in drug discrimination assays but this same tolerance was not seen with substitution of the 5-methoxy substituent.[117] In the same study, it was further revealed that removal of the 4-position methyl substituent followed by addition of a methyl substituent at the 3-position failed to produce the same behavioral responses as DOM, indicating that a substituent at the 4-position is necessary for hallucinogenic-like activity in animals. This effect is corroborated by the result that DOM displays ten times the potency of TMA-2 (**27**), also indicating that a hydrophobic substituent at the 4-position might improve the activity of this series.[118] Glennon et al. reported in a later study involving DOB that both the 2- and 5-position methoxy substituents are necessary for 5-HT_{2A} binding, and removal of the former results in complete abolishment of affinity.[119] Demethylation of the 2-methoxy substituent results in a 3-fold reduction in 5-HT_{2A} affinity. Alkylation of the terminal nitrogen via addition of a propyl substituent

drastically reduced affinity by about 30-fold, indicating that alkyl substituents on the terminal amine are not very well tolerated.[119]

As mentioned earlier, hydrophobic substituents at the 4-position of phenylisopropylamines seem to be beneficial for activating 5-HT_{2A} receptors. Glennon and coworkers[118] examined a series of analogues with variation of substituents at the 4-position of 2,5-DMA (**26**) (Table 2) with polar and hydrophobic substituents and found that polar substituents dramatically reduced the affinity at 5-HT_{2A} receptors with carboxy, hydroxy, and amino substituents displaying the lowest affinity (K_i > 25,000 nM). Lipophilic substituents on the other hand (alkyl or branched alkyl groups) were very well tolerated. Halogen substitution showed that the bromo substituent is the most favorable (K_i = 41 nM), followed by the chloro substituent (K_i = 218 nM), followed by the fluoro substituent (K_i = 1100 nM). Furthermore, two of the high affinity ligands (4-*t*-Bu and 4-pentyl analogs) were found not to generalize to DOM in drug discrimination and so were suspected of being antagonists. Four compounds, 4-hexyl (i.e., **33**) (DOHx), 4-benzyl (i.e., **35**) (DOBz), 4-octyl (i.e., **36**) (DOCT), and 4-[3-(phenyl)propyl] (i.e., **37**) (DOPP) (Table 2) analogues, were evaluated in an isolated tissue assay in rat thoracic aorta to test for agonist activity and all four were found to be antagonists.[118] This result raised the possibility of producing 5-HT_{2A} antagonists by the addition of bulk at the 4-position of phenylisopropylamines.

Although much research has involved developing structure-activity-relationships (SAR) of phenylisopropylamines, much more data are needed to fully characterize this class of compounds. For example, although there are numerous reports for the 5-HT_{2A} affinity data for this class, their functional activity at 5-HT_{2A} receptors has been limited to a relatively few compounds, e.g., DOI, DOB, DOM, DON, 2,5-DMA, and TMA.[120–122] Glennon, et al. has also conducted PI hydrolysis studies and provided intrinsic efficacy values for a series of DOX analogues and positional isomers of TMA.[123] A comprehensive affinity analysis for a series of DOX compounds

at 5-HT_{2A} and 5-HT_{2B} receptors has been conducted by Nelson et al.[111] but a greater degree of functional data at these receptors, especially 5-HT_{2B}, is still needed for these analogues.

Table 3. Affinity values of a series of DOX compounds at 5-HT_{2A} and 5-HT_{2B} receptors.[111]

Compound	Name	5-HT_{2A} K_i[nM] [^{125}I]DOI	5-HT_{2B} K_i[nM] [^{3}H]5-HT
21	DOF	41.7	227
22	DOB	0.6	26.9
23	DOI	0.7	20.0
24	DOC	1.4	31.8
26	2,5-DMA	211	1039
27	TMA-2	57.9	307
28	MEM	73.0	763
29	DOAc	80.5	313
30	DON	5.5	166
31	DOCN	45.7	774
32	DOPR	0.9	54.4
33	DOHx	0.1	30.3
34	DOTB	3.7	24.6
35	DOBz	0.4	35.0
39	M-154	94.2	341
40	D-367	88.5	521
41	QDOB	2155	>10,000

G. Quipazine

Quipazine (**45**) (Figure 14) is considered to be an enigmatic 5-HT_{2A} receptor agonist because it does not share the structural scaffold common to classical hallucinogens such as the tryptamine, phenethylamine, or ergoline scaffolds and instead contains an arylpiperazine scaffold. Despite this, quipazine binds at 5-HT_2 receptors and produces behavioral effects in drug discrimination[124] and head-twitch response (HTR)[125] assays similar to those of classical

hallucinogens, However, it is unknown if quipazine is hallucinogenic because human data are limited to anecdotal evidence.[126]

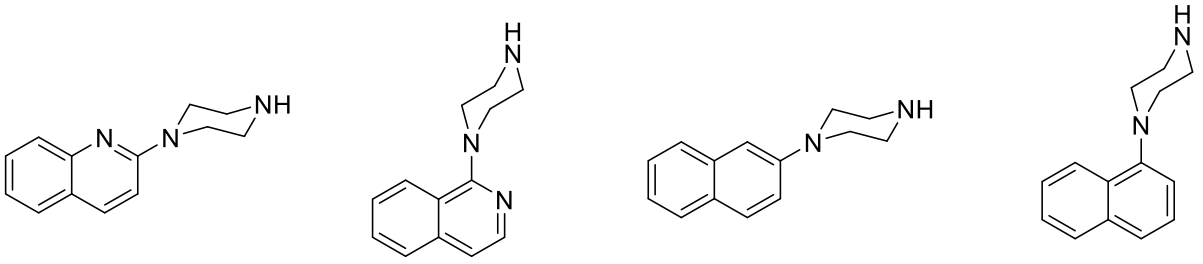

Quipazine (**45**) Isoquipazine (**46**) 2-NP (**47**) 1-NP (**48**)

Figure 14. Structures of quipazine (**45**) and its structural analogues isoquipazine (**46**), 2-NP (**47**), and 1-NP (**48**).

Originally developed having antidepressant implications, quipazine was found to antagonize the sedative effects of reserpine and tetrabenazine (similar to the clinically used antidepressant imipramine) and inhibited the mouse-killing behavior of rats, effects that were thought to be indicators of potential antidepressant activity.[127] However, in the same study it was revealed that quipazine had no effect on the inhibition of monoamine oxidase (MAO) nor on the uptake of norepinephrine or serotonin, which were known to be the mechanisms of antidepressants until that point. Subsequent studies with quipazine in drug discrimination assays revealed that quipazine can generalize to the response of LSD in rats trained to discriminate LSD from saline.[128] Similarly, rats trained to discriminate between quipazine and saline recognized the LSD cue, an effect that was blocked by 5-HT antagonists cyproheptadine, methysergide, and methiothepin but not dopamine antagonists fluphenazine and haloperidol.[129] Together these results indicated that, like LSD, quipazine might have a serotonergic component to its behavioral effects.

Other compounds in the same class (arylpiperazine) as quipazine are 1-(3-trifluoromethylphenyl)piperazine (TFMPP) (**49**) and its chloro analogue 1-(3-chlorophenyl)piperazine (mCPP) (**50**) (Figure 15), both of which are agonists at various serotonin receptors. Animals trained to recognize TFMPP in drug discrimination assays generalized to the mCPP cue. However, this effect is not seen with quipazine. Instead quipazine generalizes to DOM (and LSD as mentioned earlier), a compound with known 5-HT_{2A} receptor agonist activity, indicating that the action of quipazine is through 5-HT_{2A} receptors unlike TFMPP and mCPP.[124] The similarities of the effects of quipazine to hallucinogens such as LSD and DOM is understandable considering the similarities in their structural scaffolds: they all contain a protonatable nitrogen separated by an aliphatic chain to a substituted aromatic ring.

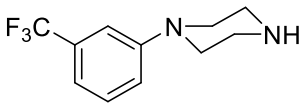

TFMPP (**49**)

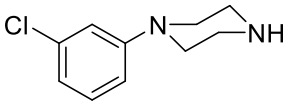

mCPP (**50**)

Figure 15. Structures of TFMPP (**49**) and mCPP (**50**).

Quipazine binds with nanomolar affinity at 5-HT_{2A} receptors as reported by multiple laboratories (Table 4). However, there are discrepancies in the binding affinity of quipazine which depend on the radioligand used in the assays. For example, quipazine binds with lower affinity at 5-HT_{2A} receptors labeled with the antagonist [^{3}H]-ketanserin, compared to when agonists [^{125}I]-DOI or [^{3}H]-DOB are used as radioligands (~4-26x lower). This is consistent with literature data showing that agonists such as 5-HT, DOI, and quipazine and partial agonist mCPP display higher affinities at 5-HT_{2A} receptors radiolabeled with [^{3}H]-DOB (~2-8x higher) than at 5-HT_{2A} receptors radiolabeled with [^{3}H]-ketanserin.[130] This same effect is not observed with antagonists spiperone, mesulergine, and ketanserin. Literature also shows that [^{3}H]-ketanserin binds to a much higher population of receptors than [^{125}I]-DOI in both brain tissue and HEK-293 cell preparations.[131,132]

Although binding assay calculations are conducted by accommodating for nonspecific binding, the higher amount of agonist needed to displace [^{3}H]-ketanserin at a higher population of 5-HT$_{2A}$ receptors might factor in to the higher affinity of agonists at [^{3}H]-DOB/[^{125}I]-DOI labeled 5-HT$_{2A}$ receptors than at [^{3}H]-ketanserin labeled receptors.

Table 4. Comparison of binding affinities of quipazine (**45**), 2-NP (**47**), isoquipazine (**46**), and 1-NP (**48**) at 5-HT$_{2A}$ receptors using radioligands [^{3}H]-ketanserin, [^{125}I]-DOI, and [^{3}H]-DOB across human, mouse, and rat species.

	Quipazine K_i [nM]	2-NP K_i [nM]	Isoquipazine K_i [nM]	1-NP K_i [nM]
[^{3}H]-Ketanserin, h5-HT$_{2A}$	5129[125]	710[125]	3,800[125]	98[125]
[^{3}H]-Ketanserin, m5-HT$_{2A}$	2506[125]	NA[b]	NA	NA
[^{3}H]-Ketanserin, h5-HT$_{2A}$	362[133]	NA	NA	NA
[^{3}H]-Ketanserin, r5-HT$_{2A}$	230[124] 447*[124,134–139]	70[124]	NA	18[124]
[^{125}I]-DOI, h5-HT$_{2A}$	129[132]	NA	NA	NA
[^{125}I]-DOI, h5-HT$_{2A}$	5[131]	NA	NA	NA
[^{3}H]-DOB, h5-HT$_{2A}$	59[133]	NA	NA	NA
[^{3}H]-DOB, r5-HT$_{2A}$	17[135] 25[139]	NA	NA	NA

*Average data collected from PDSP K_i database. [b]NA = unavailable; not reported.

Very few SAR studies have been conducted on quipazine's action at 5-HT$_{2A}$ receptors. In one study by Glennon et al.[124] quipazine and its structurally related analogues including 1-NP (**46**) and 2-NP (**47**) (Figure 14) were assessed in radioligand binding and drug discrimination assays. 2-NP (K_i = 70 nM) displayed a higher affinity at 5-HT$_{2A}$ receptors than quipazine (K_i = 230) and achieved greater selectivity for 5-HT$_2$ over 5-HT$_1$ receptors. 1-NP displayed an even higher affinity for 5-HT$_{2A}$ receptors (K_i = 18 nM) but was not selective for 5-HT$_{2A}$. These results indicate that the quinoline nitrogen atom of quipazine is not necessary for activity and might even diminish its affinity for 5-HT$_{2A}$ receptors; this might be due to some electrostatic clash with amino acids in the binding site. Furthermore translocation of the piperazine ring from the 2-position to the 1-position

of the naphthalene ring of 2-NP (as seen in 1-NP) is more favorable for binding. In drug discrimination assays, animals were trained using either TFMPP or DOM as the stimulus drug. It was found that the DOM stimulus generalized to 2-NP but not to 1-NP and the TFMPP stimulus generalized to 1-NP but not to 2-NP;[124] 1-NP has been shown to be a 5-HT_{2A} receptor antagonist.[124,125] Several other compounds were also investigated to understand the SAR of quipazine. Through these compounds it was demonstrated that the 4-position nitrogen atom of quipazine (i.e., N_4) is essential and an 8-methoxy substituent on the quinoline ring of quipazine is tolerated with respect to binding at 5-HT_{2A} receptors.

Quipazine also displayed very high affinity (K_i = 1.5 nM)[140] and potent antagonism of 5-HT_3 receptors[141] and [^{3}H]quipazine was used to label 5-HT_3 recognition sites in rat cortical membranes.[142] 5-HT_3 receptor channels are implicated in the functioning of the gastrointestinal tract in actions such as release of gastrointestinal (GI) secretions, control of vomiting, peristalsis as well as in the modulation of GI disorders such as gastroesophageal reflux disease and irritable bowel syndrome. In the few anecdotal reports[126] of quipazine's effect in humans, patients reported GI disturbances, diarrhea, vomiting, and "low dose mescaline-like effects" and similar effects were seen in monkeys except they exhibited behavior as seen upon administration of LSD, indicating that the hallucinogenic effects were stronger in monkeys than in humans. These observations have raised questions regarding the hallucinogenic action of quipazine. Specifically, it has been proposed that a higher dose of quipazine might produce hallucinogenic experiences in humans if it were not for the accompanying higher incidences of GI disturbances. Thus, administration of an antiemetic such as ondansetron prior to quipazine might allow users to consume a high enough dose of quipazine to experience its hallucinogenic action.[126] Additionally, pretreatment with ondansetron significantly reduced the fecal count of mice given quipazine.[125] Furthermore, pretreatment with ondansetron in mice administered quipazine in the HTR assay had no significant effect on the HTR counts revealing that the behavioral effects of mice in the HTR assay

by quipazine is not linked with its agonism at 5-HT_3 receptors.[125] Regardless of these indications, published data from studies with human subjects consuming quipazine are required to definitively determine if or if not quipazine is indeed hallucinogenic.

III. Specific Aims and Rationale

5-HT_{2A} and 5-HT_{2B} serotonin receptors share high sequence identity (39.96% - UniProt Allignment Data), especially in their respective ligand binding sites and transmembrane regions (Figure 16). They both contain a highly conserved aspartic acid amino acid in transmembrane 3 (TM3), a residue that is conserved across all aminergic GPCRs.[143–145] This residue serves as an anchor point for ligands of 5-HT_{2A} and 5-HT_{2B} receptors by forming salt bridge interactions (i.e. ionic bonds) between its negatively charged oxygen atoms and the positively charged amines of ligands. Agonists of both receptors interact with specific residues that share similar positions in the binding site, specifically residues in TM5 and TM6.[146,147]

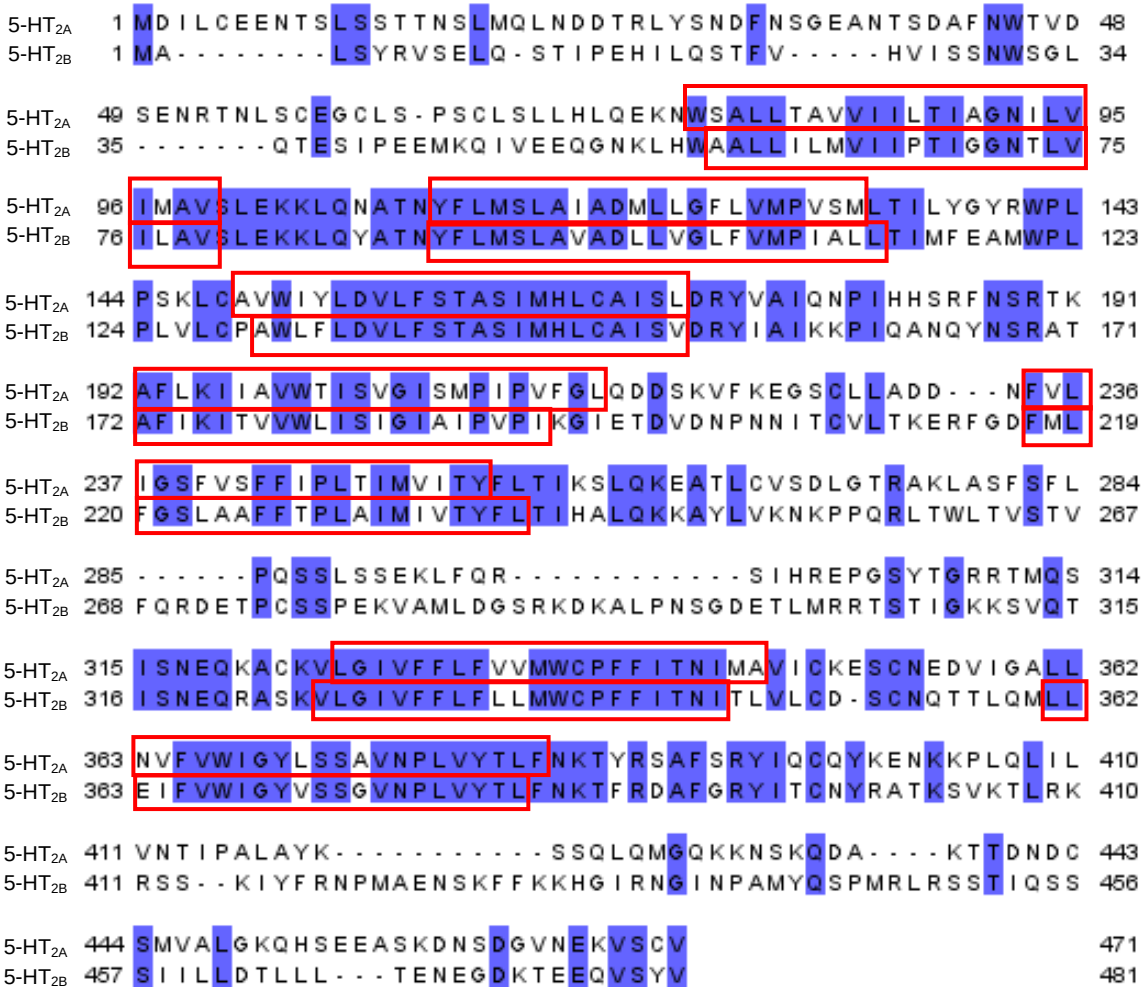

Figure 16. Sequence alignment of human 5-HT$_{2A}$ and 5-HT$_{2B}$ receptor sequences. Blue regions highlight sequence identity and red regions highlight transmembrane regions.

The similarities in the binding and activation of ligands binding at 5-HT$_{2A}$ and 5-HT$_{2B}$ receptors can be clearly elucidated by comparing bound crystal structures of the agonist LSD at both receptor subtypes, published by Roth and collegues while our investigation was in progress.[146–148] Their results indicated that LSD interacts with similar residues and only displays slight differences in the binding site of both receptors. These interactions include hydrophobic π stacking interactions with adjacent phenylalanine residues in TM6 (Phe339$^{6.51}$ and Phe340$^{6.52}$ in

5-HT_{2A} and Phe340$^{6.51}$ and Phe341$^{6.52}$ in 5-HT_{2B}). In TM5 LSD (**2**) hydrogen bonds with S242$^{5.46}$ in 5-HT_{2A} receptors. An analogous residue Ala225$^{5.46}$ at the same position in 5-HT_{2B} receptors was shown to be essential for agonism in studies with agonist methylergonovine.[146] Along with binding similarities, LSD displays similarities in its kinetic and pharmacological activity at 5-HT_{2A} and 5-HT_{2B} receptors. LSD displays relatively slow dissociation rates at both receptors (k_{off} = 0.003 ± 0.0005 min^{-1} and 0.022 ± 0.004 min^{-1}, respectively).[147,148] It has been proposed that this effect is caused by residues in extracellular loop 2 (EL2) forming a "lid" in the binding sites of both 5-HT_{2A} and 5-HT_{2B} receptors, preventing LSD from dissociating. Specific residues such as Ser242$^{5.46}$ and Leu229^{EL2} in 5-HT_{2A} and Leu209^{EL2} in 5-HT_{2B} have been implicated in the slow kinetics exhibited by LSD, as supported by mutagenesis studies. Additionally, LSD displays β-arrestin recruitment along with G-protein activation at both receptors. LSD's similarity in both binding and pharmacological activity at 5-HT_{2A} and 5-HT_{2B} receptors adds credence to the difficulty in separating activity at these receptor subtypes. This is the reason why pharmacological efforts are underway for developing pharmacophores for both receptors. Determining the minimum structural features necessary for activity at these receptors can assist in the design of more selective ligands.

Initial investigation into the pharmacophoric implications for 5-HT_{2A} functional activity was conducted by Höltje et al.[81] following Glennon et al.'s affinity SAR studies of a series of phenethylamine/phenylisopropylamine (discussed earlier) and indolalkylamine derivaties.[149] Höltje and co-workers revealed through conformational analysis using crystal structures of different isomers of phenylisopropylamines and indolalkylamines, that specific isomers might elicit more potency due to possible spatial accommodation limitations in the binding site for the α-alkyl substituent. The most important finding of this study was that a specific distance between the six-membered aromatic ring and the basic nitrogen (5.2 Å) is necessary for the agonist activities of the compounds examined. Since then, conformational analyses and computational modeling

such as CoMFA and 3D-QSAR conducted by several groups,[79,82,150–152] revealed structural overlap between agonists and antagonists as well as structural requirements for the binding of antagonists. These requirements include two aromatic center moieties separated by given distances from a basic nitrogen atom as summarized in Figure 7. Since these studies, Shah et al.[77] have refined this model using a sophisticated DRE approach and produced the pharmacophoric model seen in Figure 10. As mentioned in the background regarding the history of the development of antipsychotic drugs, EPS symptoms result from excessive D_2 receptor antagonism and so reducing the D_2 component (and increasing the 5-HT_{2A} antagonist component) has been the focus in the further development of atypical antipsychotic drugs. In the elaboration step of the DRE evaluation of risperidone, substituents can be added to the deconstructed pharmacophoric structure **14** to form new compounds. Determination of their activity across multiple receptor types, e.g., 5-HT_{2A-2C}, D_{1-5}, α_{1A}, and α_{1B} receptors, can reveal what structural features might confer selectivity for 5-HT_{2A} receptors. These receptors were chosen because atypical antipsychotic drugs have been hypothesized and/or shown to display activity at a variety of serotonin receptors, dopamine receptors, and adrenergic receptors.[153] These insights, in turn, can assist medicinal chemists in designing more effective therapeutics for schizophrenia (through improved, selective 5-HT_{2A} antagonism).

Pharmacophoric exploration of 5-HT_{2B} receptors has been much more limited than of 5-HT_{2A} receptors. Multiple researchers have performed SAR studies to produce selective antagonism at 5-HT_{2B} receptors[154–156] and one group has developed a broad antagonist pharmacophore model (Figure 17) consisting of lipophilic/aromatic centers and hydrogen bonding donor/acceptor moieties,[156] similar to the model produced for 5-HT_{2A} antagonism as seen in Figure 7. However, these studies failed to define one of the hallmarks of pharmacophoric analysis that is the minimum structural features necessary to elicit an effect. Instead high-throughput screening was used to determine hits and minor modifications were made to selected compounds

in order to develop selective and effective compounds, i.e., a thorough deconstruction analysis was not performed. The development of a selective antagonist for receptors is generally a less demanding method than developing selective agonists because of engagement of auxiliary binding sites not engaged by agonists. Because of this, antagonists can bind in a manner that is very specific to its receptor, thereby conferring high selectivity. This can also result in the loss of application of the pharmacophoric insights to antagonists with other scaffolds, as the insights might be specific to the evaluated class of compounds containing a unique scaffold. Research into the pharmacophoric requirements of 5-HT_{2B} agonism has been essentially nonexistent, although it could greatly expand on the methods to reduce 5-HT_{2B}-induced cardiac valvulopathy. Some groups, e.g. Roth and colleagues,[146] have attempted to determine specific structural features of ligands necessary for activation and functional selectivity using specific classes of compound such as ergolines. Several insights were made with respect to the activity of these compounds, however the same issue, as mentioned above, holds true in these studies: extensive deconstruction analyses were not performed to determine the minimal structural features necessary for producing activity.

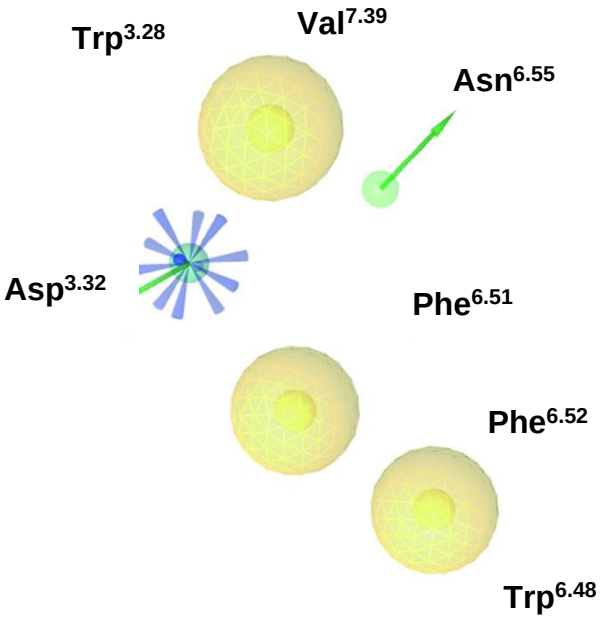

Figure 17. Broad 5-HT_{2B} antagonist pharmacophore consisting of hydrophobic regions (yellow), ionizable groups (blue), and hydrogen bond donors (green).[156]

Because of the high sequence homology between 5-HT_{2A} and 5-HT_{2B} receptors (60% in rats),[157] the binding affinities of the series of compounds in Table 3 show strong correlation between these receptors as seen in Figure 18. It would be interesting to conduct similar correlation analyses between functional activity and affinity for this series at 5-HT_{2A} receptors to test the capability of affinity to predict functional activity and vice versa. The same should be done with 5-HT_{2B} and additional correlations should be developed correlating the functional activity of compounds at 5-HT_{2A} receptors with their functional activity at 5-HT_{2B} receptors to determine which structural features are unique to the activation of 5-HT_{2B} receptors. This would aid in the development of a pharmacophore for agonism at 5-HT_{2B} receptors. Identification of a pharmacophore will reveal which specific ligand structural features to avoid to prevent 5-HT_{2B} activity, aiding in the development of more effective novel therapeutics which do not elicit cardiac valvulopathy.

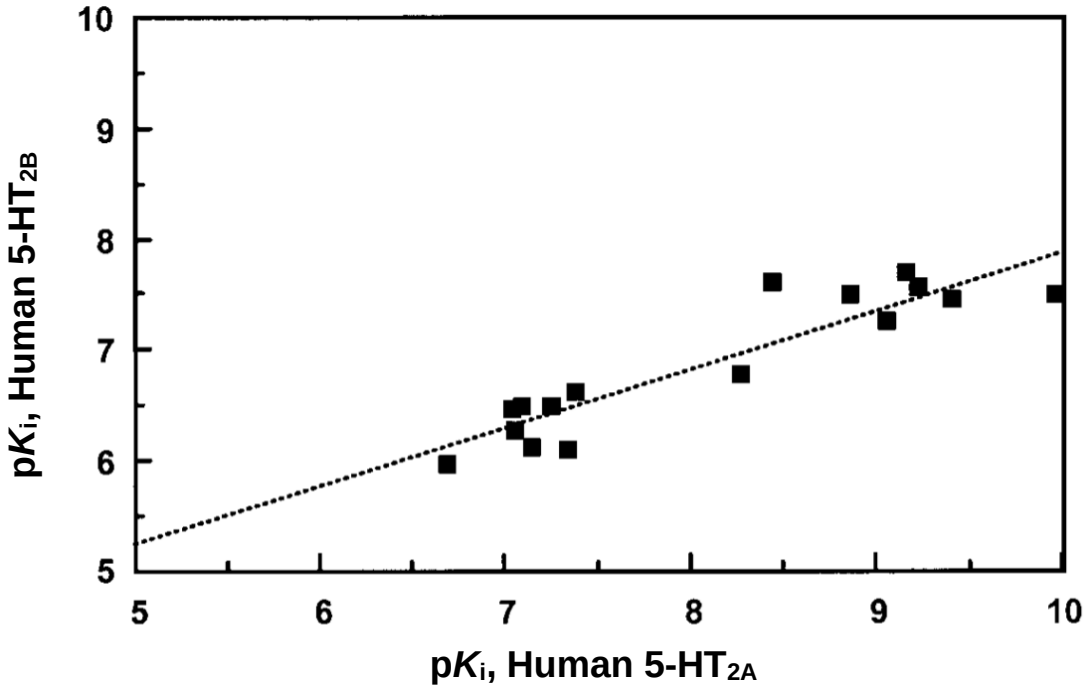

Figure 18. Correlation of DOX series compound binding data for compounds **21**-**40** (data taken from Table 3) between human 5-HT$_{2A}$ and 5-HT$_{2B}$ receptors. Slope = 0.937; r = 0.935; n = 16.[111]

Clearly the study of the pharmacophoric requirements of 5-HT$_{2A}$ and 5-HT$_{2B}$ receptor activity, specifically 5-HT$_{2A}$ antagonism and 5-HT$_{2B}$ agonism, has important therapeutic implications in schizophrenia and proper cardiac function, respectively. The goal of this project is to evaluate specific compounds that target these receptors such as 5-HT$_{2A}$ antagonists, e.g., analogues of risperidone, and certain quipazine analogues (1-NP, isoquipazine), and 5-HT$_{2B}$ agonists, e.g., DOX series of phenylisopropylamines to formulate or expand on existing pharmacophoric models.

The specific aims of this project are:

1. **Exploitation of a 5-HT$_{2A}$ receptor antagonist pharmacophore via affinity screening of compound 14 and elaboration of (i.e. adding specific substituents to) compound 14 in an attempt to delineate the structural features necessary for conferring 5-HT$_{2A}$ selectivity**

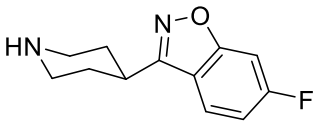

14

   a. Synthesis of **14** and analysis of affinity screening data of **14** across multiple receptors
   b. Synthesis of an analogue of **14** to determine lipophilic/bulk tolerance in 5-HT$_{2A}$ receptors through propylation of the piperidine nitrogen
   c. Affinity studies of the analogue(s) synthesized in b. and elucidation of binding requirements at 5-HT$_{2A}$ receptors

2. **In silico 3D molecular modeling studies of plausible quipazine (45) binding modes at 5-HT$_{2A}$ receptors**
   a. Docking studies of quipazine (**45**), isoquipazine (**46**), 2-NP (**47**), and 1-NP (**48**) at a crystal structure of the 5-HT$_{2A}$ receptor
   b. Hydropathic INTeraction (HINT) analysis of the identified poses in study 2a
   c. Comparison of the identified binding modes to crystal structures of known 5-HT$_{2A}$ ligand-protein complexes

3. **Development of a pharmacophore for 5-HT$_{2B}$ agonism**
   a. Molecular modeling of nFen (**20**) and DOB (**22**) at 5-HT$_{2A}$ receptors to aid in the design of specific analogues

b. Synthesis of new analogues of amphetamine (**42**) and DOB (**22**) on the basis of the above study

c. Functional studies of the synthesized analogues utilizing a calcium (Ca^{2+}) - release assay to determine potencies

d. Determination of agonist/antagonist properties of selected DOX phenylisopropylamine analogues in a Ca^{2+}-release assay

e. Formulation a pharmacophore for 5-HT_{2B} agonism based on acquired functional data

The conceptual relationship of these three studies is shown in Figure 19.

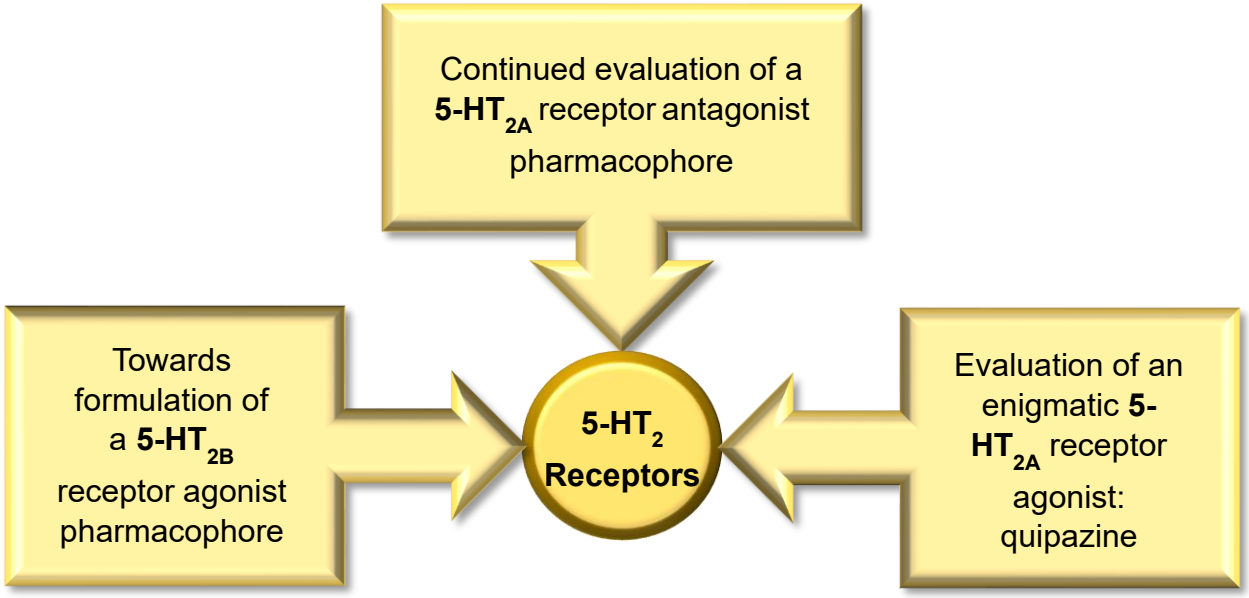

Figure 19. Relationship between the three specific aims of this investigation.

IV. Approach, Results and Discussion

A. Specific Aim 1: Exploitation of a 5-HT_{2A} receptor antagonist pharmacophore via affinity screening of compound 14 and elaboration of (i.e. adding specific substituents to) compound 14 in an attempt to delineate the structural features necessary for conferring 5-HT_{2A} selectivity

1. Approach

In the deconstruction/elaboration analysis study of risperidone conducted by our group,[76,77] it was revealed that a structure containing only the "left half" of risperidone does not bind to 5-HT_{2A} receptors whereas structures containing only the "right half" of risperidone, as seen with abbreviated analogues **14** (K_i = 71.41 nM and IC_{50} = 20.12 μM) and **15** (K_i = 12.27 nM and IC_{50} = 7.40 μM), retain both nanomolar affinity and micromolar potency at 5-HT_{2A} receptors, as compared to risperidone. This finding stresses the essential nature of the 6-fluoro-3-(4-piperidinyl)-1,2-benz[d]isoxazole moiety for the binding of risperidone. Other important findings were that a tertiary amine is optimal for binding as secondary amine-containing analogues displayed significantly lower affinity than their tertiary amine counterparts, and a 6-fluoro substituent while beneficial, is not essential for binding at 5-HT_{2A} receptors. These two findings are corroborated by similar results analyzing a series of truncated analogues of ketanserin.[158]

In the same study, to determine the structural requirements of the "left half" of risperidone, UHS-308 (**51**; Figure 20) was synthesized. UHS-308 is a truncated analogue of risperidone containing only half of the "left half" (i.e. the 2-methyl-6,7,8,9-tetrahydro-4H-pyrido[1,2-a]-pyrimidin-4-one) portion of risperidone. Specifically, the activity data of this compound at 5-HT_{2A} receptors determined if the entire "left half" portion of risperidone is necessary. It was revealed that UHS-308 displays higher affinity (K_i = 1.9 nM) and potency (IC_{50} = 5.44 nM) than risperidone, suggesting that although activity is lost with a structure containing solely the "left half" portion,

some portion of the “left half” contributes to 5-HT_{2A} receptor affinity and activity. Thus, these findings also suggest that the entire “left half” portion of risperidone is not necessary for activity.

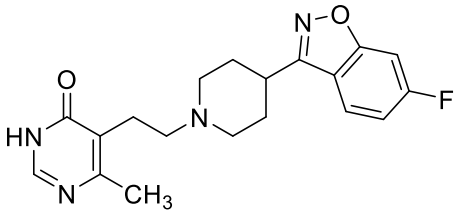

51

Figure 20. Structure of UHS-308 (**51**).

One avenue that was still yet to be explored regarded the bulk and lipophilic tolerance of the piperidinyl substituent. Thus far, it had been revealed that not all of the “left half” portion of risperidone is necessary (as in **51**) for activity and that substituting the “left half” of risperidone with the “left half” of ketanserin produces a compound (**18**, K_i = 0.37 nM and IC_{50} = 0.7 μM) with the highest affinity and potency out of all the analogues analyzed, including risperidone. However, both compounds **18** and **51** contain lipophilic elements, electronegative atoms, and 6-membered rings within their piperidinyl substituents and so at this point it was still too early to determine bulk and lipophilic tolerance of the “left half” of risperidone. Compound **15** which contains a methyl substituent on the piperidinyl nitrogen showed improvement in both affinity and potency (K_i = 12.27 nM; IC_{50} = 7.40 ± 1.45 μM) as compared to its des-methyl counterpart **14**. This indicates that alkyl substituents are well tolerated at the piperidinyl nitrogen and thus poses a question: what is the effect of extending the alkyl chain at the piperidinyl nitrogen on affinity for 5-HT_{2A} receptors?

To answer this, in the current study a series of analogues of compound **14** with piperidinyl alkyl substituents of various lengths and sizes were designed (Figure 21). Extending the alkyl chain to ethyl (i.e., **52**), propyl (i.e., **53**), and butyl (i.e., **54**) substituents would reveal what length of a purely lipophilic alkyl chain is tolerated and if at some length affinity is abolished. The benzyl

substituent of analogue **55** is the same length as the butyl substituent of **54** but differs in bulk due to the benzene ring and so **55** would be a further probe of bulk tolerance.

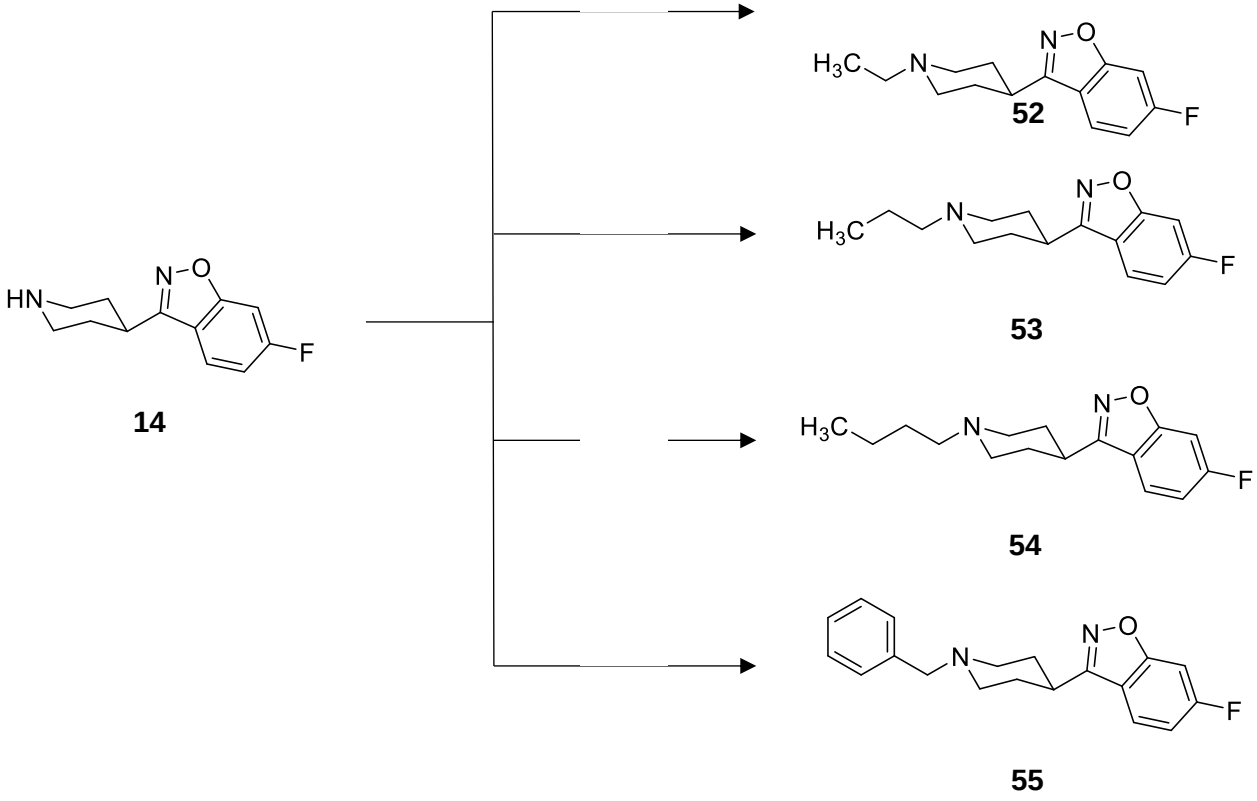

Figure 21. Proposed analogues of compound **14**.

2. Results and Discussion

a. Synthesis of 14 and analysis of affinity screening data across multiple receptors

Before initiating the synthesis of compounds **52**-**55**, compound **14** was synthesized in greater quantity for screening across various receptor types (5-HT_{2A-2C} receptors, D_{1-5} dopamine receptors, and $\alpha_{1A,1B}$ adrenergic receptors) along with its N-methyl counterpart **15**, hybrid analogues **17** and **18**, truncated analogue **51**, risperidone (**10**), and ketanserin (**16**). The synthetic scheme for compound **14** is outlined in Scheme 1.

Scheme 1. Synthesis of compound **14** and **53**.[a]

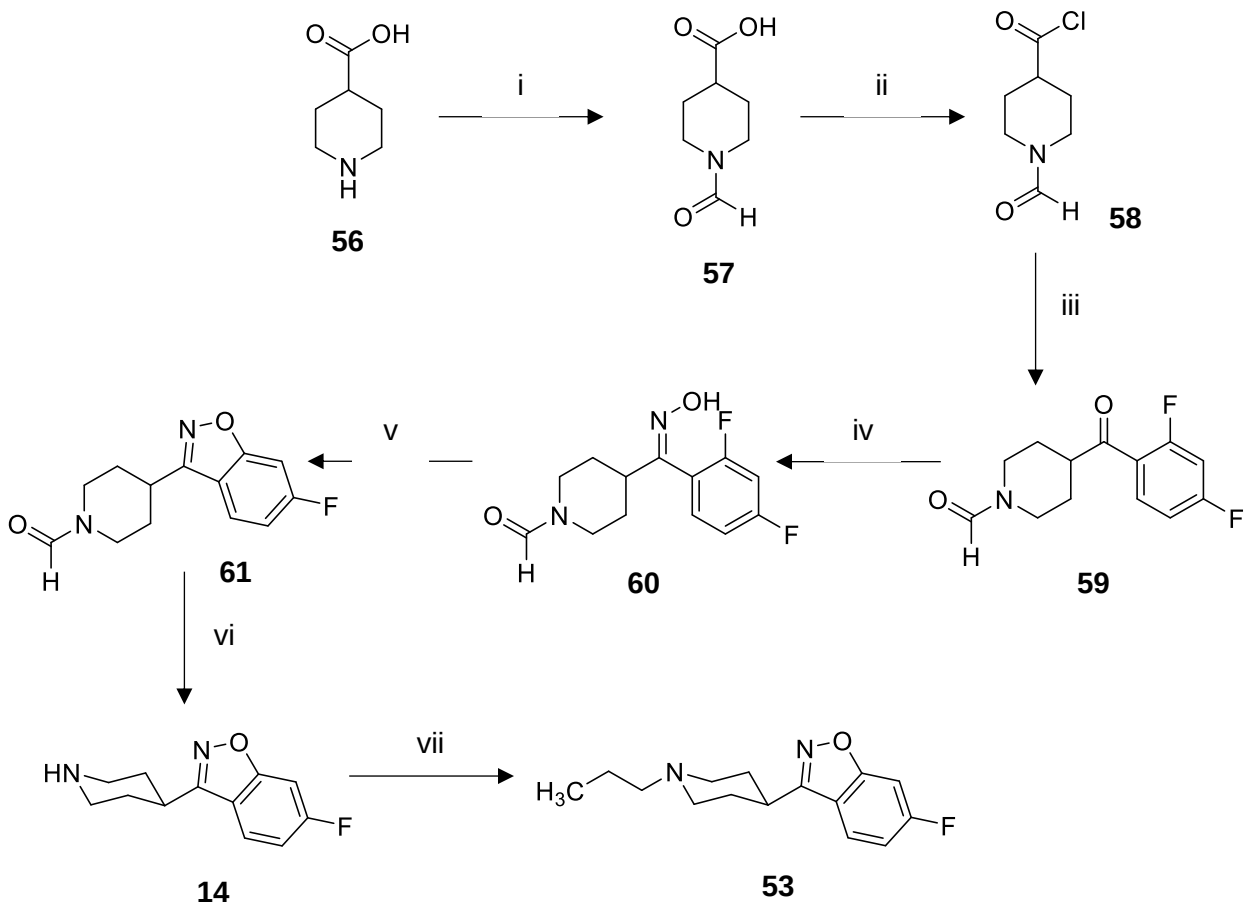

[a]Reagents and conditions: (i) Ac_2O/HCOOH, 60 °C, 1 h; (ii) $SOCl_2$/DMF, 3 h; (iii) 1,3-difluorobenzene, $AlCl_3$, reflux, 3 h; (iv) $H_2NOH{\cdot}HCl$/EtOH, NaOH/H_2O, reflux, overnight; (v) NaH/DMF, 75 °C, 4 h; (vi) conc. HCl/EtOH, reflux, 3 h; (vii) 1-iodopropane, K_2CO_3, acetonitrile.

Compound **14** was synthesized using a modified literature procedure.[159] Intermediate **57** was formed by protecting the amine of **56** using a formyl group donated by formic acid (HCOOH) to prevent the amine from forming bonds in subsequent reactions. This was a revised procedure as compared to that in the literature in that HCOOH and acetic anhydride (Ac_2O) were used as separate reagents instead of using acetic-formic anhydride as in the literature. Compound **57** was then treated with thionyl chloride ($SOCl_2$) to convert the carboxylic acid into an acid chloride. Careful attention was paid to not expose the reaction and products to air and moisture as this

resulted in the acid chloride hydrolyzing back into the carboxylic acid. This was done by utilizing a guard tube filled with calcium chloride ($CaCl_2$), flushing the reaction vessel with N_2 gas before and during the reaction, and quickly opening and closing any rubber septa or stoppers during additions and transfers of materials. Compound **58** was then coupled with 1,3-difluorobenzene using a Friedel-Crafts reaction resulting in the ketone **59**. Freshly sublimed aluminum chloride ($AlCl_3$) was used for this reaction, as using un-sublimed $AlCl_3$ resulted in multiple side products. Also, the reaction mixture was given enough time to cool to room temperature and was slowly added to water for quenching. Failure to do so resulted in the formation of a greyish, foam-like substance and decomposition of products. The carbonyl group of **59** was converted to an oxime using hydroxylamine hydrochloride ($H_2NOH{\cdot}HCl$) resulting in **60**. The crude solid formed in this reaction was dissolved in water, the recrystallization solvent; however, solid remained regardless of how much water was added. After removing the water under reduced pressure and redissolving the remaining solid, again solid remained. Melting point analysis indicated that this solid is a salt formed in the reaction, most likely NaCl, due to its very high melting point (>400 °C). Eventually, enough water was added to dissolve most of the crude solid and the remaining solid was removed using a spatula. Recrystallization using this method was successful and resulted in the formation of a solid in the form of small white crystals. This reaction did not produce a specific isomeric product so both the E and Z isomers of the oxime are formed, producing two stacked spots on TLC. However, during the ring closure reaction forming the benzisoxazole ring in **61**, only the Z isomer reacts, corresponding to one of the spots disappearing and the formation of a new spot (representing **61)**. The sodium hydride that was used for this reaction was dispersed 60% in mineral oil and so was washed in toluene prior to mixing with the other reagents. Finally, the formyl protecting group attached to the piperidine nitrogen in the first reaction was hydrolyzed and removed using hydrochloric acid (HCl), simultaneously forming the HCl salt, resulting in the target compound **14**.

The affinity data from the radioligand binding screen revealed information regarding the selectivity of compounds **14**, **15**, **17**, **18**, **51**, risperidone (**10**), and ketanserin (**16**) for 5-HT_{2A} receptors. The acquired data are shown in Table 5. The affinity data acquired for the compounds from the UNC-Chapel Hill Psychoactive Drug Screening Program at 5-HT_{2A} receptors corroborates the 5-HT_{2A} receptor radioligand binding results that we recently published.[77] Synthesized compound **14** displays nanomolar affinity (K_i = 39.1 nM) at 5-HT_{2A} receptors as expected. However, one new finding from this screen is that it also displays selectivity for 5-HT_{2A} receptors over the other receptor types analyzed. Closer analysis of the data reveals certain trends in affinity. For example, increasing the length and bulk of the piperidinyl substituent of compound **14**, as seen with compounds **15**, **51**, and **18**, results in greater 5-HT_{2A} receptor affinity (K_i = 10.6, 3.0, 0.62 nM, respectively) and greater selectivity for 5-HT_{2A} receptors over the "undesirable" receptors (5-HT_{2B}, $D_{1\text{-}4}$, and $\alpha_{1A,1B}$ adrenergic receptors). However, this same increase in the piperidinyl substituent size is correlated with an increase in D_2 receptor affinity (K_i = 1081, 374, 154 nM, respectively). Decreasing bulk of the piperidinyl nitrogen results in lower affinity for "undesirable" receptors but also results in a loss of selectivity for 5-HT_{2A} receptors.

Table 5. Radioligand binding screen of compounds risperidone (**10**), **14**, **15**, ketanserin (**16**), **17**, **18**, and **51** across multiple receptor types.[a]

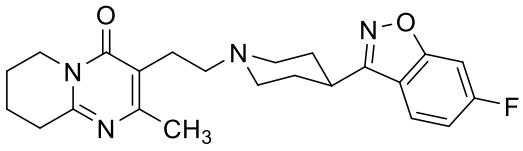

10

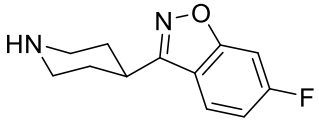

14

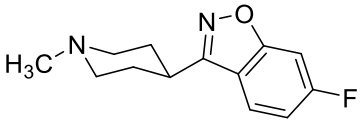

15

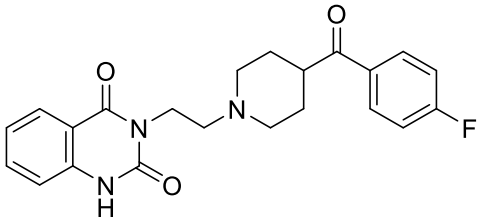

16

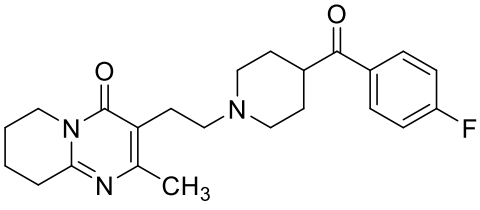

17

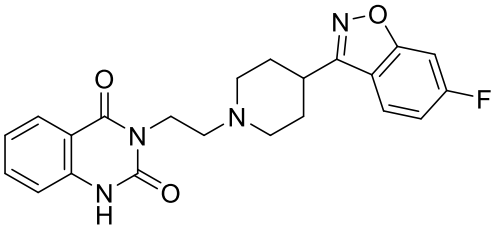

18

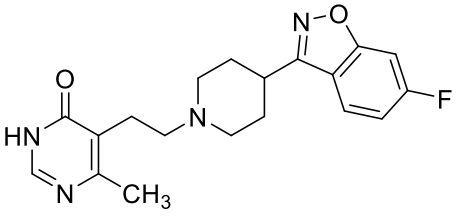

51

	Our 5-HT$_{2A}$ K_i[76,77] [^{3}H]-Ketanserin	5-HT$_{2A}$ K_i [^{3}H]-Ketanserin	5-HT$_{2B}$ K_i [^{3}H]-LSD	5-HT$_{2C}$ K_i [^{3}H]-Mesulergine	D$_1$ K_i [^{3}H]-SCH23390	D$_2$ K_i [^{3}H]-NMSP	D$_3$ K_i [^{3}H]-NMSP	D$_4$ K_i [^{3}H]-NMSP	D$_5$ K_i [^{3}H]-SCH23390	α_{1A} K_i [^{3}H]-Prazosin	α_{1B} K_i [^{3}H]-Prazosin
PH-072 (14)	71.41	39.1	736	>10,000	>10,000	2600	432	>10,000	>10,000	>10,000	1274
SAG-218 (15)	12.3	10.6	434	>10,000	141	1081	164	753	>10,000	465	295
UHS-308 (51)	1.9	3.0	99	>10,000	195	374	296	14	>10,000	44	28.3
UHS-025 (17)	3.9	2.9	30	>10,000	338	253	389	300	>10,000	240	510
SAG-136 (18)	0.37	0.62	67	>10,000	24	154	24	7.3	1177	5.4	5.5
Ketanserin (16)	15.5	2.17	372 ([^{3}H]-ketanserin)	88.1	327	>10,000 ([^{3}H]-YM 09151-2)	-	-	2.5	-	-
Risperidone (10)	5.3	0.29	41.6	11.1	249.4	4.35	9.55	18.6	289.5	5.0	9.0 ([^{125}]-HEAT)

K_i values reported in nM

[a]Highlighted regions indicate receptors of primary interest. (a) yellow represents 5-HT$_{2A}$ receptor affinity data acquired by us;[77] (b) peach represents 5-HT$_{2A}$ receptor affinity data acquired from the UNC-Chapel Hill Psychoactive Drug Screening Program (c) grey represents D$_2$ receptor affinity data acquired from the UNC-Chapel Hill Psychoactive Drug Screening Program.

b. Synthesis of an analogue of 14 to determine lipophilic/bulk tolerance in 5-HT_{2A} receptors through propylation of the piperidine nitrogen

Initially, we proposed to prepare and examine four N-substituted analogues of **14**, shown in Figure 21. As mentioned previously, antipsychotic-induced extrapyramidal stimulation is primarily precipitated by D_2 receptor antagonism. Therefore, one of the primary objectives of this study was to elaborate on the pharmacophoric requirements of 5-HT_{2A} antagonists necessary for achieving greater selectivity for 5-HT_{2A} receptors versus D_2 receptors, as well as low affinity for D_2 receptors. The results in Table 5 reveal that extension of the chain on the piperidinyl nitrogen results in greater affinity and selectivity for 5-HT_{2A} receptors, but also higher affinity for D_2 receptors. Furthermore, the N-propyl compound **53** has been reported to possess high affinity for D_2 receptors (K_i = 34 nM),[160] suggesting that extending the chain beyond the length of a propyl substituent might confer greater D_2 affinity – thus calling into question our original plan to probe the binding site of 5-HT_{2A} receptors by gradually extending the alkyl chain on the piperidinyl nitrogen. Therefore, it was our decision to change directions and forgo the synthesis of the N-ethyl (i.e., **52**), N-butyl (i.e., **54**), and N-benzyl (i.e. **55**) analogues.

Although the D_2 receptor affinity of **53** has been reported, its 5-HT_{2A} receptor affinity has not. The propyl chain of **53** might represent an intermediate substituent length (i.e. a “Goldilocks” length) in relation to the other analogues in Figure 21 and so its affinity at 5-HT_{2A} receptors might best elaborate the lipophilic and bulk requirements of the piperidinyl substituent. Hence, **53** was chosen to be synthesized and analyzed for 5-HT_{2A} receptor affinity in a radioligand binding assay using HEK293 cells stably expressing human 5-HT_{2A} receptors and [^{3}H]-ketanserin as the radioligand.

Compound **53** was synthesized using a standard alkylation reaction that proceeds through an S_N2 reaction mechanism as represented in Scheme 1. The nucleophilic nitrogen atom of the piperidine ring of **14** contains a lone pair of electrons which form a bond to the α carbon atom of

1-iodopropane, displacing the iodide atom. The purpose of the weak base K_2CO_3 is to trap the HI formed. Salt formation of the free base form of **53** was originally attempted by the dropwise addition of concentrated HCl in methanol (MeOH) directly onto the crude free base oil. However, this resulted in a black solution and TLC of the solution indicated that the free base had decomposed, resulting in numerous spots. This suggested that directly adding HCl/MeOH onto the free base is too harsh and exothermic, causing the breaking of bonds and fragment formation. Compound **53** was eventually successfully formed by dissolving its free base form in Et_2O and adding HCl/Et_2O in a dropwise manner into the solution, resulting in the formation of a white precipitate. This precipitate was initially purified using only MeOH as the recrystallization solvent, however, this resulted in a low yield of crystals. Using a two-solvent system of MeOH and Et_2O resulted in a much higher yield of precipitated crystals because of the nonpolar environment in the solution.

c. Affinity data for 53 and discussion of results

Compound **53** displayed a pK_i value of 6.97 ± 0.23 (or a K_i value of 107.3 nM) in our binding assay for 5-HT_{2A} receptors (Figure 22), relative to **15** (K_i = 12.3 nM) (Table 5).

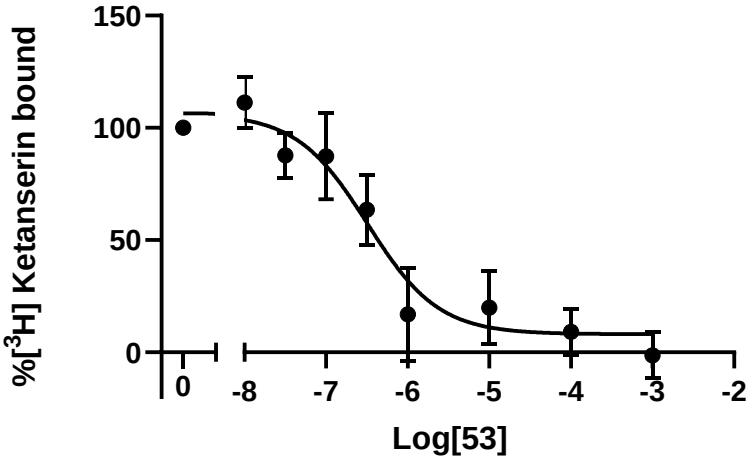

Figure 22. Saturation binding curve for **53**.

The affinity value for **53** (107.3 nM) was unexpected considering the trend of greater piperidinyl substituent length/bulk accompanied by greater affinity for 5-HT_{2A} receptors, as seen in Table 5. Adding a methyl substituent onto the piperidine nitrogen atom of **14** resulted in an increase in affinity from 71.4 nM to 12.3 nM for **15**. The next compound in Table 5, **51**, a compound that introduces a bulky aromatic ring in addition to greater piperidinyl substituent length, produced an affinity of 1.9 nM. Following this trend, one would expect a compound containing a piperidinyl substituent of intermediate length (i.e. **53**) to display an affinity higher than that of **15** but less than that of **51** (i.e. less than 12.3 but greater than 1.9 nM). Instead, we observed a jump to 107.3 nM upon increasing the chain length to a propyl chain as in **53**. This might be explained by there being a tolerance for length of simple alkyl chains on the piperidinyl nitrogen. Perhaps, only alkyl chain substituents shorter than propyl chains are well tolerated and any longer substituent requires an associated aromatic ring and/or heteroatoms as in **51**. This would be explained by phenylalanine or tyrosine residues forming π-π interactions with aromatic moieties in the molecule or hydrogen bonding between polar amino acids such as serine or threonine and heteroatoms. An alkyl chain substituent as long as a propyl chain might not make adequate interactions with these amino acids or may result in a steric clash with amino acids. To test this theory, the other compounds in Figure 21 (**52**, **54**, and **55**) can be synthesized and tested for their affinity for 5-HT_{2A} receptors. Affinity data of these compounds will reveal the limit of bulk tolerance of the region of the binding site occupied by alkyl chain substituents. With our affinity data for **53**, the most we can conclude is that a propyl chain is not well tolerated. However, the ethyl group may follow the trend in affinity mentioned above. Assuming that a three-carbon chain is the longest alkyl chain tolerated at the piperidine nitrogen atom, the N-butyl compound **54** should possess lower affinity than **53**. If an aromatic moiety contained within the substituent increases affinity via participation in π-π aromatic interactions, the N-benzyl compound **55** should have higher affinity as compared to **53** and **54**.

B. Specific Aim 2: In silico 3D molecular modeling studies of plausible quipazine (45) binding modes at 5-HT_{2A} receptors

1. Approach

Elucidation of the binding mode of quipazine (**45**) at 5-HT_{2A} receptors would be an important step toward the determination of its possible hallucinogenic activity. Due to quipazine's unique structural scaffold (as compared to other classical hallucinogens), its binding mode may represent a new way of eliciting hallucinogenic activity, via interactions with specific amino acids in the binding site of 5-HT_{2A} receptors that were never considered before. Hence, computational docking and analysis of quipazine could provide essential information. Aiding this effort, the bound crystal structures of hallucinogens 25CN-NBOH (PDB ID: 6WHA) and LSD (PDB ID: 6WGT) have been published. This allows for comparison of docked poses of quipazine to those of known hallucinogens and 5-HT_{2A} agonists, providing more evidence for, or lack thereof, of quipazine's unique manner of binding.

In this study quipazine and its isostere 2-NP (**47**), as well as its positional isomers isoquipazine (**46**) and 1-NP (**48**) were docked into the crystal structures of 5-HT_{2A} receptors. To corroborate our computational results, we obtained affinity and functional activity data for all four compounds (Table 6), from Dr. Maeso's laboratory.[125] The differences in the activity of these compounds are quite revealing. For example, comparison of the activities of quipazine and 2-NP, as well as isoquipazine and 1-NP reveals that the aromatic nitrogen atoms detract from both affinity and functional activity. Furthermore, translocating the piperazine substituent from the 2-position to the 1-position of the aromatic ring results in antagonism as seen with isoquipazine and 1-NP. Computational analyses including HINT analyses of these compounds might assist in explaining these trends in activity.

Table 6. Affinity, calcium mobilization, drug discrimination (DD), and heat twitch response (HTR) data for quipazine, 2-NP, isoquipazine, and 1-NP.

	5-HT$_{2A}$R Affinity K_i [nM][125]	**Ca^{2+} Mobilization K_i[nM][125]**	**DD ED_{50} [mg/kg][124]**	**HTR ED_{50} [mg/kg][125]**
Quipazine (45)	1995	EC_{50} = 7261	1.7	ED_{50} = 3.4
2-NP (47)	724	EC_{50} = 150	2.9	ED_{50} = 0.2
Isoquipazine (46)	3872	IC_{50} = 24,661	Not tested	Blocked quipazine
1-NP (48)	100	IC_{50} = 396	Blocked DOM	Blocked quipazine

To gain insight on how quipazine and its analogs might bind at 5-HT_{2A} receptors, we generated two models of the h5-HT_{2A} receptor-based X-ray crystal structures of the active state (PDB ID: 6WHA) and the inactive state (PDB ID: 6A94). Docking studies using the models and quipazine analogs were conducted to identify potential binding modes of the agonists and antagonists. Agonists, quipazine (**45**) and 2-NP (**47**), were docked to the active state model and antagonists, isoquipazine (**46**) and 1-NP (**48**), were docked to the inactive state model. A built-in clustering program was used to cluster the docked solutions with an RMSD cutoff of 0.75 Å. Both solutions in the most populated cluster and solutions in the highest scoring cluster were analyzed. Individual interactions were then analyzed using Hydropathic INTeractions (HINT) analysis.[161] HINT classifies and scores hydrophobic and polar interactions, collectively known as hydropathy, for each atom; the higher the score, the more favorable the interaction. The software utilizes experimental data from solvent partitioning experiments between water and 1-octanol ($LogP_{o/w}$) to determine HINT scores of interactions by assigning positive scores for favorable interactions

(hydrogen bonding, acid-base, and hydrophobic) and negative scores for unfavorable interactions (acid-acid, base-base, hydrophobic/polar).[161]

2. Results and Discussion

Docked solutions revealed two possible binding pockets occupied by the aromatic moieties of the compounds. Regardless of which binding pocket is utilized, all ligand-protein complexes formed a salt bridge between the $N_{4'}$ atom and conserved Asp155$^{3.32}$ within hydrogen bond (HB) distance (3.5 Å). The observed ionic, hydrophobic and polar interactions between ligands and protein are supported by HINT analysis (Table 7).

Table 7. GOLD and HINT interaction scores (total, hydrogen bonding, hydrophobic, acid/base) of quipazine (**45**), 2-NP (**47**), isoquipazine (**46**) and 1-NP (**48**) at 5-HT_{2A} receptors.

	Active		Inactive	
Score	**Quipazine**	**2-NP**	**Isoquipazine**	**1-NP**
GOLD	41	41	44	45
Total HINT	899	1496	1121	1454
Total H-Bond	818	1082	916	1009
Total Hydrophobic	239	501	479	649
Total Acid/Base	409	362	476	439

Examination of the various clusters as well as the HINT analysis of the compounds revealed their likely binding poses. Gold docking of quipazine and 2-NP at the active state receptor model revealed two primary clusters – one containing the highest scoring pose (in the binding pocket designated as the large principal pocket) and another containing the greatest population of solutions (in the binding pocket designated as the small sub-pocket). An analysis of the top scoring solution from each cluster is shown in Figure 23. Our selection of their probable pose was dependent on their individual interactions as elucidated by HINT. For example, HINT

revealed that the selected pose for 2-NP has a much higher total interaction score (1496) than quipazine (899). Furthermore, 2-NP has a significant hydrogen bond between the backbone oxygen atom of Ile152$^{3.29}$ and N_4, an interaction that is lacking in the quipazine docked solution. Quipazine has a moderate hydrogen bond score between Ser159$^{3.36}$ and N_1. Due to quipazine's possible proclivity for forming this reaction, it might forgo the numerous hydrophobic interactions as seen with 2-NP (forcing it to occupy a different binding site), supported by their total hydrophobic scores: 239 for quipazine and 501 for 2-NP. All these results are in accordance with the higher affinity of 2-NP as compared to that of quipazine.

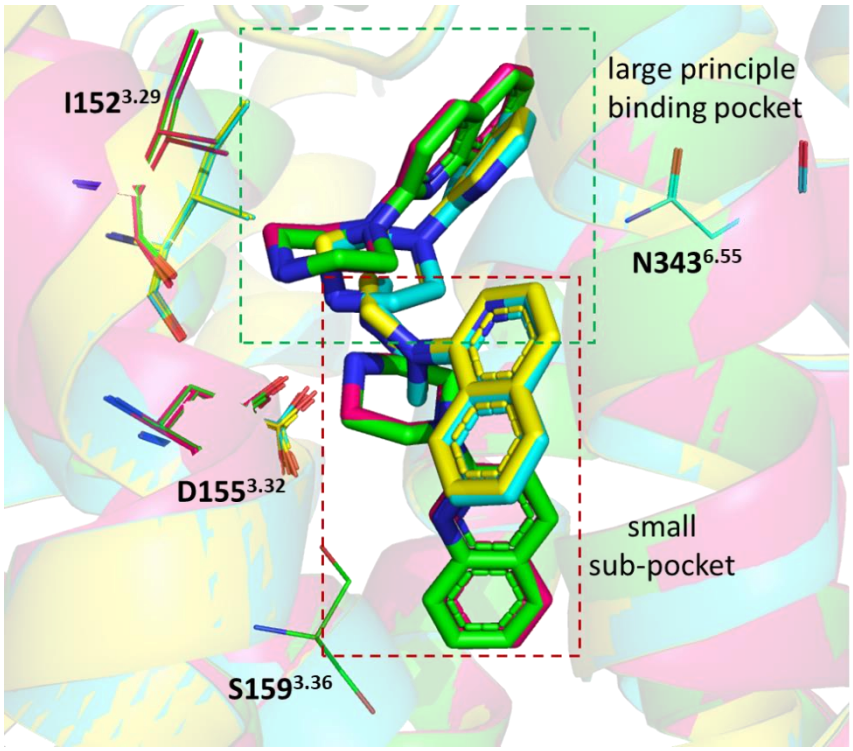

Figure 23. Top GOLD scoring solutions of quipazine (**45**) (capped sticks rendering; green carbon atoms), 2-NP (**47**) (capped sticks rendering; magenta carbon atoms), isoquipazine (**46**) (cyan carbon atoms), and 1-NP (**48**) (capped sticks rendering; yellow carbon atoms) in the binding site of their respective [i.e., active (PDB ID: 6WHA) or inactive (PDB ID: 6A94) state] 5-HT_{2A} receptor.

Gold docking of 1-NP and isoquipazine revealed two primary clusters – one containing the highest scoring pose (in the binding pocket designated as the large principal pocket) and another containing the greatest population of solutions (in the binding pocket designated as the small sub-pocket) (Figure 24). HINT analysis resulted in a higher total interaction score for the chosen pose of 1-NP (1454) than for the chosen pose of isoquipazine (1121). Inspection of individual interactions revealed an acid/base interaction between N_2 in isoquipazine and Asn343$^{6.55}$. This possible interaction might be the reason for isoqupazine occupying a different binding site compared to 1-NP. As a result, isoquipazine does not have as many hydrophobic interactions as 1-NP, supported by their total hydrophobic scores: 479 for isoquipazine and 649 for 1-NP. These results are in accordance with the higher affinity of 1-NP as compared to that of isoquipazine.

Analysis of the chosen complexes (Figure 24) revealed that the two compounds with the highest affinity (1-NP and 2-NP) faced the same binding pocket and participated in similar hydrophobic interactions – numerous interactions with Leu228^{ECL2} and Leu362$^{7.35}$. 1-NP additionally displayed hydrophobic interactions with Val235$^{5.39}$ and Val366$^{7.39}$. Quipazine and isoquipazine faced a different binding pocket, although the two molecules did not overlap. As a result, quipazine primarily displayed hydrophobic interactions with Gly369$^{7.42}$ and Val366$^{7.39}$ and isoquipazine displayed hydrophobic interactions with Val156$^{3.33}$ and Leu229^{ECL2}.

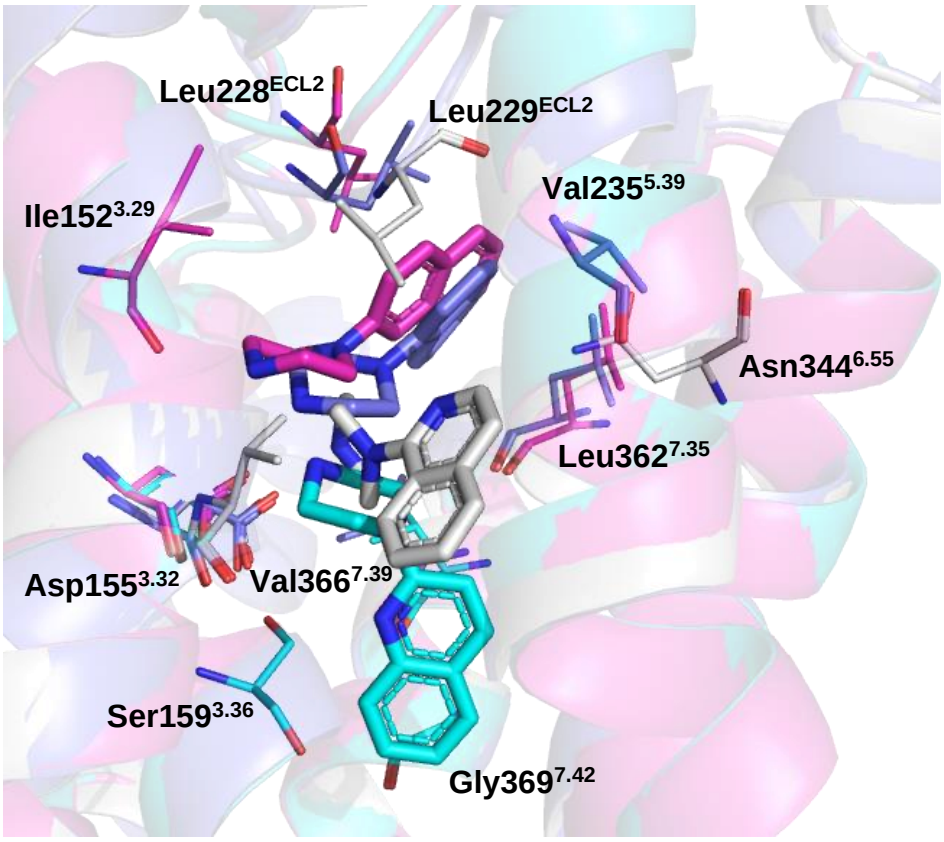

Figure 24. Binding modes of quipazine (**45**) (capped sticks rendering; cyan carbon atoms), 2-NP (**47**) (capped sticks rendering; magenta carbon atoms), isoquipazine (**46**) (white carbon atoms), and 1-NP (**48**) (capped sticks rendering; blue carbon atoms) in the binding site of the 5-HT_{2A} receptor using both the active (6WHA) and inactive (6A94) states of the receptor.

It appears that hydrophobic interactions predominate for the examined analogues to elicit binding at 5-HT_{2A}. This assertion is based on the simplicity (lack of substituents/hydrophobic nature) of the compounds along with the numerous hydrophobic interactions revealed by HINT analysis. Because 1-NP and 2-NP face a similar binding pocket, it can be suggested that compounds interacting with residues in this pocket possess the highest affinity. Furthermore $F339^{6.51}$, a residue that has been implicated in the binding of both agonists and antagonists,[162,163]

is shown to be in an edge-to-face position (4.0 - 4.6 Å) relative to the aromatic moieties of 1-NP and 2-NP (not shown by HINT analysis). Quipazine and isoquipazine, however, face away from this pocket and this might be the reason for their low affinity. These two compounds also have aromatic nitrogen atoms in their structures (which 1-NP and 2-NP lack); this suggests that heteroatoms within the aromatic ring structure of these analogues decrease their affinity and the greater the hydrophobic nature of the aromatic ring, the greater the affinity.

Our modeling results also revealed similarities in the binding of agonists quipazine and 2-NP and agonists/hallucinogens LSD and 25CN-NBOH. Similarities were also observed in the binding of antagonists isoquipazine and 1-NP and antagonist risperidone (Figure 25). The bound crystal structures of LSD (PDB ID: 6WGT), 25CN-NBOH (PDB ID: 6WHA), and risperidone (PDB ID: 6A93) have been published. The comparison of the binding modes of these ligands with the binding modes of quipazine and its analogues revealed that certain features of LSD, 25CN-NBOH, and risperidone might be essential for their binding and activity at 5-HT_{2A} receptors. Quipazine utilized amino acids common to the binding of 25CN-NBOH. Specifically the oxygen atom of the 2-hydroxy benzyl moiety of 25CN-NBOH and the nitrogen atom of the quinoline ring of quipazine participated in hydrogen bonding with $Ser159^{3.36}$. The two moieties also shared significant overlap in the binding pocket. Comparison of the binding of LSD and 2-NP revealed that the diethyl amide moiety of LSD and the naphthalene moiety of 2-NP occupy a similar region of the binding pocket indicating that they might participate in similar hydrophobic interactions. The antagonists isoquipazine and 1-NP share space with key features of the antagonist risperidone. For example, the naphthalene moiety of 1-NP shares a binding pocket occupied by the pyrimidinone moiety of risperidone. Isoquipazine on the other hand shares a distinct binding pocket occupied by the benzisoxazole moiety of risperidone. This observation is in accordance to findings previously published by our group[76,77] indicating that the entire structure of risperidone is not required for antagonism of 5-HT_{2A} receptors.

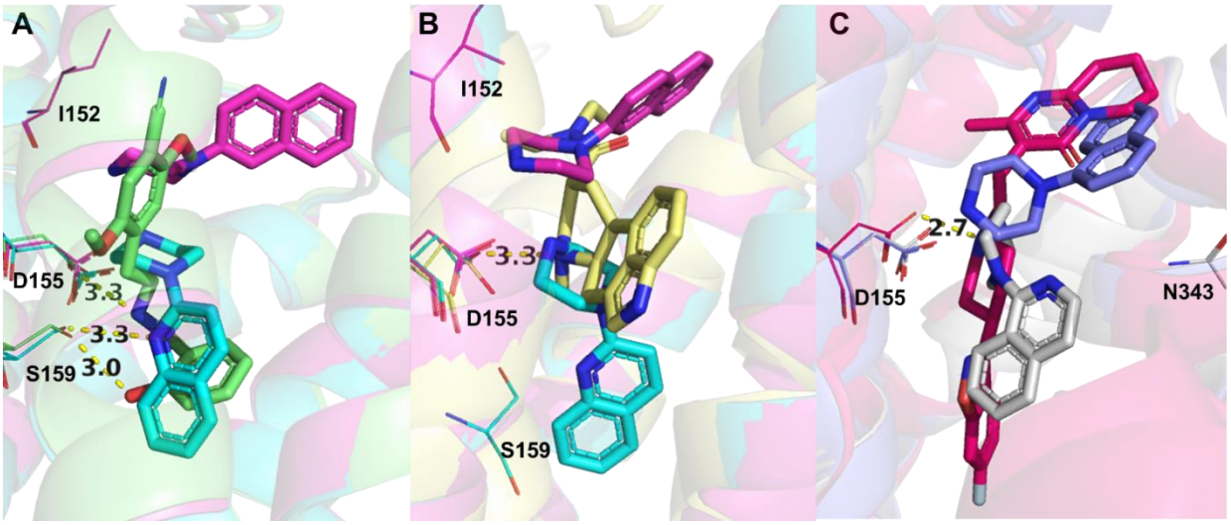

Figure 25. Comparison of binding poses of (A) quipazine (**45**) (capped sticks rendering; cyan carbon atoms) and 2-NP (**47**) (capped sticks rendering magenta carbon atoms) with 25CN-NBOH (capped sticks rendering; green carbon atoms), (B) quipazine and 2-NP with LSD (capped sticks rendering; yellow carbon atoms), and (C) isoquipazine (**46**) (capped sticks rendering; white carbon atoms), and 1-NP (**48**) (capped sticks rendering; blue carbon atoms) with risperidone (capped sticks rendering; dark pink carbon atoms) in the binding site of the 5-HT_{2A}R using both the active (6WHA) and inactive (6A94) states of the receptor. Hydrogen bonds are indicated by dashed yellow lines.

C. Specific Aim 3: Development of a pharmacophore for 5-HT_{2B} agonism

1. Approach

As mentioned previously, there is value in elucidating the structure-activity relationship of phenylisopropylamines at 5-HT_{2B} receptors in relation to prevention of cardiac valvulopathy as well as to breaking ground in pharmacophoric evaluation of 5-HT_{2B} receptors. To this aim, molecular docking and Hydropathic INTeraction (HINT) score analysis of two representative phenylisopropylamines DOB (**22**) and nFen (**20**) were performed. DOB possesses high affinity for 5-HT_{2B} receptors (K_i = 26.9 nM) and even higher affinity for 5-HT_{2A} receptors (K_i = 0.6 nM).[111] DOB exhibits agonist action at 5-HT_{2B} receptors (EC_{50} = 2.88 nM) along with its iodo-substituted counterpart, DOI (EC_{50} = 1.41 nM).[121] Both compounds, DOB and nFen, share similar structural scaffolds – both contain the structure of amphetamine (**42**) in their structures. This is a peculiar insight because both DOB and nFen have been shown to display affinity for and activity at 5-HT_{2B} receptors; however, there is no evidence for amphetamine displaying any such activity. Furthermore, there has been no evidence for amphetamine resulting in cardiac valvulopathy in patients despite being used clinically for decades, indicating amphetamine's inability to activate 5-HT_{2B} receptors. This leads to the conclusion that the 3-position CF_3 substituent of nFen must be responsible for nFen's affinity for 5-HT_{2B} receptors. Thus, the interactions of the 3-CF_3 substituent with specific amino acids in the binding pocket of 5-HT_{2B} receptors represent crucial points of interest in regard to eliciting affinity and activity at these receptors. Similar insights can be claimed when considering DOB: DOB's affinity for 5-HT_{2B} receptors must be dependent on the interactions of one or more substituents of its phenyl ring (2-OCH_3, 4-Br, 5-OCH_3) with key amino acids in the binding pocket. Because crystal structures of 5-HT_{2B} receptors had been published,[146] it was decided that computational analysis of these compounds would be the best method to begin determining the identity of these important amino acids.

2. Results and Discussion

a. Molecular docking of *R*(-)-DOB and *S*(+)-nFen using the crystal structure of the 5-HT_{2B} receptor

The 5-HT_{2B} crystal structure (PDB ID: 6DRY) was used due to its relatively high resolution (2.9 Å) and it being crystallized with the known 5-HT_{2B} agonist methylergonovine, thus representing an active state of the 5-HT_{2B} receptor appropriate for the docking of the representative agonists DOB (**22)** and nFen (**20**). Specifically *R*(-)-DOB, *S*(+)-DOB, and *S*(+)-nFen were analyzed using this crystal structure. Both isomers of DOB were analyzed because there is a lack of data distinguishing the activity of individual isomers of DOB at 5-HT_{2B} serotonin receptors. However, it should be noted that *R*(-)-DOI (K_i = 9.9 nM) binds with higher affinity than *S*(+)-DOI (K_i = 35 nM) at 5-HT_{2A} receptors;[119] hence, there is evidence for differences in the activity of individual isomers of phenylisopropylamines at serotonin receptors. *S*(+)-nFen was chosen due to its higher 5-HT_{2B} receptor affinity (K_i = 11.2 nM) and greater functional activity in phosphoinositide hydrolysis (K_{act} = 18.4 nmol/L) than its enantiomer *R*(-)-nFen (K_i = 47.8 nM and K_{act} = 357 nmol/L) and was thus deemed a better indicator for agonism at 5-HT_{2B} receptors than *R*(-)-nFen.

All three structures, *R*(-)-DOB, *S*(+)-DOB, and *S*(+)-nFen, were drawn using SYBYL-X 2.1.1 and were energy minimized utilizing the Tripos Force Field with Gasteiger-Hückel charges, a non-bonded interaction cutoff of 8 Å, dielectric constant (ε) of 4.00 D/Å, and a termination gradient of 0.05 kcal/(mol*Å). The structures were then docked at the 5-HT_{2B} receptor crystal structure using GOLD v5.6 which generated 100 protein-ligand complexes for each compound and GOLD scores, based on an in-program scoring system, for each complex. Each complex was then energy minimized using SYBYL-X 2.1.1 and evaluated by HINT score analysis within SYBYL 8.1

All of the complexes with *S*(+)-DOB docked at the 5-HT_{2B} receptor resulted in much lower GOLD and HINT scores than the complexes with *R*(-)-DOB. As a result, *S*(+)-DOB was eliminated from further consideration and focus was on *R*(-)-DOB. The most significant observation from the docking results was that the phenyl rings of *R*(-)-DOB and nFen were shifted relative to each other but they participated in similar interactions in the binding site (Figure 26). Both formed salt bridge interactions with the conserved Asp135$^{3.32}$ residue. *R*(-)-DOB participated in hydrogen bonding with Asn344$^{6.55}$ via the 5-OCH_3 group oxygen atom and the 4-Br substituent; additionally, the 4-Br substituent participated in hydrogen bonding with Ser222$^{5.43}$. One of the fluoro (F) atoms of nFen participated in bifurcated hydrogen bonds with Asn344$^{6.55}$ and Ser222$^{5.43}$; another F atom was involved in a single hydrogen bond with Asn344$^{6.55}$. These results indicate that both *R*(-)-DOB and nFen participate in the same specific hydrogen bonding interactions (with Asp135$^{3.32}$, Asn344$^{6.55}$, and Ser222$^{5.43}$). HINT analysis agreed with the observed interactions of *R*(-)-DOB and nFen (Table 8 and Table 9). The *R*(-)-DOB 4-Br substituent interactions with Asn344$^{6.55}$ and Ser222$^{5.43}$, and the hydrogen bond of the oxygen atom of the 5-OCH_3 substituent with Asn344$^{6.55}$, produced favorable HINT scores. One of the F atoms of the CF_3 substituent of nFen hydrogen bonded with Asn344$^{6.55}$ and Ser222$^{5.43}$ with positive HINT scores whereas another F atom formed favorable hydrogen bonds with Asn344$^{6.55}$ with a positive HINT score. The nitrogen atoms of *R*(-)-DOB and nFen formed bidentate hydrogen bonding interactions with the Asp135$^{3.32}$ residue with very high HINT scores, highlighting the importance of this conserved interaction.

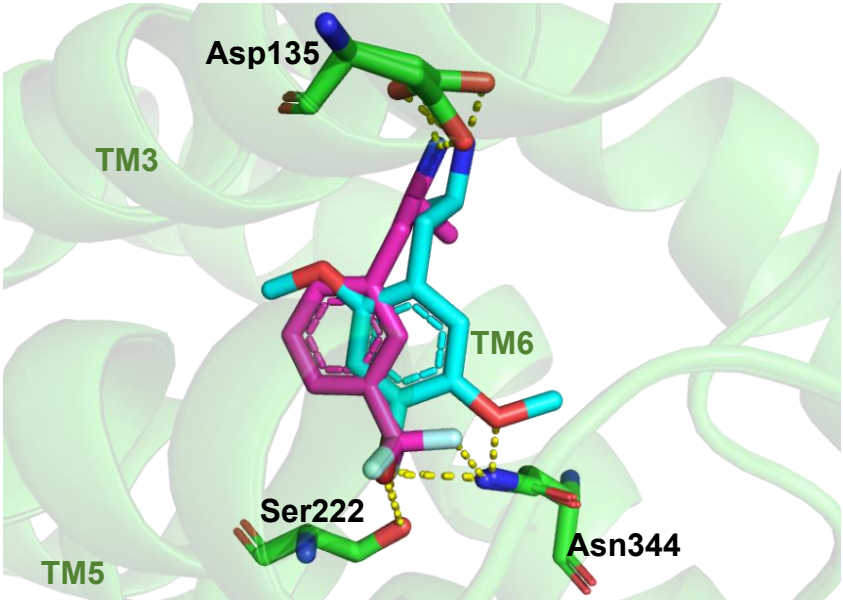

Figure 26. Docked poses of *R*(-)-DOB (capped sticks rendering; cyan carbon atoms) and nFen (capped sticks rendering; magenta carbon atoms) in the binding site of the 5-HT_{2B} receptor.

Table 8. HINT scores of *R*(-)-DOB interactions with the 5-HT_{2B} receptor.

R(-)-DOB Interactions	Hydrogen Bond HINT Score*
4-Br to Asn344	108
4-Br to Ser222	34
5-O to Asn344	39
N to Asp135	1637, 1580

*500 units = 1 kcal/mol

Table 9. HINT scores of *S*(+)-nFen interactions with the 5-HT_{2B} receptor.

nFen Interactions	Hydrogen Bond HINT Score
F to Asn344	36
F to Ser222	14
F' to Asn344	34
N to Asp135	1716, 1698

Because of the structural similarity between *R*(-)-DOB and nFen, it was expected that the phenyl moieties would be strictly superimposed in the binding site. Instead, my modeling studies showed that the phenyl moieties were skewed relative to one another, with the 4-Br substituent of *R*(-)-DOB and the 3-CF_3 group of nFen being located in the same position (Figure 26). The 4-Br atom of *R*(-)-DOB and 3-CF_3 of nFen both utilized Asn344 and Ser222 for hydrogen bonding interactions, supporting the hypothesis that these interactions are crucial for the binding of phenylisopropylamines. However, because only two F atoms of nFen participated in hydrogen bonds with the receptor, the third F might not be required for activity. Furthermore, although required for 5-HT_{2A} binding,[119] the oxygen atom of the 2-OCH_3 group of *R*(-)-DOB might not be necessary for binding at the 5-HT_{2B} receptor as shown by the lack of strong interactions (i.e. hydrogen bonding), supported by the HINT analysis. These results allowed us to propose the first working pharmacophore for 5-HT_{2B} ligands (Figure 27) which consists of an amine (N) separated by 5.2 Å from an aryl ring containing electrostatic (or possibly hydrophobic) substituents at either the 3- and/or 4-positions. Based on this putative pharmacophore, new analogs were designed to further probe the binding site of 5-HT_{2B} receptors to determine their structural requirements for activity.

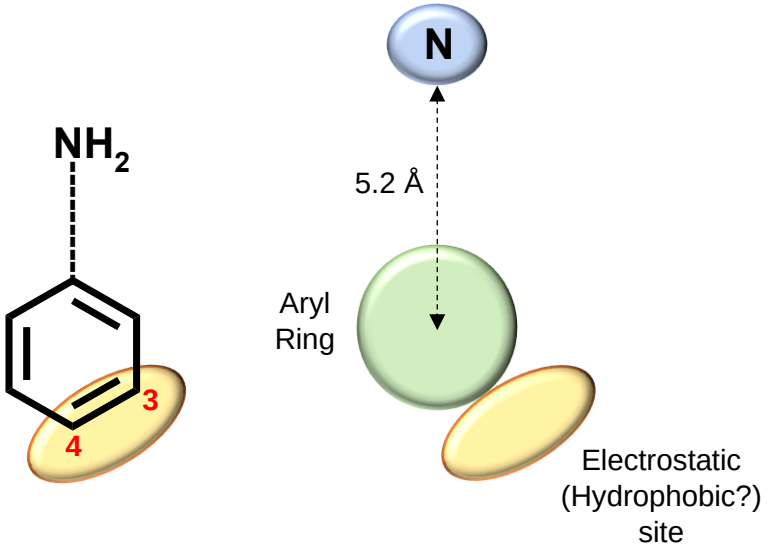

Figure 27. First working pharmacophore for 5-HT_{2B} receptors.

There are two primary questions that need to be addressed through the functional activity analysis of the designed compounds. The first question is this: is the binding of nFen at 5-HT_{2B} receptors dependent on the lipophilic or electronic character of the phenyl substituent? As surmised above, the 3-CF_3 substituent of nFen is required for binding at 5-HT_{2B} receptors. However, the CF_3 substituent forms both lipophilic and electronic interactions with the binding site (π = 0.88, σ = 0.43).[164] Therefore, compounds would need to be designed whose functional data will help elucidate this binding requirement. One of these compounds that was proposed was compound **65** (Scheme 2). Replacing the 3-CF_3 with 3-CH_3 as in **65** will allow us to determine if lipophilic character of the phenyl substituent is most essential for the binding of nFen (**20**) because the CH_3 substituent (π = 0.56, σ = -0.07) has similar lipophilic character but opposite electronic character as compared with CF_3. If **65** is equipotent to nFen then it can be concluded that lipophilic character predominates for the binding of nFen at 5-HT_{2B} receptors; if **65** is less potent than nFen, then electronic character predominates. Another proposed compound was compound **68**, a positional isomer of **65**, which contains a CH_3 substituent in the 4-position as opposed to the 3-position as in **65**. If lipophilic character of the phenyl substituent is determined to be most essential for the binding of nFen, then **68** should display similar activity as **65**. This might be possible through a relative shift of the phenyl rings of **68** as compared with **65** in the binding site (as proposed in Figure 26) to allow their phenyl substituents to participate in the appropriate interactions with residues to elicit activity at 5-HT_{2B} receptors.

The second question that must be addressed is: is the 2-position OCH_3 substituent of DOB necessary for 5-HT_{2B} receptor activity? Preliminary modeling studies indicated that there are no substantial interactions such as hydrogen bonding between the 2-OCH_3 of DOB and the binding site residues. To assess the necessity of this substituent the des-2-methoxy-DOB compound **71** will be prepared. If **71** produces similar activity as DOB in functional studies, we can conclude that the 2-OCH_3 is not required for activity. However, if activity decreases with removal of the 2-

OCH_3 substituent, then it is required and participates in electronic and/or hydrophobic interactions with the binding site of 5-HT_{2B} receptors.

Functional activity analysis of all three designed compounds as well as a series of DOX phenylisopropylamine compounds [DOF (**21**), DOB (**22**), DOI (**23**), MEM (**28**), DON (**30**), DOPR (**32**), DOHx (**33**), DOTB (**34**), and DOBz (**35**)] will be conducted to obtain EC_{50} values. This information will allow us to elaborate on the SAR of phenylisopropylamines and furthermore on the pharmacophoric requirements to activate 5-HT_{2B} receptors.

b. Synthesis of compound 65, 68, 71

The syntheses of **65** and **68** are illustrated in Scheme **2**. The nitrostyrene intermediate **64** was synthesized using a Henry reaction during which a base-catalyzed addition of nitroethane occurs followed by expulsion of water and formation of a double bond. The resulting product was successfully purified using a CombiFlash purification method and bright yellow needle-like crystals precipitated upon addition of EtOH and cooling. The nitrostyrene intermediate **67** was also synthesized using the Henry reaction; however, the purified product remained an oil rather than being converted into a solid like **64**.

Scheme 2. Synthesis of compounds **65**, **68**, and **71**.[a]

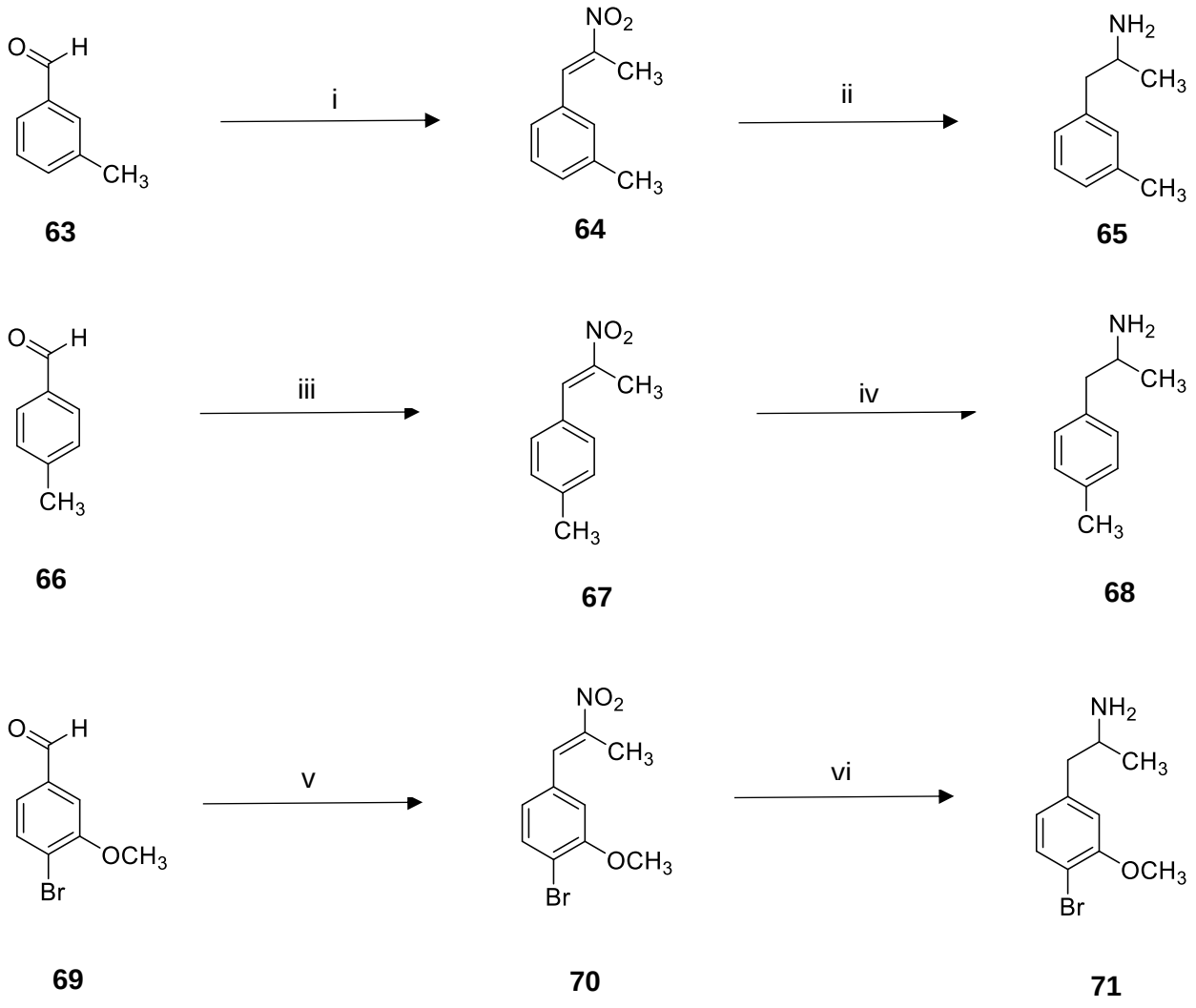

[a]Reagents and conditions: (i) NH_4OAc/Nitroethane, reflux, 48 h; (ii) $LiAlH_4$/THF, reflux, 2 h; (iii) NH_4OAc/Nitroethane, reflux, overnight; (iv) $LiAlH_4$/THF, reflux, 2 h; (v) NH_4OAc/Nitroethane, reflux, overnight; (vi) $NaBH_4$/THF, boron trifluoride diethyl etherate, 5.5 h.

The final amines **65** and **68** were synthesized from their respective nitrostyrene intermediates via a $LiAlH_4$ reduction reaction. The reduction was initially attempted with **64** before proceeding to and applying the same method to the synthesis of **68**. I initially attempted to purify the crude product of **65** using a Kugelrohr apparatus, as recommended in the literature. However,

TLC analysis of the collected fractions revealed that numerous products distilled together, thus not allowing purification. Next, an attempt was made to purify the crude oil product of **65** by precipitating the HCl salt of the final amine via addition of ethereal HCl into a solution of the crude oil dissolved in Et_2O. However, this resulted in the solution slowly turning black; a TLC analysis of this black solution revealed numerous spots, suggesting decomposition of the product. Clearly, precipitating a pure salt from a crude oil is not possible using this method and a purer oil is possibly needed to prevent decomposition. Another issue with this reaction was that I was likely not using enough $LiAlH_4$ in the reductions. Equivalences of 1:1.77 and 1:4 of the nitrostyrene:$LiAlH_4$ proved unsuccessful in completely consuming the nitrostyrene during the reaction. Finally an equivalence of 1:7 was used that successfully consumed the starting material, indicating the need of a large excess of reducing agent in the reduction of these nitrostyrenes. Using this equivalence and a purification method using the CombiFlash proved successful in producing the final amine as a pure free base in oil form which was successfully converted into an HCl salt via addition of ethereal HCl to a solution of the pure free base dissolved in Et_2O.

The synthesis of **71** is also displayed in Scheme 2. The Henry reaction was also used in the synthesis of the nitrostyrene intermediate. Based on prior knowledge of the possibility of the removal of bromo substituents from phenyl rings through the use of strong reducing agents such as $LiAlH_4$. The reduction was attempted using mild reducing agent $NaBH_4/BF_3$. After performing an acid base extraction to purify the resulting crude product, ethereal HCl was added in a dropwise manner to a solution of the purified oil in Et_2O to successfully form the HCl salt of **71**.

c. Functional activity studies of 65, 68, 71, and a series of DOX compounds

Functional analysis of the selected compounds mentioned above was initially attempted using the Flexstation 3 Multimode Microplate Reader, which is an automated instrument designed to acquire functional data of compounds in a high-throughput manner. This method utilized HEK293 cells transiently transfected with a 5-HT_{2B} plasmid using the transfection agent Lipofectamine Reagent and the fluorescent dye Fura-2 to measure the calcium signal. However, this method ultimately proved unsuccessful. Despite spending months developing proper technique in areas such as cell culturing, pipetting/aspirating, making solutions, and general laboratory procedure, as well as optimizing numerous experimental variables such as cell density, amount of Lipofectamine Reagent, and amount of 5-HT_{2B} plasmid used, the cells would not produce appreciable signals and required massive concentrations of the test compound 5-HT to elicit any effect. A representative concentration response curve is displayed in Figure 28 showing the inaccuracy of the data acquired using the Flexstation 3. The pEC_{50} of 5-HT from this curve is 3.36 while the pEC_{50} of 5-HT from the literature is 8.68.[121]

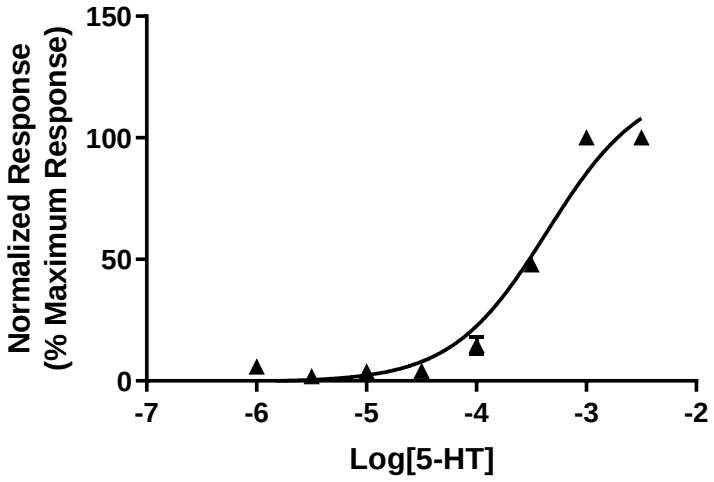

Figure 28. Representative concentration-response curve of 5-HT at 5-HT_{2B} receptors using the Flexstation 3 Multimode Microplate Reader with transiently transfected HEK293 cells. pEC_{50} = 3.36.

Because collection of proper signals from the Flexstation 3 was unsuccessful, the fluorescent microscope was employed in hopes of achieving greater sensitivity. The fluorescent microscope (Figure 29) that was used is connected to a constant perfusion system by which imaging solution and solutions of the drug of interest are constantly perfused through the wells while simultaneously being evacuated through a vacuum hose. This enables constant exposure of the cells to the drug during the drug phases of a trial and quick and thorough washing of the cells with imaging solution during the washing phases. This is in contrast to the Flexstation 3 which only has one addition of the drug solution to the wells containing the cells in imaging solution, thereby requiring the drug solution to diffuse through the imaging solution down to the cells at which point the cells very slowly react to the drug which might prevent the full potential of the signal caused by the drug from being reached. The fluorescent microscope methodology also includes individual selection of cells for the recording of data. The microscopy analysis system Live Acquisition is used during the trials to produce a video of the cells within the selected region of the wells. During activation of the receptors upon addition of an agonist, the cells display fluorescence, corresponding to the cells becoming brighter (whiter) in the video. The image processing software Fiji is then used to select individual cells that are representatives of this change in brightness. This difference is then averaged across all the selected cells from different wells and the average value represents the degree of activation of the cells. This is a much more sensitive method of recording signal as compared to the Flexstation 3. In the Flexstation 3 the overall fluorescence from the entire well is recorded by the instrument upon addition of a drug. This fluorescence is then subtracted by the baseline fluorescence, which is again a recording of the fluorescence from the entire well (but before any additions). This baseline fluorescence is quite high already due to the steady level of fluorescence constantly produced by the cells themselves. This would cause the signal from the addition of the drug to be extremely diminished. When processing data from the fluorescent microscope, the baseline fluorescence is collected for each individual cell, thus ensuring that any fluorescent signal from a drug is fully recognized for

that cell. In addition all fluorescent signals collected are subtracted by the background of the well – a black area in the video containing no cells – further amplifying the signals from the cells.

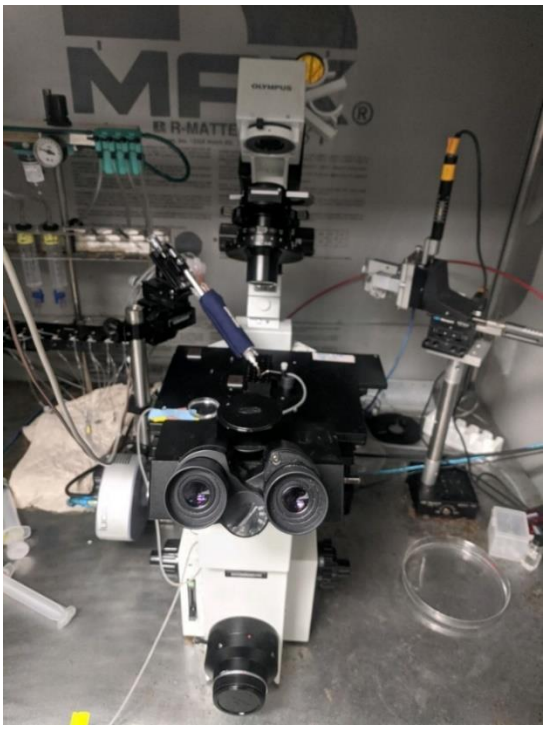

Figure 29. Photo of the fluorescent microscope used to acquire functional data of compounds at 5-HT_{2B} receptors.

When initially using the fluorescent microscope, the transfection agent Fugene and the calcium indicator GCaMP were employed. GCaMP is a fluorescent protein that is a chimera of green fluorescent protein, calmodulin (calcium binding protein), and the calmodulin interacting peptide M13.[165] During the transfection phase of the experimental preparation, both the 5-HT_{2B} plasmid and the GCaMP plasmid are transiently transfected into the HEK293 T cells using Fugene. When the cells divide and multiply, they will express the plasmids for a temporary amount

of time (i.e. transient transfection). When cells intracellularly release calcium upon agonist binding to 5-HT_{2B} receptors, calcium binds to GCaMP thus producing measurable fluorescence.

Using the fluorescent microscope, greater sensitivity in the signal from the cells was achieved. I was able to produce signal at much lower concentrations of 5-HT than used previously with the Flexstation 3 (Figure 30). Although the data acquired from the fluorescent microscope was a much better representation of the actual functional data of the compounds tested, there were still some issues which needed to be addressed. Out of all cells cultured in the 96-well plates used for experiment, only a small percentage (~30%) of cells appeared to be transfected – i.e. few cells fluoresced at 490 nm of light when viewed under the microscope. The pEC_{50} value of 5-HT (pEC_{50} = 7.44) was still not as high as that reported in the literature (pEC_{50} = 8.68)[121] where Porter et al.[121] also employed a calcium-flux assay, albeit with CHO-K1 cells stably transfected with 5-HT_{2B} receptors. Another significant issue was regarding the variability in the signal being produced, represented both by the large standard error values/standard error of mean bars in the concentration-response curves as well as in the videos of the cells producing signal on the day of the experiment. The videos revealed that, although there were cells which were transfected (i.e., accepted and expressed the GCamP plasmid), not all of the transfected cells produced signal. Furthermore, amongst the cells producing signal, there were inconsistencies in the degree of signal being produced; some cells released more calcium than others and in turn fluoresced much more brightly than other cells. This would indeed result in large variability in the concentration-response curves produced by these cells.

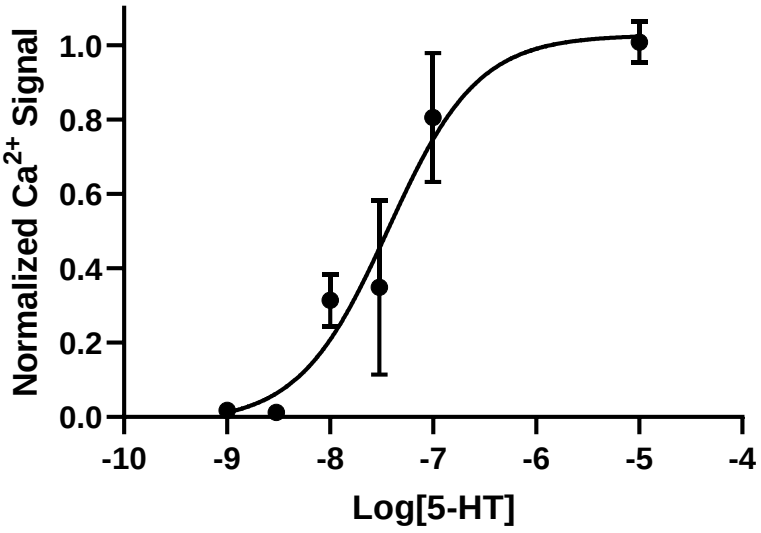

Figure 30. Normalized (to 1 μM 5-HT) concentration-response curve of 5-HT at 5-HT_{2B} receptors using the fluorescent microscope and transiently transfected HEK293 cells. pEC_{50} = 7.44 ± 0.22 (EC_{50} = ~36.73 nM).

Due to the inadequacies in transient transfection of the cells using the 5-HT_{2B} plasmid available, we surmised that the cells either did not harbor the plasmid within their DNA for very long or did not accept the 5-HT_{2B} plasmid to any great degree to begin with. The 5-HT_{2B} plasmid that was used contained a 3x-hemagglutinin (HA) tag sequence at the N-terminus of the main sequence. These HA-tags are generally added to proteins to allow for simple means of purification such as metal-affinity chromatography using a Ni^{2+} column. However, we hypothesized that this HA-tag might be interfering with some step in the transfection process, either in the transfection itself or in the post-expression translocation of the protein to the membrane of the cell. Therefore, we deemed it prudent to acquire a new plasmid of 5-HT_{2B} without the HA-tag sequence. When using this new plasmid, videos of the cells fluorescing showed that the transfection was slightly better and the cells fluoresced with slightly more consistency than with using the plasmid containing the HA-tag. In hopes of achieving greater improvement in the signal being produced

by the cells and in the degree/consistency of transfection, I decided to use this new plasmid (without the HA-tag) to produce a stable cell line containing 5-HT_{2B} receptors with the HEK-293 T cells used for experiment.

After successful production of the stable cell line, data acquired from these cells was greatly improved with regards to transfection and signal generation. A majority of the cells cultured in the 96-well plates appeared to be transfected (~90%), when viewed under the microscope with the selected wavelengths (340 and 380 nm) and the new fluorescent indicator used, Fura-2. Fura-2 is a calcium indicator which emits light at 510 nm when subjected to light with wavelengths of around 340 nm and 380 nm. A ratio of the fluorescence signal measured at both wavelengths is taken to generate a more accurate reading of Ca^{2+} release. Amongst the transfected cells ~80-90% of cells appeared to produce consistent signals (i.e. produced approximately equal levels of fluorescence) when tested with 1 μM 5-HT. A concentration-response curve representing 5-HT activity is displayed in Figure 31. The pEC_{50} value from this curve (pEC_{50} = 8.8) is much closer to the literature value (pEC_{50} = 8.68)[121] and variability in the concentration-response curve is much more mitigated as compared to when transient transfection was employed.

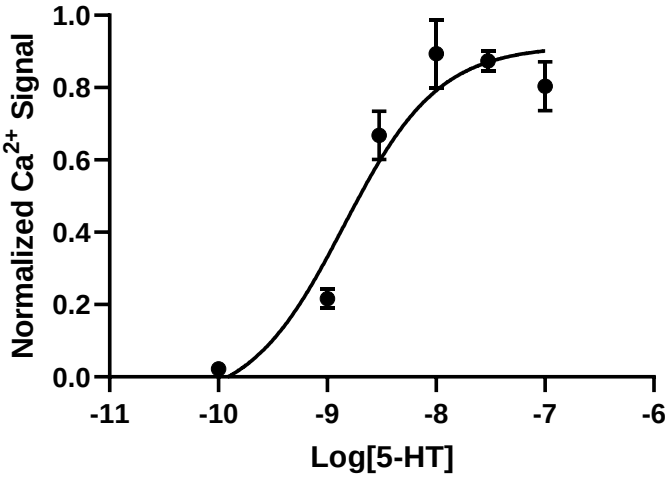

Figure 31. Normalized (to 1 μM 5-HT) concentration-response curve of 5-HT at 5-HT_{2B} receptors using the fluorescent microscope with stably transfected HEK293 cells. pEC_{50} = 8.8 ± 0.14 (EC_{50} = 1.4 nM).

Having finally developed a method by which to record accurate functional data for compounds at 5-HT_{2B} receptors, the compounds mentioned above were tested. To address the first question of this aim (Is the binding of nFen at 5-HT_{2B} receptors dependent on the electronic or lipophilic character of its 3-CF_3 substituent?) concentration-response curves were acquired for nFen (**20**), **65**, and **68** and are displayed below in Figure 32. The 3-CH_3 analogue **65** is over five-fold less potent (EC_{50} = 331 nM) than racemic nFen (EC_{50} = 65 nM), supporting the importance of the electronic character of the 3-CF_3 substituent of nFen. However, activity of nFen was not completely abolished by replacement of 3-CF_3 with 3-CH_3 and this change still results in a compound with nanomolar potency (i.e., **65**). Considering this small difference in potency, one possibility is that the 3-position substituent contributes little to nothing to the potency of the 3-unsubstituted compound (i.e., amphetamine, **42**). Hence, racemic amphetamine was evaluated for functional activity and was found to be inactive when examined at 10 μM concentration. From

this, it is evident that the 3-position substituents of **20** and **65** play an important role in agonist potency/action. There might be two possibilities: either the 3-CF_3 substituent of nFen participates in both electronic and lipophilic interactions with binding site residues, or only participates in electronic interactions although lipophilic interactions with residues in a similar binding site region also elicit activity at 5-HT_{2B} receptors (i.e. nFen and **65** participate in unique interactions via their 3-position substituents e.g., rotameric binding). Translocation of the 3-CH_3 substituent of **65** to the 4-position as in **68** resulted in similar potency (EC_{50} = 246 nM) as did **65**. This supports the possibility of activating 5-HT_{2B} receptors via lipophilic interactions with the phenyl substituents of these amphetamine analogues. Due to the similarity of the potencies of **65** and **68**, it was predicted that the methyl substituents of both compounds participate in similar interactions with common residues in the binding site. The preliminary computational model with nFen and DOB supports this prediction: just as the phenyl rings of nFen and DOB were shifted in the binding pocket to accommodate similar interactions, so too might **65** and **68** be shifted relative to one another to allow their methyl substituents to participate in common interactions with lipophilic residues.

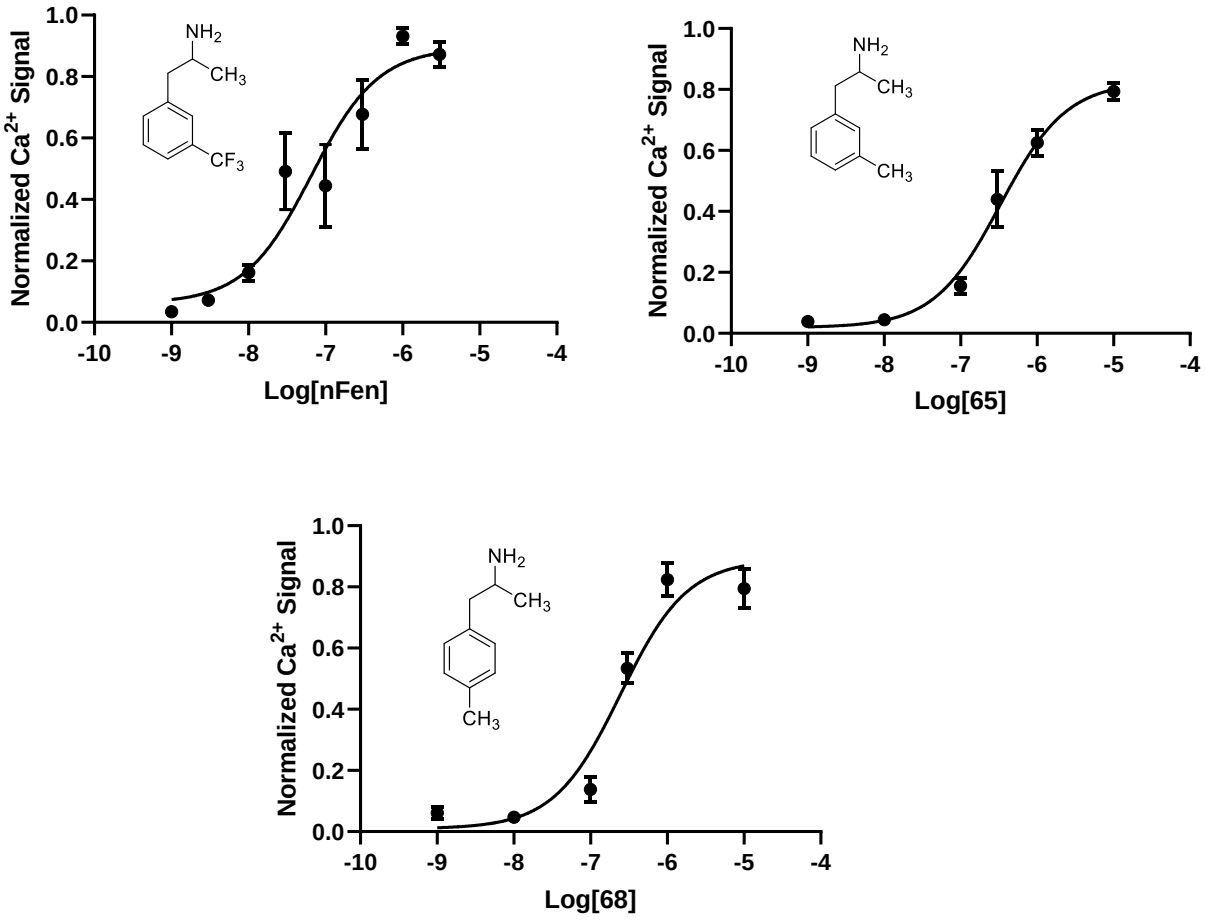

Figure 32. Normalized (to 1 μM 5-HT) concentration-response curves for functional activity of nFen (**20**), **65**, and **68** at 5-HT_{2B} receptors. pEC_{50} for nFen = 7.2 ± 0.20 (EC_{50} = 65 nM); pEC_{50} for **65** = 6.5 ± 0.11 (EC_{50} = 331 nM); pEC_{50} for **68** = 6.6 ± 0.12 (EC_{50} = 246 nM).

Computational docking and HINT analysis using the crystal structure of the 5-HT_{2B} receptor (PDB ID: 6DRY) were conducted on **65** and **68** to determine their possible binding modes. Protein-ligand complexes were chosen based on those with the highest overall HINT score. Docked poses (Figure 33) revealed that both compounds bind very similarly to nFen and all three structures are nearly superimposed in the binding pocket. As expected, all three compounds participate in hydrogen bonding with $Asp135^{3.32}$ via their amine nitrogen atoms. Just

as predicted above, **68** assumed a shifted orientation with regard to its phenyl ring and the phenyl rings of nFen and **65**, presumably to orient its phenyl substituent to be in the proper location in space for optimal interactions. Unlike in the case of norfenfluramine, HINT analysis did not reveal any hydrogen bonding between the phenyl substituents of **65** and **68** and binding site residues – which is expected as methyl groups are unable to form hydrogen bonds. Instead HINT analysis revealed several hydrophobic interactions with these substituents. For example, the 3-CH_3 substituent of **65** forms hydrophobic interactions with Val136$^{3.33}$, Leu209^{EL2}, and Phe217$^{5.38}$, according to HINT. Similarly 4-methyl substituent of **68** interacts with Val136$^{3.33}$ and Phe217$^{5.38}$; additionally, HINT revealed hydrophobic interactions between the 4-methyl substituent and Ile186$^{4.56}$, the β-carbon atom of Ser222$^{5.43}$, and Ala225$^{5.46}$. The modeling results add credence to the hypothesis that although electronic interactions with the phenyl substituents of these amphetamine compounds can elicit high activity, hydrophobic interactions with these substituents can also elicit activity, albeit to a slightly lower degree. It should be noted that HINT analysis failed to reveal any hydrophobic interactions involving the fluoro atoms of nFen; although, due to the close proximity between the fluoro atoms and hydrophobic residues (e.g. the hydrophobic residues that interact with the 3-CH_3 substituent of **65**), hydrophobic interactions may still contribute to nFen's agonist activity.

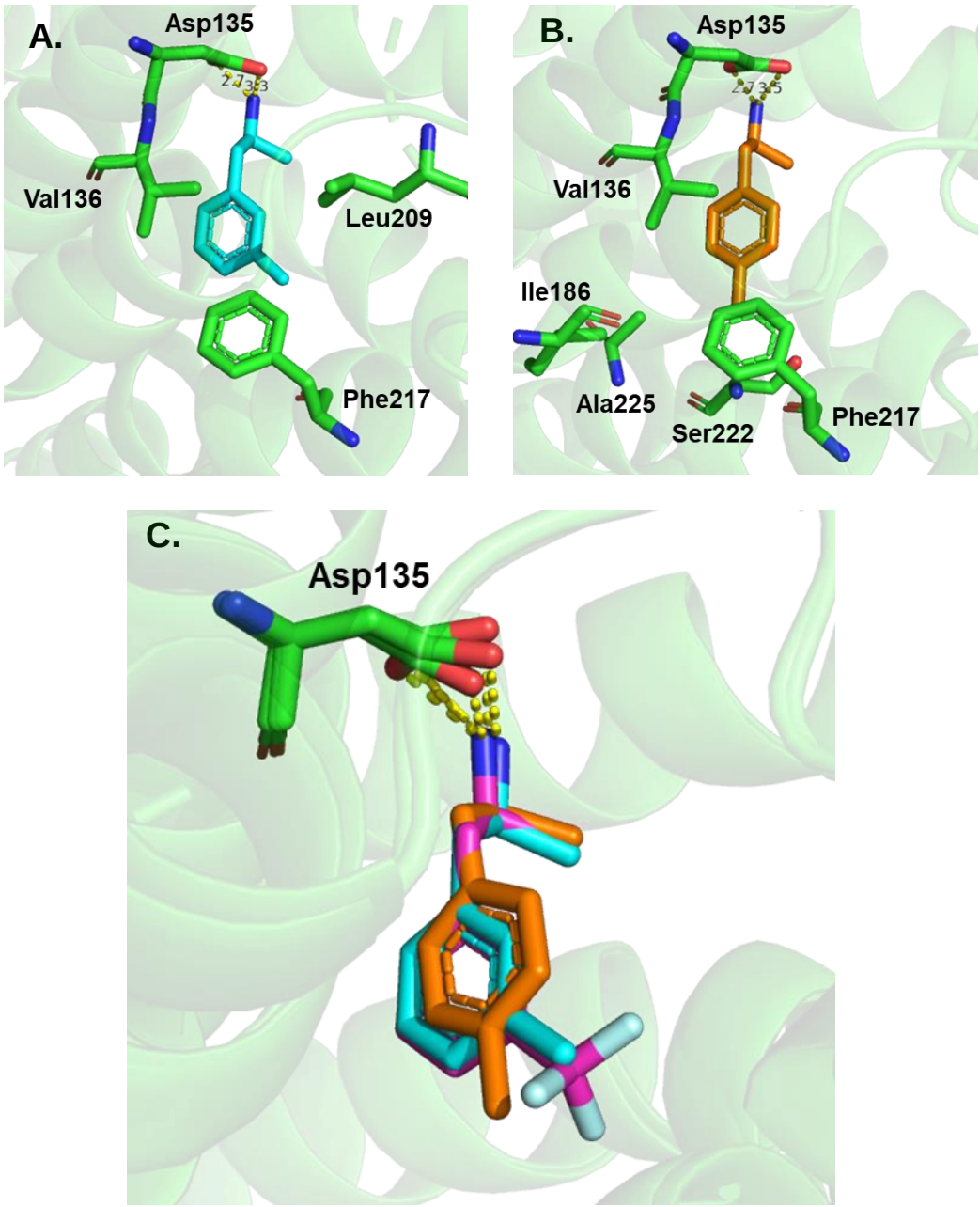

Figure 33. Docking results of **65** and **68** in the binding site of the 5-HT_{2B} receptor (cartoon helices/capped sticks rendering; green carbon atoms). A) Compound **65** (capped sticks rendering; cyan carbon atoms); B) Compound **68** (capped sticks rendering; orange carbon atoms); C) Overlay of **65**, **68**, and nFen (capped sticks rendering; magenta carbon atoms). Hydrogen bonds are indicated by yellow dashed lines.

To address the second question of this aim (Is the 2-OCH_3 substituent of DOB required for binding at 5-HT_{2B} receptors?), DOB (**22**) and its des-2-methoxy analogue **71** were examined for their functional activity at 5-HT_{2B} receptors. Concentration-response curves for both compounds are shown below in Figure 34. Removal of the 2-OCH_3 substituent of DOB (EC_{50} = 8.7 nM) as in **71** (EC_{50} = 67 nM) resulted in an almost eight-fold reduction in potency. This supports the necessity of the 2-OCH_3 substituent of DOB for activity at 5-HT_{2B} receptors. However, because **71** still retains nanomolar potency, it was concluded that although the 2-OCH_3 substituent might contribute to the greater potency of DOB through its electronic interactions with the oxygen atom or lipophilic interactions with the methyl group, it is not absolutely required for activity. These data are in accordance with very recent literature data[166] indicating an approximately six-fold reduction in 5-HT_{2B} receptor affinity of **71** as compared with DOB.

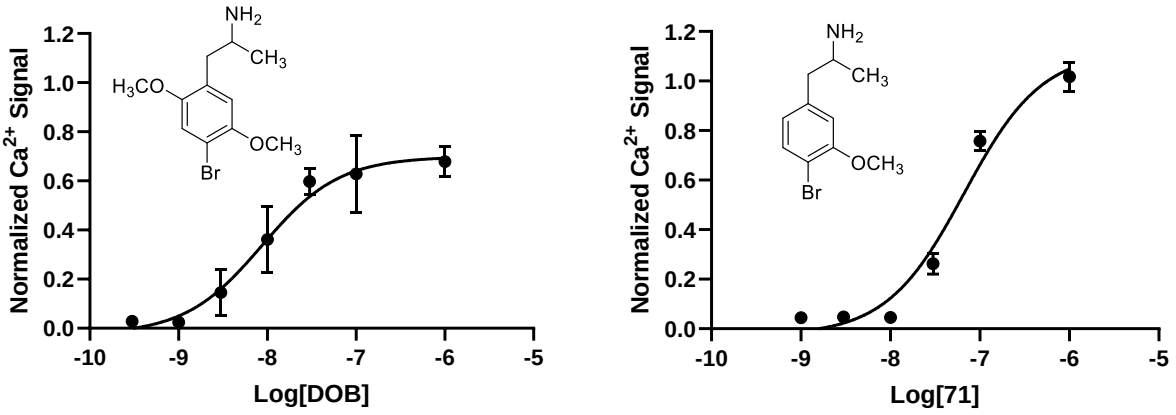

Figure 34. Normalized (to 1 µM 5-HT) concentration-response curves for functional activity of DOB (**22**) and **71** at 5-HT_{2B} receptors. pEC_{50} for DOB = 8.1 ± 0.20 (EC_{50} = 8.7 nM); pEC_{50} for **71** = 7.2 ± 0.08 (EC_{50} = 67 nM).

Computational docking and HINT analysis using the crystal structure of the 5-HT_{2B} receptor (PDB ID: 6DRY) was re-conducted on **71**; the selected protein-ligand complex produced

the highest overall total interaction HINT score (2317) and is displayed in Figure 35 (Panel A). As expected, **71** participated in hydrogen bonding with Asp135$^{3.32}$ via its amine nitrogen atom. Instead of forming a hydrogen bond with Asn344$^{6.55}$ as observed in the docked model of DOB, the 4-Br substituent of **71** formed a weaker acid/base interaction. The docked poses of **71** and DOB were oriented similarly in the binding site but were slightly shifted relative to their phenyl rings. Furthermore, the phenyl rings are flipped relative to one another so the 3-OCH_3 substituent of **71** and the 2-OCH_3 substituent of DOB are facing the same direction. As a result, the methyl groups of both substituents participate in hydrophobic interactions with exactly the same residues, according to HINT analysis. They both form hydrophobic interactions with Val136$^{3.33}$, the β-carbon of Ser139$^{3.36}$, the γ-carbon of Thr140$^{3.37}$, Ile143$^{3.40}$, Ala225$^{5.46}$, and Phe341$^{6.52}$. However, unlike DOB which failed to possess any hydrogen bonding involving the 2-OCH_3 oxygen atom, HINT analysis revealed a hydrogen bond interaction between the side-chain oxygen atom of Thr140$^{3.37}$ and the 3-OCH_3 atom of **71**. This is presumably made possible by the lower positioning of the 3-OCH_3 substituent of **71** compared to the 2-OCH_3 substituent of DOB, thus being in a closer proximity for hydrogen bonding with Thr140$^{3.37}$. Such a hydrogen bond might help salvage the activity of **71** and keep its activity in the nanomolar range, despite not producing any hydrogen bonding with Asn344$^{6.55}$ as seen with DOB.

Alternatively, docking results also produced a binding pose which most closely resembles the binding mode of DOB, with the 3-OCH_3 substituent of **71** positioned in the same location as the 5-OCH_3 substituent of DOB (Figure 35; Panel C); however, this solution had a slightly lower total interaction score (2240) than the solution in Panel A of Figure 35, described above. As a result, the 4-Br substituent and the oxygen atom of the 3-OCH_3 substituent formed hydrogen bonds with Asn344$^{6.55}$ and the 4-Br substituent formed an additional hydrogen bond with Ser222$^{5.43}$ – similar to the interactions involving DOB displayed in Figure 26. Furthermore, the methyl group of the 3-OCH_3 substituent of **71** forms the same hydrophobic interactions as the

methyl group of the 5-OCH_3 substituent of DOB: with Leu209^{EL2}, Met218$^{5.40}$, Phe340$^{6.51}$, and Leu362$^{7.35}$. Using this model, the reduced activity of **71** as compared with DOB can be supported by its lack of hydrophobic interactions: according to HINT analysis, DOB displays numerous hydrophobic interactions involving the methyl group of the 2-OCH_3 substituent. Because **71** lacks the 2-position substituent, it is unable to form these hydrophobic interactions and this might result in its lower activity. The total energy for each suggested protein-ligand complex (shown in Figure 35, panel A and C) was calculated using SYBYL. The energy for **71**'s binding pose displayed in Panel A (-888 kcal/mol) is very similar to the energy for its binding pose displayed in Panel C (-892 kcal/mol) indicating that both binding modes are equally probable.

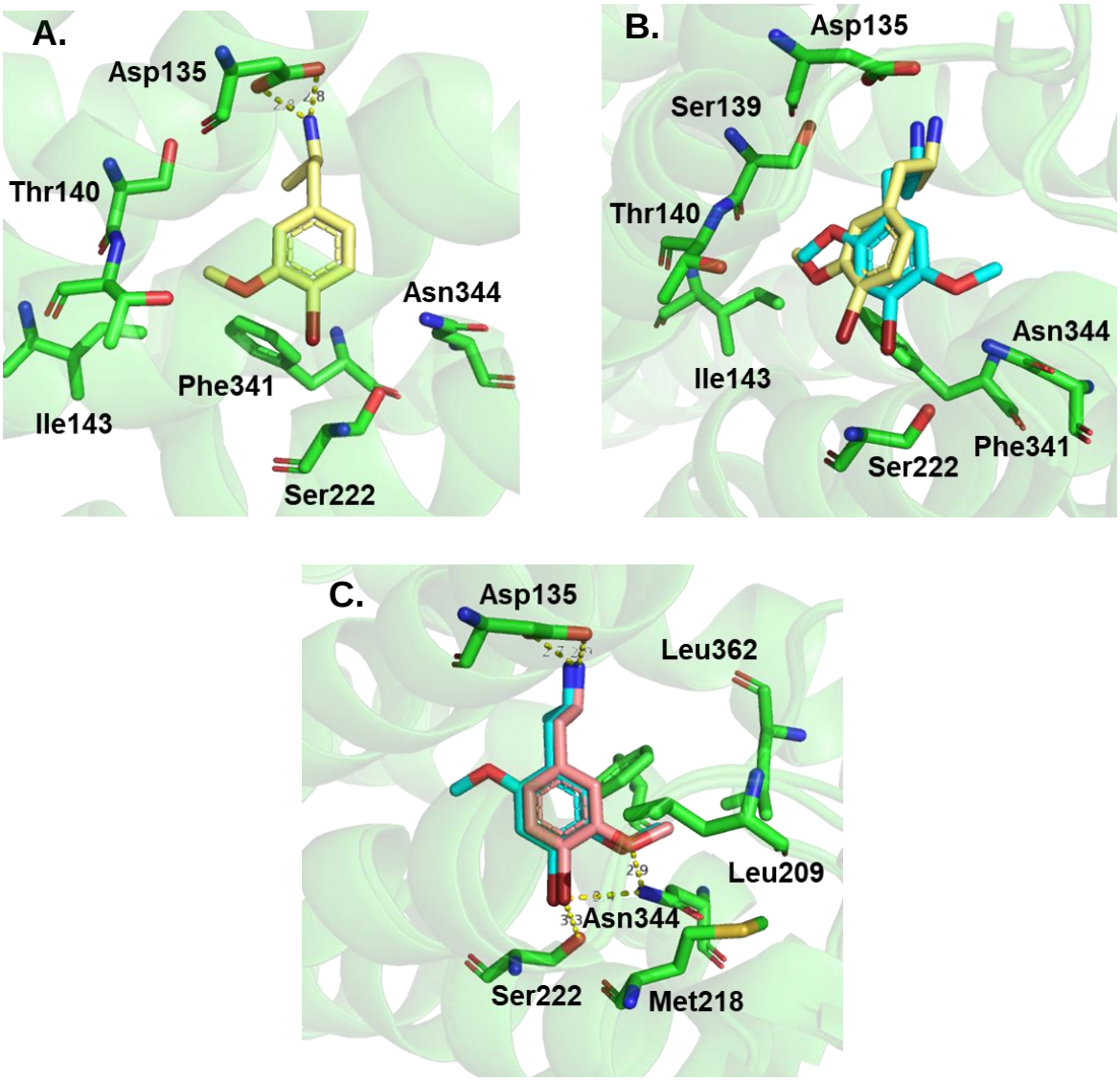

Figure 35. Docking results of **71** in the binding site of the 5-HT_{2B} receptor (cartoon helices/capped sticks rendering; green carbon atoms). A) Compound **71** (capped sticks rendering; yellow carbon atoms); B) Overlay of top total HINT interaction scoring **71** and DOB (capped sticks rendering; cyan carbon atoms); C) Overlay of top total HINT interaction scoring **71** (capped sticks rendering; peach carbon atoms) which most closely resembles the binding of DOB (capped sticks rendering; cyan carbon atoms). Hydrogen bonds are indicated by yellow dashed lines.

A series of other DOX phenylisopropylamine compounds was tested in 5-HT_{2B} cells with the intent of elaborating their SAR for functional activity at 5-HT_{2B} receptors. A total of nine phenylisopropylamine compounds with variable substituents at their 4-positions, DOB, DOI, DOF, DON, DOPR, DOTB, and MEM, were examined and concentration-response curves for six are displayed in Figure 36; data for DOB was shown in Figure 34. DOHx (**33**) and DOBz (**35**) failed to produce an agonist effect at a concentration of 10 μM. Data for seven agents are tabulated in Table 10.

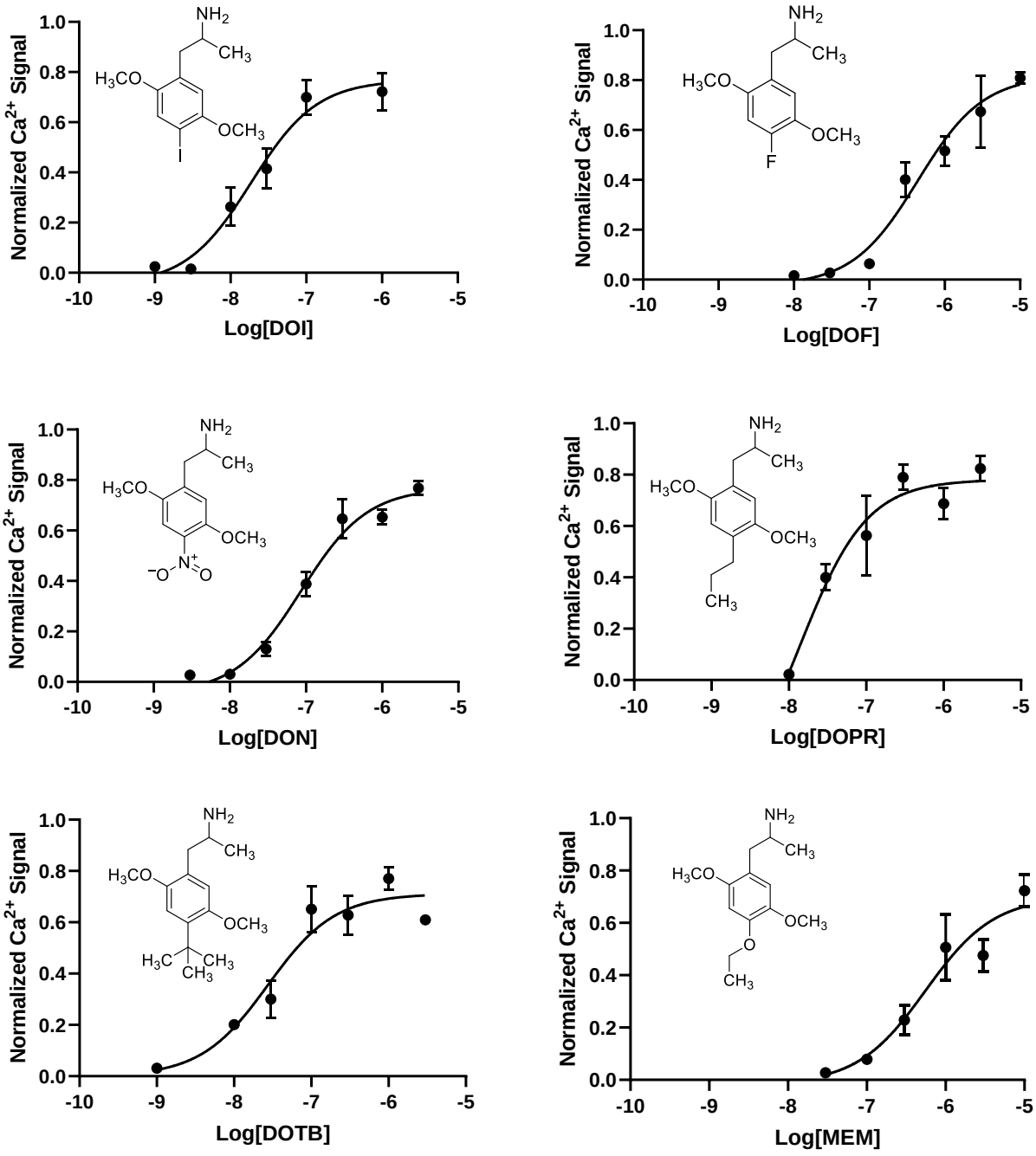

Figure 36. Normalized (to 1 μM 5-HT) concentration-response curves for DOI (**23**), DOF (**21**), DON (**30**), DOPR (**32**), DOTB (**34**), and MEM (**28**). pEC_{50} for DOI = 7.4 ± 0.17 (EC_{50} = 39 nM); pEC_{50} for DOF = 6.4 ± 0.12 (EC_{50} = 439 nM); pEC_{50} for DON = 7.1 ± 0.12 (EC_{50} = 86 nM); pEC_{50} for DOPR = 7.5 ± 0.17 (EC_{50} = 29 nM); pEC_{50} for DOTB = 7.4 ± 0.15 (EC_{50} = 37 nM); pEC_{50} for MEM = 6.3 ± 0.23 (EC_{50} = 557 nM).

Table 10. 5-HT_{2B} potency, intrinsic efficacy, and affinity values of a series of DOX compounds: DOB (**22**), DOI (**23**), DOF (**21**), DON (**30**), DOPR (**32**), DOTB (**34**), and MEM (**28**).

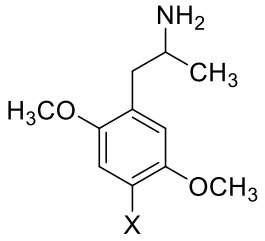

	X	5-HT_{2B} Potency, (EC_{50} ± SEM, nM)*	5-HT_{2B} Intrinsic Efficacy*	5-HT_{2B} K_i (nM)[111]
DOB (22)	Br	8.7 ± 5.5	0.70	26.9
DOI (23)	I	39 ± 15	0.71	20.0
DOF (21)	F	439 ± 120	0.82	227
DON (30)	NO_2	86 ± 24	0.77	166
DOPR (32)	*n*-Pr	29 ± 11	0.75	54.4
DOTB (34)	*t*-Bu	37 ± 13	0.69	24.6
MEM (28)	OC_2H_5	557 ± 296	0.70	763

Note: 5-HT potency and efficacy at 5-HT_{2B} receptors: 1.7 nM ± 0.59 and 0.92, respectively
*Potency and intrinsic efficacy values normalized to 1 μM 5-HT

When considering the effect of halogens occupying the 4-position of phenylisopropylamine compounds, it is evident that more lipophilic halogens with larger atomic radii are well tolerated. Compared to DOB (EC_{50} = 8.7 nM) and DOI (EC_{50} = 39 nM) which share similar functional activity, the activity of DOF is far lower (EC_{50} = 439 nM). This suggests that a strong lipophilic interaction between the 4-position substituent and lipophilic amino acids in the binding site might be beneficial for increasing activity at 5-HT_{2B} receptors. Another possibility is that the halogen atoms are interacting with polar amino acids via halogen bonding through their positively charged σ-holes. This can be resolved by considering the activity of DOPR (EC_{50} = 29 nM) and DOTB (EC_{50} = 37 nM) which both contain 4-position alkyl chains capable of forming

significant hydrophobic interactions and have similar activity as DOB and DOI. This suggests that lipophilic interactions with the 4-position substituent can increase activity; however, polar interactions may still play a part. To test the importance of polar interactions with the 4-position substituent, DON and MEM were examined that contain 4-NO_2 and 4-OCH_2CH_3 substituents, respectively. The activity of DON (EC_{50} = 86 nM) is almost 10-fold lower than its 4-bromo counterpart DOB, suggesting that charged substituents at the 4-position are tolerated but not optimal for activity. This might be due to a lack of polar amino acids capable of forming electrostatic interactions with the nitro substituent of DON such as arginine, lysine, aspartic acid, or glutamic acid in that region of the binding site. Furthermore, the activity of MEM, containing a hydrogen bond accepting oxygen atom, is far lower (EC_{50} = 557 nM) suggesting that there is even a lack of polar amino acids capable of forming hydrogen bonding interactions with the 4-position substituent.

Because 5-HT_{2B} receptor affinity data have been previously published by our group, it was of interest to correlate 5-HT_{2B} functional activity to 5-HT_{2B} affinity for the phenylisopropylamines examined above (Figure 37). These data would allow the determination of the predictive capability of affinity data to predict functional data (or vice versa) for these compounds. The correlation coefficient (*r*) for this plot is substantial (0.879), indicating that affinity and agonist potency are correlated to one another and thus K_i is a decent indicator of EC_{50}. Nevertheless, 5-HT_{2B} receptor affinity is not a valid predictor of functional activity because DOHx (**33**) and DOBz (**35**), although displaying high affinity (Table 3) were without agonist action at concentrations of up to 10,000 nM. Hence, the relationship shown in Figure 37 would seem to hold only for agonists.

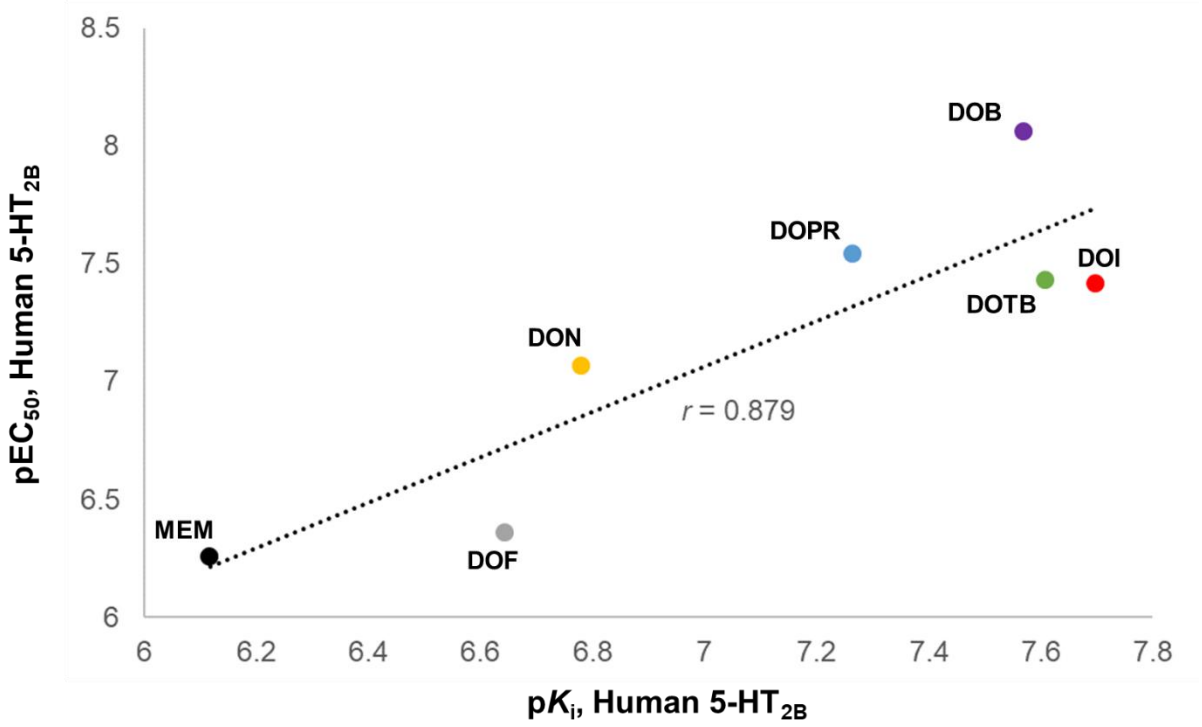

Figure 37. Relationship between 5-HT_{2B} receptor affinity (pK_i) and 5-HT_{2B} receptor potency (pEC_{50}) for seven DOX phenylisopropylamine compounds (slope = 0.962, r = 0.879).

To examine the role of a 4-position substituent for binding affinity at 5-HT_{2B} receptors, correlations were sought between 4-position substituent π-values of phenylisopropylamine agonists and their affinity at 5-HT_{2B} receptors as well as between 4-position substituent σ_p-values and affinity (Figure 38). There is a much stronger correlation between π-values and affinity (r = 0.787) than between σ_p-values and affinity (r = 0.064), suggesting that hydrophobic interactions with the 4-position substituent might be the primary driving force for the binding of these compounds at 5-HT_{2B} receptors.

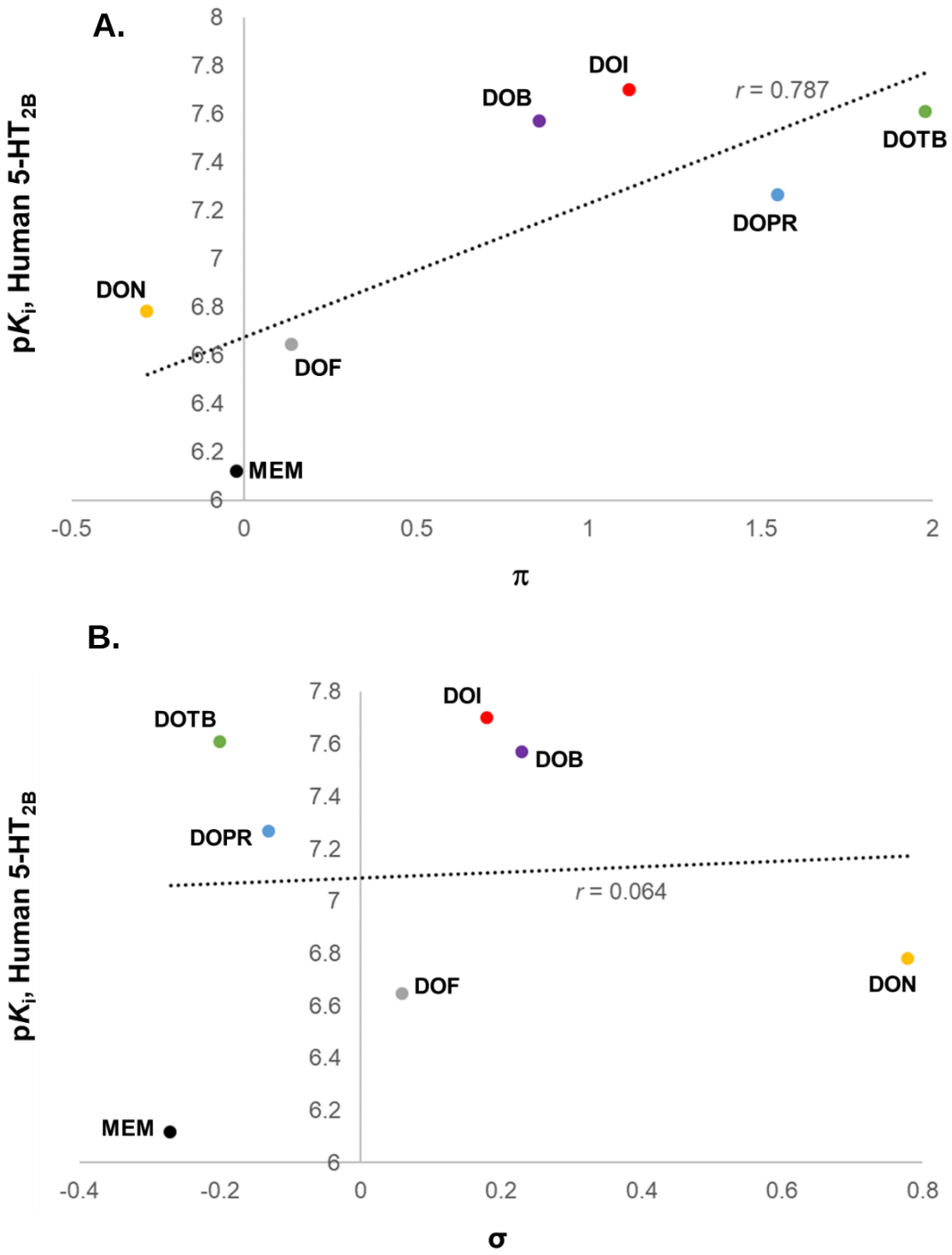

Figure 38. A) Relationship between 4-position substituent π-values of phenylisopropylamine agonists and their 5-HT_{2B} receptor affinity (pK_i) (slope = 0.554, r = 0.787). B) Relationship between 4-position substituent σ_p-values of 4-position substituents of phenylisopropylamines and their 5-HT_{2B} receptor affinity (pK_i). (slope = 0.108, r = 0.064).

To determine if the potency values of these compounds follow the same trend as their affinity values, their EC_{50} values, acquired in the present study, were analyzed and compared with both the 4-position substituent π-values of phenylisopropylamine agonists as well as with their 4-position substituent σ_p-values (Figure 39). The correlation between pEC_{50} values and π values was greater (r = 0.634) than the correlation between pEC_{50} values and σ_p-values (r = 0.193). Thus, similarly to the case of affinity, potency also might be driven by the lipophilicity of the 4-position substituent of phenylisopropylamines and the resulting hydrophobic interactions it participates in. It is entirely possible that both the lipophilic and electronic character of DOX 4-position substituents contribute to activity. Thus, a relating equation involving both π and σ might be developed. Indeed, a preliminary study was conducted employing both variables and resulted in a relating equation where $r > 0.8$. However, given that data on only seven compounds were available, the equation was not statistically valid. Additional agonists will need to be examined in order to provide additional support for this concept.

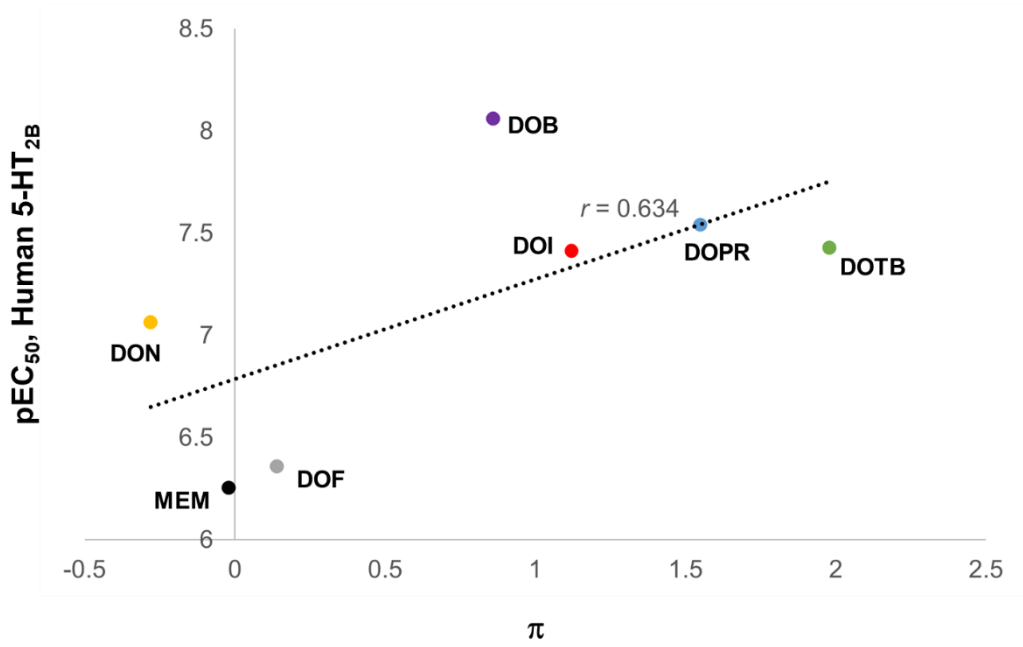

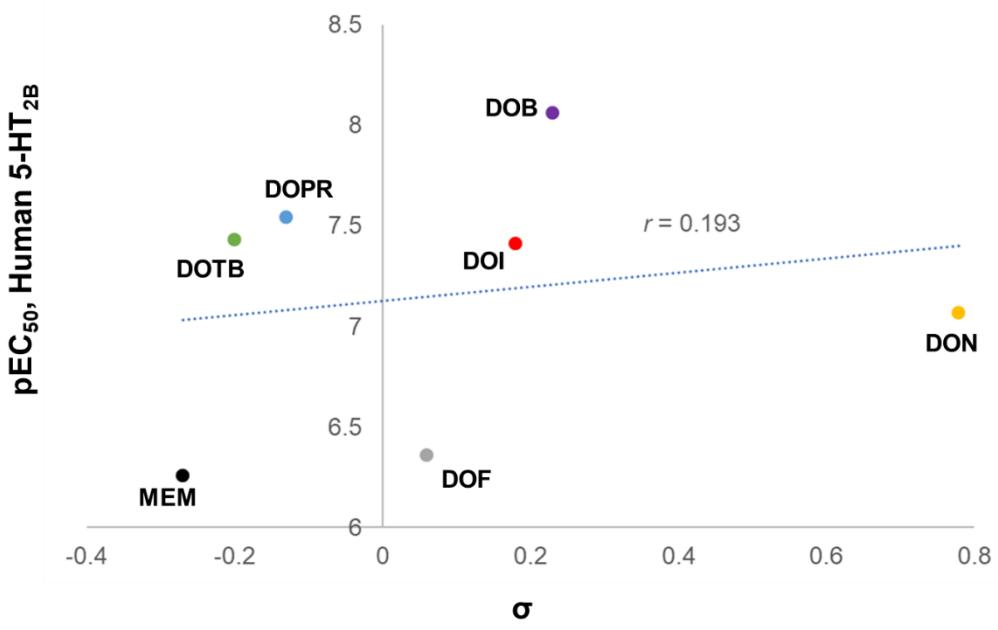

Figure 39. A) Relationship between 4-position substituent π-values of phenylisopropylamine agonists and their 5-HT_{2B} receptor potency (pEC_{50}) (slope = 0.489, *r* = 0.634). B) Relationship between 4-position substituent σ_p-values of 4-position substituents of phenylisopropylamines and their 5-HT_{2B} receptor affinity (pEC_{50}). (slope = 0.354, *r* = 0.193).

V. Conclusions

The overall goal of this project was to elaborate on the pharmacophoric requirements of 5-HT_{2A} and 5-HT_{2B} receptors. In Aim 1, the pharmacophoric requirements of 5-HT_{2A} receptor antagonism was investigated – based on the structure of risperidone and with the specific intention of "elaborating" (using the DRE approach) the fluorinated pharmacophore **14** to determine the effects of adding N-substituents on 5-HT_{2A} affinity. Previous studies revealed that the entire structure of risperidone is not required for activity and only the right half portion as in **14** is necessary for activity. A 5-HT_{2A} receptor affinity screen conducted on **14**, its N-methylated analogue **15**, and other analogues containing substituents on the piperidinyl nitrogen atom of varying length and sizes (**10**, **16**-**18**, and **51**) revealed that although increasing the length and bulk of the piperidinyl substituent is correlated with greater 5-HT_{2A} receptor affinity and selectivity, it is also correlated with increased D_2 receptor affinity. One potential application of this project was to develop a safer antipsychotic drug by increasing the 5-HT_{2A} receptor antagonism and selectivity of atypical antipsychotic drugs and concurrently decreasing their D_2 receptor antagonism (and thus increasing the safety of these drugs by reducing their incidence of EPS symptoms). In this scope, the results of the affinity screen conducted and the resulting trends surmised from the data indicate that extension of the piperidinyl substituent of **14** might not result in a compound that would make a better antipsychotic drug due to the associated trend in greater D_2 receptor affinity. In addition, affinity data of the synthesized compound **53**, containing a propyl substituent on the piperidinyl nitrogen atom, revealed that although a methyl substituent is well tolerated as in **15** and results in greater affinity (K_i = 12.3 nM) relative to **14** (K_i = 71.4 nM), increasing the length to a propyl chain results in a reduction of affinity (K_i = 107 nM). This indicates that longer alkyl chains than methyl are less tolerated at 5-HT_{2A} receptors, further supporting the indication that extension of the piperidinyl nitrogen atom substituent might not result in a good antipsychotic drug. However, putting the intention of developing safer antipsychotic drugs aside, further SAR evaluation based

on the structure of **14** is still essential for having a more comprehensive understanding of the structural requirements for 5-HT_{2A} affinity and selectivity. To accomplish this, future affinity screens of the compounds designed in this aim (**52**, **54**, and **55**) can be conducted. These data would refine the trend in SAR of simple alkyl chain substituents on the piperidinyl nitrogen atom on 5-HT_{2A} affinity and selectivity. Possibly, the reason why the affinity of **53** decreases relative to **15** is that longer substituents than a methyl group require an aromatic and/or a heteroatom-containing moiety. If there exists an aromatic requirement, **55** should result in greater affinity than **53** and **54**. Other longer alkyl chains (containing four carbon atoms or more) containing amine or hydroxy moieties should also be examined to determine if electrostatic interactions are crucial to 5-HT_{2A} affinity.

To further refine the SAR for 5-HT_{2A} receptor activity, quipazine (**45**), isoquipazine (**46**), 2-NP (**47**), and 1-NP (**48**) were examined in Aim 2 in a computational modeling study using crystal structures of the 5-HT_{2A} receptor. Specifically, the intention was to determine probable binding modes of these compounds to suggest reasons for their peculiar activities. HINT analysis results of the chosen binding poses are in accordance with the binding activities of these compounds. For example, the higher affinity compounds 2-NP and 1-NP display greater total interaction scores (1496 and 1454, respectively) than their structural counterparts and lower affinity compounds quipazine (899) and isoquipazine (1121), respectively. It is predicted that hydrophobic interactions might be paramount for the high affinity of this class of compounds as both 2-NP and 1-NP occupy a distinct binding pocket that contains more hydrophobic residues as compared to the binding pocket occupied by quipazine and isoquipazine. This is supported by the higher total hydrophobic scores of 2-NP (501) and 1-NP (649) compared with quipazine (239) and isoquipazine (479). One important question of this aim was: why does the addition of a nitrogen atom in the aromatic rings of 2-NP and 1-NP (as with quipazine and isoquipazine) result in such a reduction of affinity? The identified binding poses for these compounds addresses this question. Both quipazine and

isoquipazine formed electrostatic interactions with Ser159$^{3.36}$ and Asn343$^{6.55}$, respectively. It is predicted that because they participate in these interactions, quipazine and isoquipazine are "forced" to occupy a distinct pocket as compared to 2-NP and 1-NP, thus rendering them unable to participate in hydrophobic interactions that would otherwise confer higher affinity.

It should be noted that isoquipazine and 1-NP, the antagonists in this study, are structurally simple compounds and represent another pharmacophore for 5-HT_{2A} receptor antagonism. It could be argued that 1-NP represents a truer antagonist pharmacophore as compared to that derived in Aim 1 (des-fluoro analogue of **14**) due to its simpler structure: while both structures contain biaryl ring moieties bonded to unconjugated six-membered nitrogen atom-containing rings, 1-NP contains one fewer heteroatom in its structure. Based on the structure of 1-NP, simple deconstruction analyses can be conducted, particularly one that determines the necessity of the tertiary nitrogen atom. The piperazine ring can also be broken open, resulting in a long chain, to determine the importance of the ring for activity. If the piperazine ring is important for activity, the ring nitrogen atoms can be translocated through the ring to determine their optimal location.

The premise for the third aim was contrived from preliminary modeling studies utilizing docked structures DOB and nFen in the binding site of the 5-HT_{2B} receptor. These modeling studies drew attention to potential electrostatic interactions employed by both molecules to bind with residues. Specifically, HINT analysis revealed hydrogen bonds/acid base interactions involving the 5-OCH_3 and 4-Br substituents of DOB and the 3-CF_3 substituent of nFen. These results thus called into question the necessity of the 2-OCH_3 substituent of DOB and the electrastic/hydrophobic participation of the 3-CF_3 substituent of nFen (because fluoro atoms are capable of forming both hydrogen bonds and hydrophobic interactions with residues). To determine the involvement of these substituents, **65**, **68**, and **71** were synthesized and examined in a Ca^{2+}-release assay utilizing HEK-293T cells stably transfected with the 5-HT_{2B} receptor

plasmid, along with nFen and DOB as standards. To confirm that nFen's agonist activity at 5-HT_{2B} receptors is dependent on the 3-CF_3 substituent, amphetamine was also examined. Results indicated amphetamine is inactive as an agonist (at 10 μM) at 5-HT_{2B} receptors, confirming the essential nature of the 3-CF_3 substituent. Furthermore, this substituent most likely interacts with the binding site in a hydrophobic or both a hydrophobic and an electrostatic manner with the binding site, supported by functional activity results: although **65** (EC_{50} = 331 nM) resulted in over five-fold lower potency as compared with nFen (EC_{50} = 65 nM); both **65** and its positional isomer **68** (EC_{50} = 246 nM) resulted in low-nanomolar potency suggesting that hydrophobic interactions are very favorable for 5-HT_{2B} agonist activity. If electrostatic interactions were paramount for agonist activity, it is unlikely to observe such a large increase in agonist activity when comparing amphetamine to **65**. Not only did we observe high potency for the 3-CH_3 analogue **65**, we also observed similarly high potency for the 4-CH_3 analogue **66**, suggesting hydrophobic interactions might be so crucial, interaction can occur with both the 3- and 4-position substituents without much difference in potency.

Computational docking studies of nFen, **65**, and **68** revealed a similar positioning of their phenyl substituents in the binding site of the 5-HT_{2B} receptor as well as numerous hydrophobic residues near this region capable of interacting with 3- and 4-position substituents of these amphetamine analogues, supporting the hypothesis that hydrophobic interactions are paramount for the activity of nFen.

Functional activity analysis of **71** revealed that although the 2-OCH_3 substituent of DOB is not absolutely essential for functional activity, it does contribute: compound **71** (EC_{50} = 67 nM) resulted in an almost eight-fold reduction in potency as compared to DOB (EC_{50} = 8.7 nM). Computational docking results produced a potential binding pose for **71** based on the highest total interaction score from HINT analysis. This binding pose does not have its 3-OCH_3 substituent superimposed with the 5-OCH_3 substituent of DOB. Instead, **71**'s 3-OCH_3 substituent faces the

same direction as the 2-OCH_3 substituent of DOB, enabling methyl groups from both substituents to participate in identical hydrophobic interactions with the same binding site residues, supported by HINT. The 3-OCH_3 oxygen atom also forms a hydrogen bond with Thr140$^{3.37}$, which might contribute to **71**'s retention of nanomolar potency; **71** lacks the hydrogen bonds with Ser222$^{5.43}$ and Asn344$^{6.55}$ as observed in the model of DOB, therefore the hydrogen bonding with Thr140$^{3.37}$ might make up for this deficit of interaction.

A more logical representation of the binding of **71** at 5-HT_{2B} receptors is depicted in Panel C of Figure 35 which displays **71** essentially superimposed with DOB in the binding site. Due to the structural similarity between **71** and DOB, logic would suggest that both compounds would bind similarly. Although this binding pose did not produce the highest total interaction HINT score, it was still amongst the top 20 highest scoring solutions out of the 100 solutions generated and examined. Thus, this model is still a very viable candidate for the accurate representation of **71**'s binding. HINT analysis revealed that **71** participates in identical hydrogen bond interactions with Ser222$^{5.43}$ and Asn344$^{6.55}$ via its 4-Br and 3-OCH_3 substituents, as compared with DOB. The almost eight-fold lower potency of **71** compared with DOB can be explained by its lack of a 2-OCH_3 substituent, thus rendering it unable to participate in hydrophobic interactions via the methyl group (as observed with DOB). This model is a better representation of this difference in activity than the model discussed previously. In the previous model, **71** did not display any hydrogen bonding with Ser222$^{5.43}$ nor with Asn344$^{6.55}$ via its 4-Br substituent. Such a loss of hydrogen bond interaction is likely to result in a much more drastic reduction in potency, due to the high energy of these bonds. Instead, the slightly lower potency of **71** compared with DOB is much better explained by the lower hydrophobic interactions (a weaker type of bond) experienced by **71**.

Another explanation is that the majority of DOB's agonist effect is elicited by hydrophobic interactions via its 4-Br substituent, which would be more congruent with the hypothesis stated above (hydrophobic interactions are paramount for the 5-HT_{2B} activity of these analogues).

Continuing with the same reasoning, the methoxy substituents of DOB may contribute very little to its potency. It was determined in this study that the 2-OCH_3 substituent is not essential for activity, however there is also evidence that the 5-OCH_3 might not be necessary as supported by the high potency of **65** that contains no substituents capable of forming electrostatic interactions such as a methoxy substituent. Because of the similar lipophilicity of bromo (π = 0.86)[164] and methyl (π = 0.56)[164] substituents, simply a 4-Br substituent with no other phenyl substituents might be enough to elicit high potency. However, the bromo and methyl substituents contain opposite electronic character (σ_p = 0.23 and -0.17, respectively), thus there is still a possibility for electronic contribution of the 4-Br substituent of DOB. To conclude, the 2-OCH_3 substituent of DOB is not required for its agonist activity at 5-HT_{2B} receptors, unlike in the case of 5-HT_{2A} receptors where removal of the 2-OCH_3 substituent results in abolishment of affinity. With this simple revelation, we can already begin to separate the activity of compounds at 5-HT_{2A} and 5-HT_{2B} receptors. Furthermore, removal of the 5-OCH_3 substituent results in a drastic reduction of affinity for 5-HT_{2A} receptors. Future studies examining other amphetamine analogues such as 4-bromoamphetamine should be conducted to definitively test for the necessity of the 3-OCH_3 substituent of **71**.

Another goal of this aim was to gain understanding with regards to the SAR of phenylisopropylamines at 5-HT_{2B} receptors. To accomplish this, a series of phenylisopropylamines (DOB, DOI, DOF, DON, DOPR, DOTB, and MEM) were examined for their functional activity at 5-HT_{2B} receptors. It was discovered that larger, more lipophilic halogen substituents are best tolerated, as supported by the vast difference in activity of DOF (EC_{50} = 439 nM) which contains a smaller, less lipophilic 4-F substituent, compared to the activity of DOB (EC_{50} = 8.7 nM) and DOI (EC_{50} = 39 nM) which contain larger and much more lipophilic 4-position substituents. The importance of the lipophilic nature of the 4-position substituent is substantiated by the data obtained from DOPR and DOTB. Both compounds produced approximately equal

potency, similar to that produced by DOI. Assuming that these phenylisopropylamines bind similarly to the proposed binding mode of the amphetamine analogues examined above (**65** and **68**, Figure 33), and **71** and DOB (Figure 35), numerous hydrophobic residues (Val136$^{3.33}$, Leu209^{EL2}, Phe217$^{5.38}$, Ile186$^{4.56}$, and Ala225$^{5.46}$) are available within interacting distance of the 4-position substituent, thus explaining the high activities of DOPR (EC_{50} = 29 nM) and DOTB (EC_{50} = 37 nM) which both contain lipophilic 4-position alkyl chain substituents capable of forming hydrophobic interactions. DOB and DOI might additionally participate in hydrogen bonding interactions with residues such as Ser222$^{5.43}$ and Asn344$^{6.55}$ as depicted in the docked model of DOB (Figure 35), contributing to their high activities. The lower activity of MEM might suggest that electron withdrawing substituents are not very well tolerated at the 4-position.

Given the combined results from Aim 3, the pharmacophore model in Figure 27 can be refined. It was proposed that the phenyl substituents of the pharmacophore can contain substituents either in the 3- or 4-positions capable of forming electrostatic or hydrophobic interactions with the binding site. Our functional assay data for **65** and **68** revealed that methyl substituents are well tolerated at both the 3- and 4-positions of the phenyl rings. Thus our model can be refined to specify that both hydrophobic interactions with 3- and 4-position phenyl substituents of amphetamine-like compounds elicit activity at 5-HT_{2B} receptors (Figure 40); however, electrostatic interactions might still contribute to greater activity as portrayed by the higher potency of nFen as compared with either **65** or **68**.

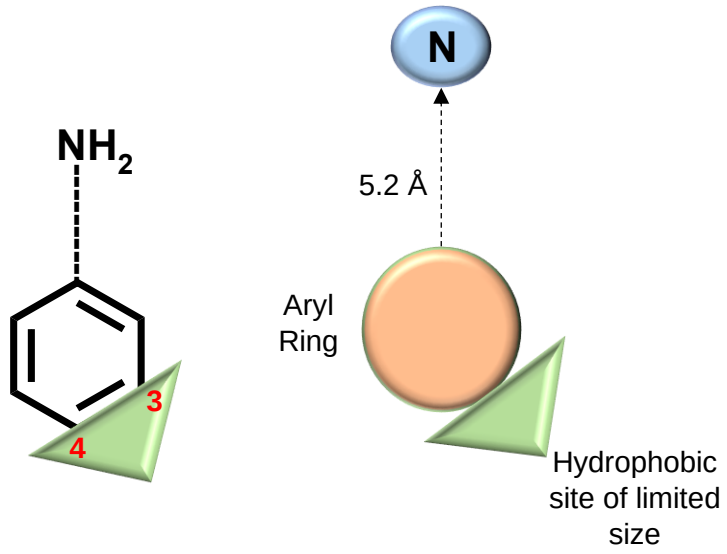

Figure 40. Revised pharmacophore for 5-HT_{2B} receptor agonist action.

This revised model also accounts for the agonist actions of the DOX analogues. Although a role for possible electrostatic interactions cannot be eliminated, it would appear that hydrophobic interactions play a dominant role, but that the site these substituents interact with is of limited size. Compounds with large lipophilic substituents bind (e.g., DOHx, DOBz) with affinities nearly comparable to DOB, but are without agonist action.

VI. Experimental

A. Synthesis

Compounds were characterized using mass spectrometry (MS), proton nuclear magnetic resonance (^{1}H NMR), and melting point analysis using the Thomas Hoover melting point apparatus. The ^{1}H NMR used was a Bruker AXR 400 MHz spectrometer using tetramethylsilane (TMS) as an internal standard. The positions of the peaks in the ^{1}H NMR spectra were reported as parts per million (δ). The coupling constants (*J*, Hz) and integration values were reported for all compounds. The splitting pattern of the peaks were also reported as containing either singlets (s), doublets (d), triplets (t), quartets (dd) doublet of doublets (td), triplet of doublets, (td), or multiplets (m). Reactions were monitored using thin layer chromatography (TLC) using silica gel GHLF plates. Purification of compounds was done using flash chromatography (ComiFlash Companion/TS) and recrystallization methods. All compounds were prepared as hydrochloride salts.

6-Fluoro-3-(piperidin-4-yl)benz[d]isoxazole Hydrochloride (**14**)

Crude compound **61** (1.0 g, 4.03 mmol) was dissolved in anhydrous EtOH (25 mL) and was added to a stirred mixture of HCl (1.4 mL) in anhydrous EtOH (10 mL) under an N_2 atmosphere. The resulting mixture was heated at reflux for 3 h and was allowed to stand at room temperature for five days. The resulting precipitate was collected by filtration and was recrystallized from MeOH/Et_2O to yield 0.07 g of **14** (8%) as a buff colored solid: mp 298-302 °C (lit.[159] 293-295 °C). No further characterization of the compound was conducted.

6-Fluoro-3-(1-propyl-4-piperidyl)-1,2-benzoxazole Hydrochloride (**53**)

Compound **14** (1.0 g, 4.5 mmol) was dissolved in acetonitrile and 1-iodopropane (0.53 mL, 5.45 mmol) and K_2CO_3 (1.9 g, 13.6 mmol) were added. The mixture was heated at reflux for 15 h,

cooled to rt and K_2CO_3 was filtered and washed with acetonitrile. The filtrate was concentrated to an oil and the oil was purified using column chromatography (EtOAc/MeOH). Ethereal HCl was added in a dropwise manner to the freebase dissolved in Et_2O forming the final compound **53** as an HCl salt which was purified by recrystallization using MeOH/Et_2O yielding 0.07 g of **53**: mp 200-204 °C (lit.[160] mp 208-210 °C); ^{1}H NMR (DMSO-d_6) δ 0.88-1.04 (m, 3H, CH_3), 1.62 (s, 1H, CH), 1.80-2.23 (m, 4H, CH_2, CH_2), 2.70-3.01 (m, 4H, CH_2, CH_2), 3.01-3.26 (m, 2H, CH_2), 3.27-3.50 (m, 1H, CH), 3.60-3.75 (m, 2H, CH_2), 7.01-7.27 (m, 1H, CH), 7.54 (dd, J = 4.99, 3.77 Hz, 1H, CH), 8.32 (dd, J = 5.11, 3.78 Hz, 1H, NH^+); HRMS (ESI-TOF) m/z $[M + H]^+$ calcd for $C_{15}H_{20}FN_2O$, 236.1556; found, 236.1550.

***N*-Formylpiperidine-4-carboxylic acid** (**57**)

AC_2O (28.5 mL) and HCOOH (11.4 mL) were stirred for 1 h at 60 °C under an N_2 atmosphere and gradually cooled to 0 °C using an ice-bath. Isonipecotic acid (6.5 g, 50.3 mmol) was added portionwise and the reaction mixture was stirred for 16 h at room temperature. The solvent was evaporated under reduced pressure and the resulting pale white solid was recrystallized from *i*-PrOH to yield 5.3 g (68%) of **57** as a white solid: mp 134-137 °C (lit.[167] 136-138 °C).

***N*-Formylpiperidine-4-carboxylic acid chloride** (**58**)

Compound **57** (5.3 g, 34.0 mmol) was added portionwise to $SOCl_2$ (5.1 mL) which had been stirred and cooled to 0 °C. DMF was added and the reaction mixture was allowed to stir at room temperature overnight under an N_2 atmosphere. $SOCl_2$ was evaporated under reduced pressure to yield 9.0 g of an orange oil. The crude oil was used without further characterization for the preparation of **59**.

***N*-Formyl-4-(2,4-difluorobenzoyl)piperidine** (**59**)

$AlCl_3$ (11.7 g, 87.7 mmol) was added portionwise to a stirred mixture of **58** (9.0 g, 51.3 mmol) in 1,3-difluorobenzene (36.2 mL), under an N_2 atmosphere. The reaction mixture was heated at reflux for 3 h and was quenched by pouring the reaction mixture into ice-H_2O. The aqueous mixture was extracted with $CHCl_3$ (3 x 50 mL) and the combined organic portion was washed with H_2O (1 x 50 mL), dried ($MgSO_4$) and evaporated under reduced pressure to yield 11.9 g of a dark brown oil. The oil was purified using column chromatography to yield 3.0 g (23%) of **59** as a brown oil.

***N*-Formyl-4-((2,4-difluorophenyl)(hydroxyimino)methyl)piperidine** (**60**)

Compound **59** (3.0 g, 12 mmol) was dissolved in anhydrous EtOH (45 mL) and the resulting solution was added dropwise to a stirred solution of hydroxylamine hydrochloride (2.5 g, 36 mmol) in anhydrous EtOH (48 mL) under an N_2 atmosphere. A solution of NaOH (1.49 g, 37.2 mmol) in H_2O (9.3 mL) was added to the reaction mixture. The reaction mixture was heated at reflux overnight under an N_2 atmosphere. The resulting precipitate was removed by filtration and the filtrate was evaporated under reduced pressure, yielding a yellow solid which was recrystallized from H_2O, yielding 1.2 g (36%) of **60** as a pale yellow solid: mp 182-186 °C (lit.[159] 182-184 °C).

***N*-Formyl-4-(6-fluorobenz[d]isoxazol-3-yl)piperidine** (**61**)

Compound **60** (1.2 g, 4.4 mmol) was dissolved in anhydrous DMF (12 mL) and was stirred under an N_2 atmosphere. The solution was added dropwise to toluene-washed NaH (0.2 g, 8.7 mmol). The reaction mixture was heated at 75 °C for 4 h and was allowed to stir under an N_2 atmosphere for 96 h. The reaction mixture was quenched by pouring the mixture into H_2O. The aqueous mixture was extracted with EtOAc (3 x 30 mL) and the combined organic portion was washed with H_2O (1 x 50 mL), dried ($MgSO_4$) and concentrated under reduced pressure, yielding 1.0 g (93%) of **61** as an orange oil which was used crude in the preparation of **14**.

(*E*)-1-Methyl-3-(2-nitropropen-1-yl)benzene (**64**)

3-Methylbenzaldehyde (**63**, 2.0 g, 16.6 mmol) and NH_4OAc (1.8 g, 22.7 mmol) were stirred and heated at reflux in nitroethane (33.3 mL for 48 h. The reaction mixture was poured into H_2O (10 mL). The mixture was extracted (3 x 30 mL) with EtOAc and the combined EtOAc fraction was washed with brine and dried ($MgSO_4$). Evaporation of EtOAc under reduced pressure resulted in a crude oil which was purified using column chromatography resulting in 1.6 g (54%) of the pure oil **64** which was used in the preparation of **65**.

1-(3-Methylphenyl)propan-2-amine Hydrochloride (**65**)

A suspension of $LiAlH_4$ (2.4 g, 62.5 mmol) in THF (47 mL) was added using an addition funnel to **64** (1.6 g, 8.9 mmol). The solution was heated under reflux for 2 h. Reaction mixture was quenched with H_2O (2.4 mL), 15% NaOH aq. solution (2.4 mL), and H_2O (7.1 mL), resulting in white crystals (Li and Al salts) which were filtered off and washed with Et_2O. The filtrate was dried ($MgSO_4$) and concentrated to an oil. The oil was purified using column chromatography (silica gel; $CHCl_3$/MeOH). The oil was dissolved in Et_2O and concentrated ethereal HCl was added in a dropwise manner until the solution turned acidic. 0.2 g (13%) of the solid **65** was collected by vacuum filtration: mp 134-135 °C (lit.[168] mp 113-115 °C); 1.15 (d, *J* = 6.5 Hz, 3H, CH_3), 2.35 (s, 3H, CH_3), 2.66 (dd, *J* = 9.4 Hz, 1H, CH_2), 3.07 (dd, *J* = 4.9 Hz, 1H CH), 3.38-3.43 (m, 1H, CH), 7.07-7.13 (m, 3H, CH), 7.27 (tr, *J* = 7.5 Hz, 1H, CH), 8.22 (s, 3H, NH_3^+).

(*E*)-1-Methyl-4-(2-nitropropen-1-yl)benzene (**67**)

4-Methylbenzaldehyde (**66**, 2.0 g, 16.6 mmol) and NH_4OAc (1.8 g, 22.7 mmol) were stirred and heated at reflux in nitroethane (33.3 mL) overnight. The reaction mixture was poured into H_2O (10 mL). The mixture was extracted with EtOAc (3 x 30 mL) and the combined EtOAc fraction was washed with brine and dried ($MgSO_4$). Evaporation of EtOAc under reduced pressure resulted in

a crude oil, which mostly solidified under vacuum. The solid was filtered and washed with cold EtOH. The solid was recrystallized from EtOH affording 1.52 g (52%) of **67** as a yellow colored solid. **67** was used in the preparation of **68**. mp 55-56 °C (lit.[169] mp 53-54 °C).

1-(4-Methylphenyl)propan-2-amine Hydrochloride (**68**)

A suspension of $LiAlH_4$ (1.5 g, 39.5 mmol) in THF (30 mL) was added using an addition funnel to **67** (1 g, 5.6 mmol). The solution was heated at reflux for 2 h. The reaction mixture was quenched with H_2O (1.5 mL), 15% NaOH aq. solution (1.5 mL), and H_2O (4.5 mL), resulting in white crystals (Li and Al salts) which were filtered off and washed with Et_2O. The filtrate was dried ($MgSO_4$) and concentrated to an oil. The oil was purified using column chromatography (silica gel; $CHCl_3$/MeOH). The resulting oil was dissolved in Et_2O and concentrated ethereal HCl was added in a dropwise manner until the solution turned acidic. The resulting solid was collected by vacuum filtration affording 0.04 g (13%) of the final compound **68** as a white solid. mp 155-156 °C (lit.[168] mp 148-150 °C); ^{1}H NMR (DMSO-d_6) δ 1.10 (d, J = 6.5 Hz, 3H, CH_3), 2.29 (s, 3H, CH_3), 2.62 (dd, J = 9.2 Hz, 1H, CH_2), 2.99 (dd, J = 13.2 Hz, 1H, CH_2), 3.34 (m, 1H, CH), 7.14 (dd, J = 8.2 Hz, 2H, CH), 8.09 (s, 3H, NH_3^+).

(*E*)-1-Bromo-2-methoxy-4-(2-nitropropen-1-yl)benzene (**70**)

3-Methoxy-4-bromobenzaldehyde (**69**, 0.3 g, 1.4 mmol) and NH_4OAc (0.7 g, 9.1 mmol) were heated to reflux in nitroethane (10 mL) overnight. The reaction mixture was poured into H_2O (10 mL). The mixture was extracted with EtOAc (3 x 15 mL) and the EtOAc layer was washed with brine and dried over $MgSO_4$. Evaporation of EtOAc under reduced pressure resulted in a crude oil, which was purified using column chromatography (silica gel; hexane/EtOAc) affording 0.2 g of **70** (63%) as a brown oil. Compound **70** was used in the preparation of **71**.

1-(4-Bromo-3-methoxyphenyl)propan-2-amine Hydrochloride (**71**)

$NaBH_4/BF_3$ (0.97 g, 2.6 mmol) was added to a round bottom flask and cooled to 0 °C. THF (7 mL) was added, the ice bath was removed, and the contents were stirred for 15 min; **70** in THF (3 mL) was added and the reaction mixture was stirred at reflux for 5.5 h. The mixture was cooled to rt, quenched with H_2O (6.8 mL), acidified (1 N HCl, 6.8 mL) and heated at 85 °C for 2 h. The mixture was cooled to rt and the acid layer was washed with Et_2O (2 x 10 mL) and basified with 5 M NaOH. The solution was extracted with Et_2O (3 x 15 mL). The organic layer was dried ($MgSO_4$) and concentrated to an oil. The oil was dissolved in Et_2O and ethereal HCl was added to form a solid. The solid was filtered and recrystallized with MeOH/Et_2O affording 0.048 g (32%) of **71**. mp = 145-150 °C (lit.[166] mp = 151-152 °C); ^{1}H NMR (DMSO-d_6) δ (d, J = 1.15, 6.5 Hz, 3H, CH_3), (dd, J = 2.72, 8.2 Hz 1H, CH), (dd, J = 2.97, 5.8 Hz 1H, CH), (s, J = 3.45, 1H CH), (s, J = 3.86, 3H, CH_3), (d, J = 6.78, 8 Hz, 1H, CH), (s, J = 7.04, 8.2 Hz, 1H, CH), (d, J = 7.51, 8 Hz, 1H, CH), (s, J = 8.11, 3H, NH_3^+)

B. Computational Docking

All compounds were sketched using SYBYL-X 2.1.1 and were energy minimized utilizing the Tripos Force Field with Gasteiger-Hückel charges, a non-bonded interaction cutoff of 8 Å, dielectric constant (ε) of 4.00 D/Å, and a termination gradient of 0.05 kcal/(mol*Å). The structures were then docked at either the 5-HT_{2B} receptor crystal structure (active, PDB: 6DRY) or 5-HT_{2A} crystal structures [active (PDB: 6WHA) or inactive (PDB: 6A94)] using GOLD v5.6 which generated up to 100 protein-ligand complexes for each compound and GOLD scores, based on an in-program scoring system, for each complex. Complexes were then energy minimized using SYBYL-X 2.1.1 and evaluated by HINT score analysis within SYBYL 8.1. A built-in GOLD clustering program (using an RMSD cutoff of 0.75 Å) was used in conjunction with the docking of quipazine (**45**), isoquipazine (**46**), 2-NP (**47**), and 1-NP (**48**). The resulting clusters were analyzed according to which one contained the highest scoring GOLD solution [highest scoring cluster

(HSC)] and which one contained the most number of solutions [most populated cluster (MPC)]. The final binding poses for quipazine and isoquipazine were selected because they were the highest GOLD-scoring solutions. The binding poses for 2-NP and 1-NP were selected because they were the highest scoring solutions within the MPC. The binding mode of *R*(-)-DOB was selected because it produced the highest GOLD score. The binding mode of *S*(+)-nFen was selected because it produced the highest GOLD-scoring solution that most closely resembled the binding mode of *R*(-)-DOB. The binding modes for *S*-**64**, *S*-**68**, and *R*-**71** were selected because they produced the highest overall HINT interaction scores. An additional binding mode for *R*-**71** was proposed because it was the highest HINT interaction-scoring pose which most closely resembled the binding mode of *R*(-)-DOB. PYMOL was used to produce high quality images of docked structures.

C. Functional Activity Studies

Functional activity studies of the compounds were conducted using a Ca^{2+} binding assay using the epifluorescent microscope (Olympus IX71). Cells used for experiments were cultured using Dulbecco's Modified Eagle Medium (DMEM) containing 10% fetal bovine serum (FBS) and 5% penicillin/streptomycin. The fluorescent indicator used during experiments was Fura 2-AM. Cells were analyzed using wavelengths of 340 nm and 380 nm, bandwidth of 12 nm, light intensity of 15%, and exposure of 70 ms. Three wells containing cells were analyzed for each concentration per experiment day. Two experiments were conducted for each drug. All data was processed used Fiji software by ImageJ2 which allowed manual selection of cells and measurement of fluorescence. Logarithmic concentration-response curves were generated using Graphpad Prism 8. Curves were generated with a Hill slope of 1.0 to allow easier comparison of potencies of the various compound analyzed.

References

1. Glennon, R. A.; Dukat, M. Serotonin receptors and drugs affecting serotonergic neurotransmission. Foye's Principles of Medicinal Chemistry. 7th ed, T. L. Lemke, D. A Williams, V. F. Roche, S. W. Zito, Lippincott Williams and Wilkins, Baltimore, Chapter 11, 2013, pp 365-396.
2. Aghajanian, G. K.; Sanders-Bush, E. Serotonin. In *Neuropsychopharmacology – 5th Generation of Progress*, Ed. 5; Davis, K. L., Charney, D., Coyle, J. T., Nemeroff, C., Eds.; Lippincott, Williams, & Williams: Philadelphia, 2002; pp 15-34.
3. Vialli, M.; Erspamer, V. Ricerche sul secreto delle cellule enterocromaffini. *Boll. Soc. Med-Chir. Pavia* **1937**, *51*, 357-363.
4. Twarog, B. M.; Page, I. H. Serotonin content of some mammalian tissues and urine and a method for its determination. *Am. J. Physiol.* **1953**, *175*, 157-161.
5. Nichols, D. E.; Nichols, C. D. Serotonin receptors. *Chem. Rev.* **2008**, *108*, 1614-1641.
6. Mohammad-Zadeh, L. F.; Moses, L.; Gwaltney-Brant, S. M. Serotonin: A review. *J. Vet. Pharmacol. Ther.* **2008**, *31*, 187-199.
7. Ruddell, R. G.; Mann, D. A.; Ramm, G. A. The function of serotonin within the liver. *J. Hepatol.* **2008**, *48*, 666-675.
8. Gaddum, J. H.; Picarelli, Z. P. Two kinds of tryptamine receptor. *Br. J. Pharmacol.* **1957**, *120*, 134-139.
9. Peroutka, S. J.; Snyder, S. H. Multiple serotonin receptors: Differential binding of [^{3}H]5-hydroxytryptamine, [^{3}H]lysergic acid diethylamide and [^{3}H]spiroperidol. *Mol. Pharmacol.* **1979**, 687-699.
10. Bradley, P. B.; Engel, G.; Feniuk, W.; Fozard, J. R.; Humphrey, P. P. A.; Middlemiss, D. N.; Mylecharane, E. J.; Richardson, B. P.; Saxena, P. R. Proposals for the classification

and nomenclature of functional receptors for 5-hydroxytryptamine. *Neuropharmacology* **1986**, *25*, 563-576.

11. McCorvy, J.; Roth, B. Structure and function of serotonin G protein-coupled receptors. *Pharmacol. Ther.* **2015**, *150*, 129-142.
12. Leysen, J. E.; Niemegeers, C. J. E.; Tollenaere, J. P.; Laduron, P. M. Serotonergic component of neuroleptic receptors. *Nature* **1978**, *272*, 168-171.
13. Burnet, P. W. J.; Eastwood, S. L.; Lacey, K.; Harrison, P. J. The distribution of 5-HT_{1A} and 5-HT_{2A} receptor mRNA in human brain. *Brain Res.* **1995**, *676*, 157-168.
14. Wong, D. F.; Lever, J. R.; Hartig, P. R.; Dannals, R. F.; Villemagne, V.; Hoffman, B. J.; Wilson, A. A.; Ravert, H. T.; Links, J. M.; Scheffel, U.; Wagner, H. N. Localization of serotonin 5-HT_2 receptors in living human brain by positron emission tomography using N1-([^{11}C]-methyl)-2-Br-LSD. *Synapse* **1987**, *1*, 393-398.
15. Lairez, O.; Cognet, T.; Schaak, S.; Calise, D.; Guilbeau-Frugier, C.; Parini, A.; Mialet-Perez, J. Role of serotonin 5-HT_{2A} receptors in the development of cardiac hypertrophy in response to aortic constriction in mice. *J. Neural Transm.* **2013**, *120*, 927-935.
16. Gómez-Gil, E.; Gastó, C.; Díaz-Ricart, M.; Carretero, M.; Salamero, M.; Catalán, R.; Escolar, G. Platelet 5-HT_{2A}-receptor-mediated induction of aggregation is not altered in major depression. *Hum. Psychopharmacol.* **2002**, *17*, 419-424.
17. Tierney, A. J. Invertebrate serotonin receptors: A molecular perspective on classification and pharmacology. *J. Exp. Biol.* **2018**, *221*, 1-11.
18. Vane, J. R. A sensitive method for the assay of 5-hydroxytraptamine. *Br. J. Pharmacol*. **1997**, *120*, 142-147.
19. Hoyer, D.; Hannon, J. P.; Martin, G. R. Molecular, pharmacological and functional diversity of 5-HT receptors. *Pharmacol. Biochem. Behav.* **2002**, *71*, 533-554.

20. Choi, D. S.; Birraux, G.; Launay, J. M.; Maroteaux, L. The human serotonin 5-HT_{2B} receptor: Pharmacological link betweeen 5-HT_2 and 5-HT_{1D}. *FEBS Lett.* **1994**, *352*, 393-399.
21. Duxon, M. S.; Flanigan, T. P.; Reavley, A. C.; Baxter, G. S.; Blackburn, T. P.; Fone, K. C. F. Evidence for expression of the 5-hydroxyramine-2B receptor protein in the rat central nervous system. *Neuroscience* **1997**, 323-329.
22. Launay, J. M.; Hervé, P.; Peoc'h, K.; Tournois, C.; Callebert, J.; Nebigil, C. G.; Etienne, N.; Drouet, L.; Humbert, M.; Simonneau, G.; Maroteaux, L. Function of the serotonin 5-hydroxytryptamine 2B receptor in pulmonary hypertension. *Nat. Med.* **2002**, *8*, 1129-1135.
23. Hoffman, B. J.; Mezey, E. Distribution of serotonin 5-HT_{1c} receptor mRNA in adult rat brain. *FEBS Lett.* **1989**, *247*, 453-462.
24. Clemett, D. A.; Punhani, T.; Duxon, M. S.; Blackburn, T. P.; Fone, K. C. F. Immunohistochemical localisation of the 5-HT_{2C} receptor protein in the rat CNS. *Neuropharmacology* **2000**, *39*, 123-132.
25. Heisler, L. K.; Zhou, L.; Bajwa, P.; Hsu, J.; Tecott, L. H. Serotonin 5-HT_{2C} receptors regulate anxiety-like behavior. *Genes, Brain Behav.* **2007**, *6*, 491-496.
26. Müller, C. P.; Carey, R. J. Intracellular 5-HT_{2C}-receptor dephosphorylation: A new target for treating drug addiction. *Trends Pharmacol. Sci*. **2006**, *27*, 455-458.
27. Alex, K. D.; Yavanian, G. J.; McFarlane, H. G.; Pluto, C. P.; Pehek, E. A. Modulation of dopamine release by striatal 5-HT_{2C} receptors. *Synapse* **2005**, *55*, 242-251.
28. Millan, M. J. Serotonin 5-HT_{2C} receptors as a target for the treatment of depressive and anxious states: Focus on novel therapeutic strategies. *Therapie* **2005**. *60*, 441-460.
29. Bonhaus, D. W.; Weinhardt, K. K.; Taylor, M.; Desouza, A.; Mcneeley, P. M.; Szczepanski, K.; Fontana, D. J.; Trinh, J.; Rocha, C. L.; Dawson, M. W.; Flippin, L. A.; Eglen, R. M. RS-102221: A novel high affinity and selective, 5-HT_{2C} receptor antagonist. *Neuropharmacology* **1997**, *36*, 621-629.

30. Reynolds, G. P.; Hill, M. J.; Kirk, S. L. The 5-HT_{2C} receptor and antipsychotic-induced weight gain - mechanisms and genetics. *J. Psychopharmacol.* **2006**, *20*, 15-18.
31. Aghajanian, G. K.; Marek, G. J. Serotonin model of schizophrenia: Emerging role of glutamate mechanisms. *Brain Res. Rev.* **2000**, *31*, 302-312.
32. Gaddum, J. H. Antagonism between lysergic acid diethylamide and 5-hydroxytryptamine. *J. Physiol.* **1953**, *121*, 15P.
33. Shaw, E.; Woolley, D. W. Some serotoninlike activities of lysergic acid diethylamide. *Science* **1956**, *124*, 121-122.
34. Woolley, D. W.; Shaw, F. N. Evidence for the participation of serotonin in mental processes. *Ann. N. Y. Acad. Sci.* **1957**, *66*, 649-667.
35. Balestrieri, A.; Fontanari, D. Acquired and crossed tolerance to mescaline, LSD-25, and BOL-148. *AMA Arch. Gen. Psychiatry* **1959**, *1*, 279-282.
36. Glennon, R. A.; Titeler, M.; McKenney, J. D. Evidence for 5-HT_2 involvement in the mechanism of action of hallucinogenic agents. *Life Sci.* **1984**, *35*, 2505-2511.
37. Vollenweider, F. X.; Vollenweider-Scherpenhuyzen, M. F. I.; Bäbler, A.; Vogel, H.; Hell, D. Psilocybin induces schizophrenia-like psychosis in humans via a serotonin-2 agonist action. *Neuroreport* **1998**, *9*, 3897-3902.
38. Winblad, B.; Bucht, G.; Gottfries, C. G.; Roos, B. E. Monoamines and monoamine metabolites in brains from demented schizophrenics. *Acta Psychiatr. Scand.* **1979**, *60*, 17-28.
39. Abi-Dargham, A.; Laruelle, M.; Aghajanian, G. K.; Charney, D.; Krystal, J. The role of serotonin in the pathophysiology and treatment of schizophrenia. *J. Neuropsychiatry Clin. Neurosci.* **1997**, *9*, 1-17.
40. Carlsson, A.; Lindqvist, M. Effect of chlorpromazine or haloperidol on formation of 3-methoxytyramine and normetanephrine in mouse brain. *Acta Pharmacol. Toxicol. (Copenh).* **1963**, *20*, 140-144.

41. Preskorn, S. H. The evolution of antipsychotic drug therapy: Reserpine, chlorpromazine, and haloperidol. *J. Psychiatr. Pract.* **2007**, *13*, 253-257.
42. Carlsson, A.; Lindqvist, M.; Magnusson, T. 3,4-Dihydroxyphenylalanine and 5-hydroxytryptophan as reserpine antagonists. *Nature* **1957**, *180*, 1200.
43. Snyder, S. H. The dopamine hypothesis of schizophrenia: Focus on the dopamine receptor. *Am. J. Psychiatry* **1976**, *133*, 197-202.
44. Davis, K. L.; Kahn, R. S.; Ko, G.; Davidson, M. Dopamine in schizophrenia: A review and reconceptualization. *Am. J. Psychiatry* **1991**, *148*, 1474-1486.
45. Pycock, C. J.; Kerwin, R. W.; Carter, C. J. Effect of lesion of cortical dopamine terminals on subcortical dopamine receptors in rats. *Nature* **1980**, *286*, 74-77.
46. Scatton, B.; Worms, P.; Lloyd, K. G.; Bartholini, G. Cortical modulation of striatal function. *Brain Res.* **1982**, *232*, 331-343.
47. Sesack, S. R.; Carr, D. B.; Omelchenko, N.; Pinto, A. Anatomical substrates for glutamate-dopamine interactions: Evidence for specificity of connections and extrasynaptic actions. *Ann. N. Y. Acad. Sci.* **2003**, *1003*, 36-52.
48. Javitt, D. C.; Zukin, S. R. Recent advances in the phencyclidine model of schizophrenia. *Am. J. Psychiatry* **1991**, *148*, 1301-1308.
49. Luby, E. D.; Cohen, B. D.; Rosenbaum, G.; Gottlieb, J. S.; Kelley, R. Study of a new schizophrenomimetic drug-sernyl. *Arch. Neurol. Psychiatry* **1959**, *81*, 363-369.
50. Anis, N. A.; Berry, S. C.; Burton, N. R.; Lodge, D. The dissociative anaesthetics, ketamine and phencyclidine, selectively reduce excitation of central mammalian neurones by N-methyl-aspartate. *Br. J. Pharmacol.* **1983**, *79*, 565-575.
51. Javitt, D. C.; Zukin, S. R. The role of excitatory amino acids in neuropsychiatric illness. *J. Neuropsychiatry Clin. Neurosci.* **1990**, *2*, 44-52.

52. Wong, E. H. F.; Kemp, J. A.; Priestley, T.; Knight, A. R.; Woodruff, G. N.; Iversen, L. L. The anticonvulsant MK-801 is a potent *N*-methyl-D-aspartate antagonist. *Proc. Natl. Acad. Sci. U. S. A.* **1986**, *83*, 7104-7108.
53. Cohen, S. M.; Tsien, R. W.; Goff, D. C.; Halassa, M. M. The impact of NMDA receptor hypofunction on GABAergic neurons in the pathophysiology of schizophrenia. *Schizophr. Res.* **2015**, *167*, 98-107.
54. Mortensen, M.; Patel, B.; Smart, T. G. GABA potency at $GABA_A$ receptors found in synaptic and extrasynaptic zones. *Front. Cell. Neurosci*. **2012**, *6*, 1-10.
55. Padgett, C. L.; Slesinger, P. A. $GABA_B$ receptor coupling to G-proteins and ion channels. *Adv. Pharmacol.* **2010**, *58*, 123-147.
56. Li, K.; Xu, E. The role and the mechanism of γ-aminobutyric acid during central nervous system development. *Neurosci. Bull*. **2008**, *24*, 195-200.
57. Chiapponi, C.; Piras, F.; Piras, F.; Caltagirone, C.; Spalletta, G. GABA system in schizophrenia and mood disorders: A mini review on third-generation imaging studies. *Front. Psychiatry* **2016**, *7*, 1-10.
58. de Jonge, J. C.; Vinkers, C. H.; Hulshoff Pol, H. E.; Marsman, A. GABAergic mechanisms in schizophrenia: Linking postmortem and in vivo studies. *Front. Psychiatry* **2017**, *8*, 1-10.
59. Volk, D. W.; Austin, M. C.; Pierri, J. N.; Sampson, A. R.; Lewis, D. A. Decreased glutamic acid decarboxylase$_{67}$ messenger RNA expression in a subset of prefrontal cortical γ-aminobutyric acid neurons in subjects with schizophrenia. *Arch. Gen. Psychiatry* **2000**, *57*, 237-245.
60. Hashimoto, T.; Volk, D. W.; Eggan, S. M.; Mirnics, K.; Pierri, J. N.; Sun, Z.; Sampson, A. R.; Lewis, D. A. Gene expression deficits in a subclass of GABA neurons in the prefrontal cortex of subjects with schizophrenia. *J. Neurosci.* **2003**, *23*, 6315-6326.
61. Cowan, R. L.; Wilson, C. J.; Emson, P. C.; Heizmann, C. W. Parvalbumin-containing gabaergic interneurons in the rat neostriatum. *J. Comp. Neurol.* **1990**, *302*, 197-205.

62. Hashimoto, T.; Arion, D.; Unger, T.; Maldonado-Avilés, J. G.; Morris, H. M.; Volk, D. W.; Mirnics, K.; Lewis, D. A. Alterations in GABA-related transcriptome in the dorsolateral prefrontal cortex of subjects with schizophrenia. *Mol. Psychiatry* **2008**, *13*, 147-161.
63. Ohnuma, T.; Augood, S. J.; Arai, H.; McKenna, P. J.; Emson, P. C. Measurement of GABAergic parameters in the prefrontal cortex in schizophrenia: Focus on GABA content, $GABA_A$ receptor α-1 subunit messenger RNA and human GABA transporter-1 (hGAT-1) messenger RNA expression. *Neuroscience* **1999**, *93*, 441-448.
64. López-Muñoz, F.; Alamo, C.; Cuenca, E.; Shen, W. W.; Clervoy, P.; Rubio, G. History of the discovery and clinical introduction of chlorpromazine. *Ann. Clin. Psychiatry* **2005**, *17*, 113-135.
65. Meyer, J. M.; Simpson, G. M. From chlorpromazine to olanzapine: A brief history of antipsychotics. *Psychiatr. Serv.* **1997**, *48*, 1137-1139.
66. Shen, W. W. A history of antipsychotic drug development. *Compr. Psychiatry* **1999**, *40*, 407-414.
67. Carpenter, W. T.; Davis, J. M. Another view of the history of antipsychotic drug discovery and development. *Mol. Psychiatry* **2012**, *17*, 1168-1173.
68. Baumeister, A. A. The chlorpromazine enigma. *J. Hist. Neurosci.* **2013**. *22*, 14-29.
69. Shore, P. A.; Silver, S. L.; Brodie, B. B. Interaction of reserpine, serotonin, and lysergic acid diethylamide in brain. *Science* **1955**, *122*, 284-285.
70. Meltzer, H. Y. Update on typical and atypical antipsychotic drugs. *Annu. Rev. Med*. **2013**, *64*, 393-406.
71. Jafari, S.; Fernandez-Enright, F.; Huang, X. F. Structural contributions of antipsychotic drugs to their therapeutic profiles and metabolic side effects. *J. Neurochem*. **2012**, *120*, 371-384.

72. Avram, S.; Berner, H.; Milac, A. L.; Wolschann, P. Quantitative structure - activity relationship studies on membrane receptors inhibition by antipsychotic drugs. Application to schizophrenia treatment. *Monatsh. Chem.* **2008**, *139*, 407-426.
73. Barceló, M.; Raviña, E.; Varela, M. J.; Brea, J.; Loza, M. I.; Masaguer, C. F. Potential atypical antipsychotics: Synthesis, binding affinity and SAR of new heterocyclic bioisosteric butyrophenone analogues as multitarget ligands. *MedChemComm* **2011**, *2*, 1194-1200.
74. Sekhar, K. V. G. C.; Kumar Vyas, D. R.; Nagesh, H. N.; Rao, V. S. Pharmacophore hypothesis for atypical antipsychotics. *Bull. Korean Chem. Soc.* **2012**, *33*, 2930-2936.
75. Awadallah, F. M. Synthesis, pharmacophore modeling, and biological evaluation of novel 5H-thiazolo[3,2-a]pyrimidin-5-one derivatives as 5-HT_{2A} receptor antagonists. *Sci. Pharm.* **2008**, *76*, 415-448.
76. Younkin, J.; Gaitonde, S. A.; Ellaithy, A.; Vekariya, R.; Baki, L.; Moreno, J. L.; Shah, S.; Drossopoulos, P.; Hideshima, K. S.; Eltit, J. M.; González-Maeso, J.; Logothetis, D. E.; Dukat, M.; Glennon, R. A. Reformulating a pharmacophore for 5-HT_{2A} serotonin receptor antagonists. *ACS Chem. Neurosci.* **2016**, *7*, 1292-1299.
77. Shah, U. H.; Gaitonde, S. A.; Moreno, J. L.; Glennon, R. A.; Dukat, M.; González-Maeso, J. Revised pharmacophore model for 5-HT_{2A} receptor antagonists derived from the atypical antipsychotic agent risperidone. *ACS Chem. Neurosci.* **2019**, *10*, 2318-2331.
78. Glennon, R. Pharmacophore identification for sigma-1 (σ_1) receptor binding: Application of the “deconstruction - reconstruction - elaboration” approach. *Mini-Reviews Med. Chem.* **2005**, *5*, 927-940.
79. Mokrosz, M. J.; Strekowski, L.; Kozak, W. X.; Duszyńska, B.; Bojarski, A. J.; Kłodzinska, A.; Czarny, A.; Cegła, M. T.; Dereń-Wesołek, A.; Chojnacka-Wójcik, E.; Dove, S.; Mokrosz, J. L. Structure-activity relationship studies of CNS agents, part 25: 4,6-

Di(heteroaryl)-2-(*N*-methylpiperazino)pyrimidines as new, potent 5-HT_{2A} receptor ligands: A verification of the topographic model. *Arch. Pharm. (Weinheim)* **1995**, *328*, 659-666.

80. Westkaemper, R.; Glennon, R. A. Application of ligand SAR, receptor modeling and receptor mutagenesis to the discovery and development of a new class of 5-HT_{2A} ligands. *Curr. Top. Med. Chem.* **2005**, *2*, 575-598.
81. Höltje, H. -D.; Jendretzki, U. K. Construction of a detailed serotoninergic 5-HT_{2A} receptor model. *Arch. Pharm. (Weinheim)* **1995**. *328*, 577-584.
82. Andersen, K.; Liljefors, T.; Gundertofte, K.; Perregaard, J.; Bøgesø, K. P. Development of a receptor-interaction model for serotonin 5-HT_2 receptor antagonists. Predicting selectivity with respect to dopamine D_2 receptors. *J. Med. Chem.* **1994**, *37*, 950-962.
83. Robiolio, P. A.; Rigolin, V. H.; Wilson, J. S.; Harrison, J. K.; Sanders, L. L.; Bashore, T. M.; Feldman, J. M. Carcinoid heart disease: Correlation of high serotonin levels with valvular abnormalities detected by cardiac catheterization and echocardiography. *Circulation* **1995**, *92*, 790-795.
84. Roberts, W. C. A unique heart disease associated with a unique cancer: Carcinoid heart disease. *Am. J. Cardiol.* **1997**, *80*, 251-256.
85. Sheline, Y. I.; Freedland, K. E.; Carney, R. M. How safe are serotonin reuptake inhibitors for depression in patients with coronary heart disease? *Am. J. Med.* **1997**, *102*, 54-59.
86. Diaz, S. L.; Maroteaux, L. Implication of 5-HT_{2B} receptors in the serotonin syndrome. *Neuropharmacology* **2011**, *61*, 495-502.
87. Diaz, S. L.; Doly, S.; Narboux-Nme, N.; Fernández, S.; Mazot, P.; Banas, S. M.; Boutourlinsky, K.; Moutkine, I.; Belmer, A.; Roumier, A.; Maroteaux, L. 5-HT_{2B} receptors are required for serotonin-selective antidepressant actions. *Mol. Psychiatry* **2012**, *17*, 154-163.
88. Nebigil, C. G.; Hickel, P.; Messaddeq, N.; Vonesch, J. L.; Douchet, M. P.; Monassier, L.; György, K.; Matz, R.; Andriantsitohaina, R.; Manivet, P.; Launay, J. M.; Maroteaux, L.

Ablation of serotonin 5-HT_{2B} receptors in mice leads to abnormal cardiac structure and function. *Circulation* **2001**, *103*, 2973-2979.

89. Nebigil, C. G.; Jaffré, F.; Messaddeq, N.; Hickel, P.; Monassier, L.; Launay, J. M.; Maroteaux, L. Overexpression of the serotonin 5-HT_{2B} receptor in heart leads to abnormal mitochondrial function and cardiac hypertrophy. *Circulation* **2003**, *107*, 3223-3229.
90. Janssen, W.; Schymura, Y.; Novoyatleva, T.; Kojonazarov, B.; Boehm, M.; Wietelmann, A.; Luitel, H.; Murmann, K.; Krompiec, D. R.; Tretyn, A.; Pullamsetti, S. S.; Weissmann, N.; Seeger, W.; Ghofrani, H. A.; Schermuly, R. T. 5-HT_{2B} receptor antagonists inhibit fibrosis and protect from RV heart failure. *Biomed Res. Int.* **2015**, *2015*, 1-8.
91. Barceloux, D. G. Serotoninergic and mixed agents. In *Medical Toxicology of Drug Abuse*; **2012**, Ed. 1; John Wiley & Sons, Inc.:Hoboken, NJ, 2012; pp 255-274.
92. Connolly, H. M.; Crary, J. L.; McGoon, M. D.; Hensrud, D. D.; Edwards, B.S.; Edwards, W. D. . S.; V, H. V. Valvular heart disease associated with fenfluramine–phentermine. *N. Engl. J. Med.* **1997**, *337*, 1772-1776.
93. Rothman, R. B.; Baumann, M. H. Serotonergic drugs and valvular heart disease. *Expert Opin. Drug Saf*. **2009**, *8*, 317-329.
94. Roth, B. L. Drugs and valvular heart disease. *N. Engl. J. Med.* **2007**, *356*, 6-9.
95. Raleigh, M. J.; Brammer, G. L.; Ritvo, E. R.; Geller, E.; McGuire, M. T.; Yuwiler, A. Effects of chronic fenfluramine on blood serotonin, cerebrospinal fluid metabolites, and behavior in monkeys. *Psychopharmacology (Heidelberg, Ger.)* **1986**, *90*, 503-508.
96. Celada, P.; Martín, F.; Artigas, F. Effects of chronic treatment with dexfenfluramine on serotonin in rat blood, brain and lung tissue. *Life Sci.* **1994**, *55*, 1237-1243.
97. Sherman, J.; Factor, D. C.; Swinson, R.; Darjes, R. W. The effects of fenfluramine (hydrochloride) on the behaviors of fifteen autistic children. *J. Autism Dev. Disord.* **1989**, *19*, 533-543.

98. Setola, V.; Hufeisen, S. J.; Grande-Allen, K. J.; Vesely, I.; Glennon, R. A.; Blough, B.; Rothman, R. B.; Roth, B. L. 3,4-Methylenedioxymethamphetamine (MDMA, “Ecstasy”) induces fenfluramine-like proliferative actions on human cardiac valvular interstitial cells in vitro. *Mol. Pharmacol.* **2003**, *63*, 1223-1229.

99. Droogmans, S.; Cosyns, B.; D’haenen, H.; Creeten, E.; Weytjens, C.; Franken, P. R.; Scott, B.; Schoors, D.; Kemdem, A.; Close, L.; Vandenbossche, J. L.; Bechet, S.; Van Camp, G. Possible association between 3,4-methylenedioxymethamphetamine abuse and valvular heart disease. *Am. J. Cardiol.* **2007**, *100*, 1442-1445.

100. Schade, R.; Andersohn, F.; Suissa, S.; Haverkamp, W.; Garbe, E. Dopamine agonists and the risk of cardiac-valve regurgitation. *N. Engl. J. Med.* **2007**, *356*, 29-38.

101. Setola, V.; Dukat, M.; Glennon, R. A.; Roth, B. L. Molecular determinants for the interaction of the valvulopathic anorexigen norfenfluramine with the 5-HT_{2B} receptor. *Mol. Pharmacol.* **2005**, *68*, 20-33.

102. Finder, R. M.; Brogden, R. N.; Sawyer, P. R.; Speight, T. M.; Avery, G. S. Fenfluramine: A review of its pharmacological properties and therapeutic efficacy in obesity. *Drugs* **1975**, *10*, 241-323.

103. Vickers, S. P.; Clifton, P. G.; Dourish, C. T.; Tecott, L. H. Reduced satiating effect of d-fenfluramine in serotonin 5-HT_{2C} mutant mice. *Psychopharmacology (Heidelberg, Ger.)* **1999**, *143*, 309-314.

104. Vickers, S. P.; Dourish, C. T.; Kennett, G. A. Evidence that hypophagia induced by d-fenfluramine and d-norfenfluramine in the rat is mediated by 5-HT_{2C} receptors. *Neuropharmacology* **2001**, *41*, 200-209.

105. Schoonjans, A. S.; Ceulemans, B. An old drug for a new indication: Repurposing fenfluramine from an anorexigen to an antiepileptic drug. *Clin. Pharmacol. Ther.* **2019**, *106*, 929-932.

106. Vavers, E.; Svalbe, B.; Lauberte, L.; Stonans, I.; Misane, I.; Dambrova, M.; Zvejniece, L. The activity of selective sigma-1 receptor ligands in seizure models in vivo. *Behav. Brain Res.* **2017**, *328*, 13-18.

107. Guo, L.; Chen, Y.; Zhao, R.; Wang, G.; Friedman, E.; Zhang, A.; Zhen, X. Allosteric modulation of sigma-1 receptors elicits anti-seizure activities. *Br. J. Pharmacol.* **2015**, *172*, 4052-4065.

108. Venzi, M.; David, F.; Bellet, J.; Cavaccini, A.; Bombardi, C.; Crunelli, V.; Di Giovanni, G. Role for serotonin2A (5-HT2A) and 2C (5-HT2C) receptors in experimental absence seizures. *Neuropharmacology* **2016**, *108*, 292-304.

109. Rothman, R. B.; Baumann, M. H.; Savage, J. E.; Rauser, L.; McBride, A.; Hufeisen, S. J.; Roth, B. L. Evidence for possible involvement of 5-HT_{2B} receptors in the cardiac valvulopathy associated with fenfluramine and other serotonergic medications. *Circulation* **2000**, *102*, 2836-2841.

110. Favrod-Coune, T.; Broers, B. The health effect of psychostimulants: A literature review. *Pharmaceuticals* **2010**, *3*, 2333-2361.

111. Nelson, D. L.; Lucaites, V. L.; Wainscott, D. B.; Glennon, R. A. Comparisons of hallucinogenic phenylisopropylamine binding affinities at cloned human 5-HT_{2A}, 5-HT_{2B} and 5-HT_{2C} receptors. *Naunyn-Schmiedeberg's Arch. Pharmacol.* **1999**, *359*, 1-6.

112. Glennon, R. A. The 2014 Philip S. Portoghese Medicinal Chemistry Lectureship: The "phenylalkylaminome" with a focus on selected drugs of abuse. *J. Med. Chem*. **2017**, *60*, 2605-2628.

113. Nichols, D. E. Structure-activity relationships of serotonin 5-HT_{2A} agonists. *Wiley Interdiscip. Rev.: Membr. Transp. Signaling*. **2012,** *1*, 559-579.

114. Shulgin, A. T.; Sargent, T.; Naranjo, C. Structure-activity relationships of one-ring psychotomimetics. *Nature* **1969**, *221*, 537-541.

115. Parrish, J. C.; Braden, M. R.; Gundy, E.; Nichols, D. E. Differential phospholipase C activation by phenylalkylamine serotonin 5-HT_{2A} receptor agonists. *J. Neurochem.* **2005**, *95*, 1575-1584.

116. Glennon, R. A.; Bondarev, M. L.; Khorana, N.; Young, R.; May, J. A.; Hellberg, M. R.; McLaughlin, M. A.; Sharif, N. A. β-Oxygenated analogues of the 5-HT_{2A} serotonin receptor agonist 1-(4-bromo-2,5-dimethoxyphenyl)-2-aminopropane. *J. Med. Chem.* **2004**, *47*, 6034-6041.

117. Glennon, R. A.; Young, R.; Rosecrans, J. A. Discriminative stimulus properties of DOM and several molecular modifications. *Pharmacol. Biochem. Behav.* **1982**, *16*, 553-556.

118. Seggel, M. R.; Yousif, M. Y.; Glennon, R. A.; Lyon, R. A.; Titeler, M.; Roth, B. L.; Suba, E. A. A structure-affinity study of the binding of 4-substituted analogues of 1-(2,5-dimethoxyphenyl)-2-aminopropane at 5-HT_2 serotonin receptors. *J. Med. Chem.* **1990**, 1032-1036.

119. Glennon, R. A.; Lyon, R. A.; McKenney, J. D.; Titeler, M. 5-HT_1 and 5-HT_2 binding characteristics of 1-(2,5-dimethoxy-4-bromophenyl)-2-aminopropane analogues. *J. Med. Chem.* **1986**, *29*, 194-199.

120. Moya, P. R.; Berg, K. A.; Gutiérrez-Hernandez, M. A.; Sáez-Briones, P.; Reyes-Parada, M.; Cassels, B. K.; Clarke, W. P. Functional selectivity of hallucinogenic phenethylamine and phenylisopropylamine derivatives at human 5-hydroxytryptamine (5-HT)$_{2A}$ and 5-HT_{2C} Receptors. *J. Pharmacol. Exp. Ther.* **2007**, *321*, 1054-1061.

121. Porter, R. H. P.; Benwell, K. R.; Lamb, H.; Malcolm, C. S.; Allen, N. H.; Revell, D. F.; Adams, D. R.; Sheardown, M. J. Functional characterization of agonists at recombinant human 5-HT_{2A}, 5-HT_{2B} and 5-HT_{2C} receptors in CHO-K1 cells. *Br. J. Pharmacol.* **1999**, *128*, 13-20.

122. Acuña-Castillo, C.; Villalobos, C.; Moya, P. R.; Sáez, P.; Cassels, B. K.; Huidobro-Toro, J. P. Differences in potency and efficacy of a series of

phenylisopropylamine/phenylethylamine pairs at 5-HT_{2A} and 5-HT_{2C} receptors. *Br. J. Pharmacol.* **2002**, *136*, 510-519.

123. Glennon, R. A.; Dukat, M.; Grella, B.; Hong, S. S.; Costantino, L.; Teitler, M.; Smith, C.; Egan, C.; Davis, K.; Mattson, M. V. Binding of β-carbolines and related agents at serotonin (5-HT_2 and 5- HT_{1A}), dopamine (D_2) and benzodiazepine receptors. *Drug Alcohol Depend.* **2000**, *60*, 121-132.
124. Glennon, R. A.; Slusher, R. M.; McKenney, J. D.; Lyon, R. A.; Titeler, M. 5-HT_1 and 5-HT_2 binding characteristics of some quipazine analogues. *J. Med. Chem.* **1986**, *29*, 2375-2380.
125. De La Fuente Revenga, M.; Shah, U. H.; Nassehi, N.; Jaster, A. M.; Hemanth, P.; Sierra, S.; Dukat, M.; González-Maeso, J. Psychedelic-like properties of quipazine and its structural analogues in mice. *ACS Chem. Neurosci.* **2021**, *12*, 831-844.
126. Winter, J. C. The stimulus effects of serotonergic hallucinogens in animals. *NIDA Res. Monogr.* **1994**, *146*, 157-182.
127. Rodríguez, R.; Pardo, E. G. Quipazine, a new type of antidepressant agent. *Psychopharmacologia* **1971**, *21*, 89-100.
128. Kuhn, D. M.; White, F. J.; Appel, J. B. Discriminable stimuli produced by hallucinogens. *Psychopharmacol. Commun.* **1976**, *2*, 345-348.
129. White, F. J.; Kuhn, D. M.; Appel, J. B. Discriminative stimulus properties of quipazine. *Neuropharmacology* **1977**, *16*, 827-832.
130. Sleight, A. J.; Stam, N. J.; Mutel, V.; Vanderheyden, P. M. L. Radiolabelling of the human 5-HT_{2A} receptor with an agonist, a partial agonist and an antagonist: Effects on apparent agonist affinities. *Biochem. Pharmacol.* **1996**, *51*, 71-76.
131. McKenna, D. J.; Peroutka, S. J. Differentiation of 5-hydroxytryptamine$_2$ receptor subtypes using ^{125}I-R-(-)2,5-dimethoxy-4-iodo-phenylisopropylamine and ^{3}H-ketanserin. *J. Neurosci.* **1989**, *9*, 3482-3490.

132. Knight, A. R.; Misra, A.; Quirk, K.; Benwell, K.; Revell, D.; Kennett, G.; Bickerdike, M. Pharmacological characterisation of the agonist radioligand binding site of 5-HT_{2A}, 5-HT_{2B} and 5-HT_{2C} receptors. *Naunyn-Schmiedeberg's Arch. Pharmacol.* **2004**, *370*, 114-123.

133. Egan, C.; Grinde, E.; Dupre, A.; Roth, B. L.; Hake, M.; Teitler, M.; Herrick-Davis, K. Agonist high and low affinity state ratios predict drug intrinsic activity and a revised ternary complex mechanism at serotonin 5-HT_{2A} and 5-HT_{2C} receptors. *Synapse* **2000**, *35*, 144-150.

134. Battaglia, G.; Shannon, M.; Borgundvaag, B.; Titeler, M. pH-Dependent modulation of agonist interactions with [^{3}H]-ketanserin-labelled S_2 serotonin receptors. *Life Sci.* **1983**, *33*, 2011-2016.

135. Lyon, R. A.; Davis, K. H.; Titeler, M. ^{3}H-DOB (4-bromo-2,5-dimethoxyphenylisopropylamine) labels a guanyl nucleotide-sensitive state of cortical 5-HT_2 receptors. *Mol. Pharmacol.* **1986**, *31*, 194-199.

136. Hoyer, D. Molecular pharmacology and biology of 5-HT_{1C} receptors. *Trends Pharmacol. Sci.* **1988**, *9*, 89-94.

137. Engel, G.; Göthert, M.; Hoyer, D.; Schlicker, E.; Hillenbrand, K. Identity of inhibitory presynaptic 5-hydroxytryptamine (5-HT) autoreceptors in the rat brain cortex with 5-HT_{1B} binding sites. *Naunyn-Schmiedeberg's Arch. Pharmacol.* **1986**, *332*, 1-7.

138. Hoyer, D.; Engel, G.; Kalkman, H. O. Molecular pharmacology of 5-HT_1 and 5-HT_2 recognition sites in rat and pig brain membranes: Radioligand binding studies with [^{3}H]5-HT, [^{3}H]8-OH-DPAT, (-)[^{125}I]iodocyanopindolol, [^{3}H]mesulergine and [^{3}H]ketanserin. *Eur. J. Pharmacol.* **1985**, *118*, 13-23.

139. Titeler, M.; Lyon, R. A.; Davis, K. H.; Glennon, R. A. Selectivity of serotonergic drugs for multiple brain serotonin receptors. Role of [^{3}H]-4-bromo-2,5-dimethoxyphenylisopropylamine ([^{3}H]DOB), a 5-HT_2 agonist radioligand. *Biochem. Pharmacol.* **1987**, *36*, 3265-3271.

140. Glennon, R. A.; Ismaiel, A. E.; McCarthy, B. M.; Peroutka, S. J. Binding of arylpiperazines to 5-HT_3 serotonin receptors: Results of a structure-affinity study. *Eur. J. Pharmacol.* **1989**, *168*, 387-392.

141. Round, A.; Wallis, D. I. Further studies on the blockade of 5-HT depolarizations of rabbit vagal afferent and sympathetic ganglion cells by MDL 72222 and other antagonists. *Neuropharmacology* **1987**, *26*, 39-48.

142. Peroutka, S. J.; Hamik, A. [^{3}H]Quipazine labels 5-HT_3 recognition sites in rat cortical membranes. *Eur. J. Pharmacol.* **1988**, *148*, 297-299.

143. Chien, E. Y. T.; Liu, W.; Zhao, Q.; Katritch, V.; Han, G. W.; Hanson, M. A.; Shi, L.; Newman, A. H.; Javitch, J. A.; Cherezov, V.; Stevens, R. C. Structure of the human dopamine D_3 receptor in complex with a D_2/D_3 selective antagonist. *Science* **2010**, *330*, 1091-1095.

144. Shimamura, T.; Shiroishi, M.; Weyand, S.; Tsujimoto, H.; Winter, G.; Katritch, V.; Abagyan, R.; Cherezov, V.; Liu, W.; Han, G. W.; Kobayashi, T.; Stevens, R. C.; Iwata, S. Structure of the human histamine H_1 receptor complex with doxepin. *Nature* **2011**, *475*, 65-72.

145. Wacker, D.; Fenalti, G.; Brown, M. A.; Katritch, V.; Abagyan, R.; Cherezov, V.; Stevens, R. C. Conserved binding mode of human *β*2 adrenergic receptor inverse agonists and antagonist revealed by X-ray crystallography. *J. Am. Chem. Soc.* **2010**, *132*, 11443-11445.

146. McCorvy, J. D.; Wacker, D.; Wang, S.; Agegnehu, B.; Liu, J.; Lansu, K.; Tribo, A. R.; Olsen, R. H. J.; Che, T.; Jin, J.; Roth, B. L. Structural determinants of 5-HT_{2B} receptor activation and biased agonism. *Nat. Struct. Mol. Biol.* **2018**, *25*, 787-796.

147. Kim, K.; Che, T.; Panova, O.; DiBerto, J. F.; Lyu, J.; Krumm, B. E.; Wacker, D.; Robertson, M. J.; Seven, A. B.; Nichols, D. E.; Shoichet, B. K.; Skiniotis, G.; Roth, B. L. Structure of a hallucinogen-activated Gq-coupled 5-HT_{2A} serotonin receptor. *Cell* **2020**, *182*, 1574-1588.

148. Wacker, D.; Wang, S.; McCorvy, J. D.; Betz, R. M.; Venkatakrishnan, A. J.; Levit, A.; Lansu, K.; Schools, Z. L.; Che, T.; Nichols, D. E.; Shoichet, B. K.; Dror, R. O.; Roth, B. L. Crystal structure of an LSD-bound human serotonin receptor. *Cell* **2017**, *168*, 377-389.

149. Glennon, R. A. Central serotonin receptors as targets for drug research. *J. Med. Chem.* **1987**, *30*, 1-12.

150. Jendretzki, U. K.; Elz, S.; Holtje, H. D. Computer aided molecular analysis of 5-HT_{2A} agonists. *Pharm. Pharmacol. Lett.* **1994**, *3*, 260-263.

151. Brea, J.; Rodrigo, J.; Carrieri, A.; Sanz, F.; Cadavid, M. I.; Enguix, J.; Mengod, G.; Caro, Y.; Masaguer, C. F.; Ravin, E. New serotonin 5-HT_{2A}, 5-HT_{2B}, and 5-HT_{2C} receptor antagonists: Synthesis, pharmacology, 3D-QSAR, and molecular modeling of (aminoalkyl)benzo and heterocycloalkanones. *J. Med. Chem.* **2002**, *45*, 54-71.

152. Runyon, S. P.; Savage, J. E.; Taroua, M.; Roth, B. L.; Glennon, R. A.; Westkaemper, R. B. Influence of chain length and N-alkylation on the selective serotonin receptor ligand 9-(aminomethyl)-9,10-dihydroanthracene. *Bioorg. Med. Chem. Lett.* **2001**, *11*, 655-658.

153. Reynolds, G. P.; Kirk, S. L. Metabolic side effects of antipsychotic drug treatment - pharmacological mechanisms. *Pharmacol. Ther.* **2010**, *125*, 169-179.

154. Zhou, Y.; Ma, J.; Lin, X.; Huang, X. P.; Wu, K.; Huang, N. Structure-based discovery of novel and selective 5-hydroxytryptamine 2B receptor antagonists for the treatment of irritable bowel syndrome. *J. Med. Chem.* **2016**, *59*, 707-720.

155. Audia, J. E.; Evrard, D. A.; Murdoch, G. R.; Droste, J. J.; Nissen, J. S.; Schenck, K. W.; Fludzinski, P.; Lucaites, V. L.; Nelson, D. L.; Cohen, M. L. Potent, selective tetrahydro-β-carboline antagonists of the serotonin 2B ($5HT_{2B}$) contractile receptor in the rat stomach fundus. *J. Med. Chem.* **1996**, *39*, 2773-2780.

156. Gabr, M. T.; Abdel-Raziq, M. S. Pharmacophore-based tailoring of biphenyl amide derivatives as selective 5-hydroxytryptamine 2B receptor antagonists. *MedChemComm* **2018**, *9*, 1069-1075.

157. Kursar, J. D.; Nelson, D. L.; Wainscott, D. B.; Cohen, M. L.; Baez, M. Molecular cloning, functional expression, and pharmacological characterization of a novel serotonin receptor (5-hydroxytryptamine$_{2F}$) from rat stomach fundus. *Mol. Pharmacol.* **1992**, *42*, 549-557.

158. Herndon, J. L.; Ismaiel, A.; Glennon, R. A.; Ingher, S. P.; Teitler, M. Ketanserin analogues: Structure-affinity relationships for 5-HT$_2$ and 5-HT$_{1C}$ serotonin receptor binding. *J. Med. Chem.* **1992**, *35*, 4903-4910.

159. Strupczewski, J. T.; Allen, R. C.; Gardner, B. A.; Schmid, B. L.; Stache, U.; Glamkowski, E. J.; Jones, M. C.; Ellis, D. B.; Huger, F. P.; Dunn, R. W. Synthesis and neuroleptic activity of 3-(1-substituted-4-piperidinyl)-1,2-benzisoxazoles. *J. Med. Chem.* **1985**, *28*, 761-769.

160. Mattsson, C.; Andreasson, T.; Waters, N.; Sonesson, C. Systematic in vivo screening of a series of 1-propyl-4-arylpiperidines against dopaminergic and serotonergic properties in rat brain: A scaffold-jumping approach. *J. Med. Chem.* **2012**, *55*, 9735-9750.

161. Kellogg, G. E.; Abraham, D. J. Hydrophobicity: Is logP(o/w) more than the sum of its parts? *Eur. J. Med. Chem.* **2000**, *35*, 651-661.

162. Braden, M. R.; Parrish, J. C.; Naylor, J. C.; Nichols, D. E. Molecular interaction of serotonin 5-HT$_{2A}$ receptor residues Phe339$^{(6.51)}$ and Phe340$^{(6.52)}$ with superpotent *N*-benzyl phenethylamine agonists. *Mol. Pharmacol.* **2006**, *70*, 1956-1964.

163. Choudhary, M. S.; Craigo, S.; Western, C.; Roth, B. L. A single point mutation (Phe^{340}->Leu^{340}) of a conserved phenylalanine abolishes 4-[^{125}I]iodo-(2,5-dimethoxy)phenylisopropylamine and [^{3}H]mesulergine but not [^{3}H]ketanserin binding to 5-hydroxytryptamine$_2$ receptors. *Mol. Pharmacol.* **1993**, *43*, 755-761.

164. Hansch, C.; Leo, A.; Unger, S. H.; Kim, K. H.; Nikaitani, D.; Lien, E. J. “Aromatic” substituent constants for structure-activity correlations. *J. Med. Chem.* **1973**, *16*, 1207-1216.

165. Chen, T. W.; Wardill, T. J.; Sun, Y.; Pulver, S. R.; Renninger, S. L.; Baohan, A.; Schreiter, E. R.; Kerr, R. A.; Orger, M. B.; Jayaraman, V.; Looger, L. L.; Svoboda, K.; Kim, D. S.

Ultrasensitive fluorescent proteins for imaging neuronal activity. *Nature* **2013**, *499*, 295-300.

166. Marcher-Rørsted, E.; Halberstadt, A. L.; Klein, A. K.; Chatha, M.; Jademyr, S.; Jensen, A. A.; Kristensen, J. L. Investigation of the 2,5-dimethoxy motif in phenethylamine serotonin 2A receptor agonists. *ACS Chem. Neurosci.* **2020**, *11*, 1238-1244.
167. Basappa; Mantelingu, K.; Sadashiva, M. P.; Rangappa, K. S. A simple and efficient method for the synthesis of 1,2-benzisoxazoles: A series of its potent acetylcholinesterase inhibitors. *Indian J. Chem.* **2004**, *43*, 1954-1957.
168. Power, J. D.; Clarke, K.; McDermott, S. D.; McGlynn, P.; Barry, M.; White, C.; O'Brien, J.; Kavanagh, P. The identification of 4-methylamphetamine and its synthesis by-products in forensic samples. *Forensic Sci. Int.* **2013**, *228*, 115-131.
169. Kawai, Y.; Inaba, Y.; Tokitoh, N. Asymmetric reduction of nitroalkenes with baker's yeast. *Tetrahedron: Asymmetry* **2001**, *12*, 309-318.

Vita

Prithvi Hemanth was born on June 24, 1994 to Dr. Hemanth K. Thippeswamy and Roopa Hemanth in Morgantown, West Virginia. He received his bachelors of science degree in chemistry with a concentration in biochemistry from Virginia Commonwealth University in Richmond Virginia in August 2017, following which he enrolled in the doctoral program in the Department of Medicinal Chemistry, School of Pharmacy at Virginia Commwealth University.